Diplomarbeit

Sparsity - based Spectrum Estimators for Nonstationary Random Processes

ausgeführt am
Institut für Nachrichtentechnik und Hochfrequenztechnik (E 389)
der Technischen Universität Wien

unter der Leitung von

Dipl.-Ing. Dr. techn. Georg Tauböck
Ao. Univ.-Prof. Dipl.-Ing. Dr. Franz Hlawatsch

von
Alexander Jung
Gattring 11
A-3143 Pyhra

Gattring, Mai 2008 _____

Acknowledgements

I am grateful for the help I received from G. Tauböck.

Thanks to F. Hlawatsch, whose spirit of work will always be an motivating but unreachable ideal for me.

I also want to thank Gerald Matz who kindly shared his expertise in statistical signal processing.

I'd like to express my thanks to my parents. Their support made my study of electrical engineering possible.

Finally and most importantly i'd like to express my deep gratefulness for Julia and Helene for being with me. While continuously supporting and motivating me throughout writing this thesis, they regularly reminded me on what's really important in life.

To my aunt Gerti ...

Abstract

In recent years, say 10 to 15, there has been an tremendous effort in studying over-complete signal representations in the signal processing community. Overcompleteness has the advantage of allowing tailoring the description to the corresponding situation. This is in obvious analogy to the system of human language. One of the ground-breaking papers in this direction was authored by Mallat and Zhang, introducing the "Matching Pursuit" [37].

More recently, it has been recognized that over completeness can also be used to perform a compression, i.e., we use less linear measurements (the measurement process is represented by multiplying the signal vector with a "fat" measurement matrix) than the original signal dimension with the additional constraint that the original signal is sparse. The corresponding area of research is often labeled by Compressed Sensing (CS).

Relying on the existing theoretical results for over complete representations it has been shown in a number of papers (e.g. [6, 13]) that not only one can achieve extremely good compression performance without loosing significant information but also the recovery (or decoding) can be performed in an efficient and practically feasible manner.

In this thesis we try to find synergies of the results of CS with recent results on the problem of estimating the spectrum of an underspread process. The resulting CS-based estimators are intended to work with a reduced data rate at the input.

Zusammenfassung

In den letzten 10 bis 15 Jahren hat sich ein enormes Interesse an redundanten linearen Signaldarstellungen gezeigt. Eine redundante Darstellung hat den Vorteil sich besser auf die jeweilige Problemstellung anpassen zu können. Hier gibt es eine Analogie zum System der menschlichen Sprache. Eine grundlegende Arbeit auf diesem Gebiet geht zurück auf Mallat and Zhang, die dabei den sogenannten "Matching Pursuit" entwickelten [37]. Vor kurzem hat man erkannt, dass man die Theorie der redundanten linearen Darstellungen verwenden kann um Kompressionsverfahren zu studieren. Der daraus entstandene Forschungsbereich wird oftmals mit dem Namen "Compressed Sensing" identifiziert. Aufbauend auf den Ergebnissen zu den redundanten Signaldarstellungen konnte gezeigt werden (z.B. [6, 13]), dass man unter gewissen Bedingungen extrem gute Kompressionsleistungen erzielen kann. Darüber hinausgehend hat man effiziente Verfahren gefunden um aus den komprimierten Daten die originalen zurückzugewinnen. In dieser Diplomarbeit wird versucht die Ergebnisse aus Compressed Sensing zu verwenden um Spektrumschätzer für Zufallsprozesse zu entwickeln, die mit einer reduzierten Datenrate am Eingang arbeiten.

Contents

Chapter 1

Introduction

1.1 Motivation

In this thesis we try to combine the results of two subfields of signal processing. On one hand we have the traditional and well developed field of statistical time-frequency signal processing. On the other hand, we have the relative new area of Compressed Sensing (CS). The main scope of this thesis is to investigate the impacts of the new results on CS for statistical (using time-frequency methods/concepts) signal processing. A central point of this thesis is to compare different combinations of CS-results with time-frequency methods. The presented combination of results focuses mainly on new designs of spectrum estimators for underspread processes. We think that this application will illustrate nicely the power of CS for statistical signal processing problems.

Although this thesis is clearly located more on the theoretical side and not on the practical, we would like to illustrate the potential of the results from the CS theory with the help of some applications:

- **Cognitive Radio.** The term "cognitive radio" stands for wireless communication systems, where each participant continuously monitors the environment for radiation. If he finds a frequency band that is not already occupied he uses it for transmission. Two main requirements in the technical realization of this concept are: a wide frequency band of interest and second, fast response times of the transceivers. When using conventional sampling techniques operating at nyquist rate, the technical realization is rather hard. Recently there has been proposed the usage of compressed sensing for cognitive radios [54]. There it is shown, that sampling the radio signal at half the nominal nyquist rate, still yields acceptable performance.

- **Analog to Information Converter.** The concept of an Analog to Information Converter is the direct usage of the compressed sensing theory to build new types of analog to digital

converter. In a recent paper [21] a concept was proposed, where the CS theory was applied by modulating the analog signal with a pseudo random chipping sequence and then using a conventional anti-aliasing analog to digital converter stage. It has been demonstrated there, that under specific sparsity restrictions on the input signal, sampling with only a sixth of the nominal Nyquist rate still yields usable results. A closely related approach is proposed in [19], where the input signals are assumed to be locally Fourier - sparse (see [19] for the exact meaning of this notion). The input signal is then sampled at non uniform randomly distributed time instants. A further flavor of implementing an AIC is to use a FIR filter structure at the (high) Nyquist rate and use random variables as tap weights. The output of this random filter [56] is then downsampled onto rates which are confirmed by the CS theory.

- **Compressive Imaging.** A very exciting approach in optics is to implement the multiplication of a sparse vector with a random matrix by "passive" hardware. This is done with the help of a DMD[1] (Digital Micromirror device), an array of electrostatic controllable small mirrors. Here the term "projection matrix" gets a very practical meaning, because it really projects the incoming light onto a photodiode. The theory behind it and the technical realization is presented in [22].

- **High Resolution Radar via Compressed Sensing.** The authors of [24] propose the usage of CS methods to mitigate the limitations of the radar uncertainty principle which is a fundamental performance limit for conventional radar systems.

These examples show that the motivation behind the exploration of the CS theory is really driven by applications. An almost complete list of references to papers about the theory and applications of CS and other material related to Compressed Sensing can be found on the web page **http://www.dsp.ece.rice.edu/cs/** .

1.2 Notations and Definitions

The conjugate complex of a complex number x will be denoted by x^*. We will denote a linear operator by bold capital letters (e.g. $\mathbf{H}$). The kernel of a linear operator $\mathbf{X}$ will be denoted by $h_{\mathbf{X}}(t,t')$ where for the subscript the same symbol as for the linear operator is used. The adjoint of a linear operator $\mathbf{H}$ will be denoted by $\mathbf{H}^*$, it is given via the following relationship of its kernel: $h_{\mathbf{H}^*}(t_1,t_2) = h^*_{\mathbf{H}}(t_2,t_1)$. Given a hermitian linear operator $\mathbf{H}$ ($\mathbf{H} = \mathbf{H}^*$), we denote by $\|\mathbf{H}\|_2^2$ the squared Hilbert-Schmidt (HS) norm: $\|\mathbf{H}\|_2^2 \triangleq \int_{t,t'} |h_{\mathbf{H}}(t,t')|^2 dtdt' = \sum_k \lambda_k^2$ where λ_k denotes the real-valued eigenvalues of $\mathbf{H}$. Signals (functions) will be denoted by lower case letters (e.g.

[1] To the best knowledge of the author, the term "DMD - Digital Micromirror Device" is originated by its inventors at Texas Instruments. See **www.ti.com** for reference

$u(t) \in L^2(\mathbb{R})$). A matrix will also be set in bold face: $\mathbf{A} \in \mathbb{C}^{m\times n}$. The hermitian transpose of a matrix $\mathbf{A}$ will be denoted by $\mathbf{A}^H$. For finite dimensional vectors (e.g. $\in \mathbb{C}^n$) we use the same notation as for matrices because a finite dimensional vector will be identified throughout this thesis with a single column matrix. We denote the k-th coefficient or element of a vector $\mathbf{x} \in \mathbb{C}^n$ by $\mathbf{x}_k$. Given a matrix $\mathbf{A}$, we denote by $\mathbf{A}_{k,l}$ the element of $\mathbf{A}$ which is located in the k-th row and the l-th column. Given two functions $u(t)$ and $v(t)$, both assumed to be in $L^2(\mathbb{R})$), we define the inner product $\langle u, v\rangle$ as $\langle u, v\rangle \triangleq \int_t u(t)v^*(t)dt$. The partial Fourier transform $\hat{u}(f, \tau)$ of a 2D- function $u(t, \tau)$ is denoted by:

$$\hat{u}(f, \tau) = \mathcal{F}_{x\to f} u(t, \tau) \triangleq \int_t u(t, \tau)e^{-j2\pi tf} dt. \tag{1.1}$$

1.3 Assumptions

The fundamental object of interest within this thesis is a complex-valued, circular-symmetric and non stationary random process, denoted by $X(t)$. We assume that $X(t)$ fulfills two requirements:

- First, it is underspread, i.e. it has a limited time-frequency correlation horizon. The exact meaning of "underspread" will be discussed in Chapter 3.
- Second, it is sparsely representable by a Gabor expansion. More specifically, most of the Gabor analysis coefficients of $X(t)$ are effectively zero.

It seems to be the first time that these two fundamental (but independent) assumptions are investigated in a joint fashion. To keep the derivations simple we place a further constraint on the process $X(t)$. We assume that every realization $x(t)$ (which is a deterministic function of time t) of $X(t)$ lies in $L^2(\mathbb{R})$. This assumption removes technical (in a mathematical sense) difficulties. In order to investigate the stochastic properties of the random process $X(t)$, we use a (linear) correlation operator, denoted by $\mathbf{R}_X$. The kernel $r_X(t_1, t_2)$ of this linear operator is defined as $r_X(t_1, t_2) \triangleq \mathrm{E}\{X(t_1)X^*(t_2)\}$ where the asterisk * denotes complex conjugation. We also assume that $X(t)$ has zero mean: $\mathrm{E}\{X(t)\} \equiv 0$, therefore $\mathbf{R}_X$ is a complete description of the second order statistics of $X(t)$.[2] From the definition of $\mathbf{R}_X$ it follows that it is a self-adjoint operator. Since one can show the equation: $\mathrm{E}\{\langle X, u\rangle\langle X, v\rangle^*\} = \langle \mathbf{R}_X v, u\rangle$, it is evident that $\mathbf{R}_X$ is a positive semi-definite operator. A further property of $\mathbf{R}_X$ is a consequence of our assumption that $x(t) \in L^2(\mathbb{R})$. This implies that the trace of $\mathbf{R}_X$, denoted by $\mathrm{tr}\{\mathbf{R}_X\} \triangleq \int_t r_X(t, t)dt$, is finite. A finite trace of $\mathbf{R}_X$, in turn, implies that $\mathbf{R}_X$ has finite Hilbert-Schmidt norm: $\|\mathbf{R}_X\|_2^2 \triangleq \int_{t'} \int_{t''} |r_X(t', t'')|^2 < \infty$. Finally because $\mathbf{R}_X$ is HS (the phrase "the operator is HS" means that the operator has a finite HS-norm), it is necessarily a compact operator. For a compact and self-adjoint operator $\mathbf{R}_X$ the

[2] If $X(t)$ is moreover known to be a Gaussian process, then $\mathbf{R}_X$ provides a full statistical description.

spectral decomposition theorem with real-valued weights holds [43], i.e., $\mathbf{R}_X$ can be decomposed as follows[3]:

$$\mathbf{R}_X = \sum_k \lambda_k u_k \otimes u_k \tag{1.2}$$

where $\lambda_k \in \mathbb{R}$ and the set of functions $\{u_k(t)\}_k$ forms an ONB of $L^2(\mathbb{R})$. Equivalently, $\mathbf{R}_X$ allows an eigenvalue decomposition (EVD) with an orthonormal system of eigenvectors u_k (which are complete in $L^2(\mathbb{R})$) and a corresponding sequence of real-valued non-negative eigenvalues λ_k. The EVD of $\mathbf{R}_X$ is essential for performing the so called $Karhunen - Love$ transform (we will discuss this in detail below).

1.4 Overview

The outline of the thesis is organized as follows:

- In **Chapter 2** we present some key concepts of time-frequency signal processing, as far as they concern our thesis. We will introduce the notion of a Wigner-Ville spectrum (WVS) and the expected ambiguity function (EAF). Furthermore we will give a short introduction to the important concept of Gabor frames and the related topic of local cosine bases (LCB).

- In **Chapter 3** we review the main properties of those specific class of nonstationary random processes which consists of all processes that are underspread. We derive the smoothness of the WVS of underspread processes and the corresponding sampling theorems. Furthermore, we discuss the correlations structure of the Gabor coefficients of the underspread process w.r.t. to a given Gabor frame in more detail. Finally a simple heuristic design of a WVS estimator for underspread processes is presented.

- In **Chapter 4** we introduce the main concepts and results for Compressed Sensing (CS). In that chapter we will consider the main approaches for the key problem in CS, i.e., recovery of the original signal or data from incomplete (therefore compressed) and inaccurate (because of noise) measurements.

- The key element of this thesis is **Chapter 5**. There, we will show that the combination of Compressed Sensing and existing concepts for WVS estimation for underspread processes lead to implementations that allow to use significant lower sampling rates in the front end of the estimator, while still allowing for a reasonable estimation performance. There we will discuss the notion of (TF-) sparsity of a process in more detail. We will discuss methods to

[3]The product $x \otimes y$ where $x(t)$ and $y(t)$ are functions in $L^2(\mathbb{R})$ is defined to be the specific linear operator whose kernel $h(t_1, t_2)$ is given by $h(t_1, t_2) = x(t_1)y^*(t_2)$.

quantify the sparsity of the underlying process using the concepts of Gabor expansion and the Wigner-Ville spectrum.

- In **Chapter 6** we present the main results of the numerical investigations related to the theoretical concepts of the previous chapter. We furthermore give a detailed discussion of the problem of generating sparse underspread processes in an efficient manner.
- The final **Chapter 7** lists the most important conclusions that have been found in the course of this thesis and points out questions that have not been answered in this thesis but seem to be a reasonable continuation of the work started with this thesis.

Chapter 2

Time-Frequency Concepts in Signal Processing

2.1 Introduction

The purpose of this chapter is to give a brief introduction/review of the main methods and concepts of time-frequency (TF) signal processing as far as it is necessary for our context. Within this thesis we can divide the TF-concepts for analyzing random processes or deterministic functions generally into two big categories. Furthermore, to each method belonging to one of the two categories there belongs always a stochastic and a deterministic instance. The stochastic instances of the TF-methods are used to analyze a random process $X(t)$. On the other hand, the deterministic instances are used to analyze a deterministic function $x(t)$, which may be a single realization of the process $X(t)$. In almost all cases and for all methods used in this thesis the stochastic instance can be written as the mean of a deterministic TF method. This is sometimes reflected already in the naming: The stochastic instance of a TF-method is in some cases labeled exactly with the same name as its deterministic counterpart with the only difference of preceding "expected" (e.g. the expected ambiguity function/ambiguity function).

From this connection via the expectation operation, it follows that every property of a TF-method in the stochastic setting which is valid for every random process, induces the *same* property of the corresponding TF-method in the deterministic setting, because a deterministic function can be viewed as a special case of a random process.[1]

The first category of TF-methods compares the properties of a random process $X(t)$/deterministic

[1]Note that this is only true for the properties of the *methods* and not for properties of the *signals/processes*, i.e, a property that a random process has with respect to a TF-representation needs not to carry over to a corresponding property of any realization of that process.

function $x(t)$ with absolute time t and absolute frequency f. The basic method for this comparison is a "TF-spectrum". Loosely speaking, the spectrum of a process $X(t)$ tells us how much energy the process/signal $X(t)/x(t)$ has at neighborhood around time t and frequency f[2] A practical interpretation could be, that the value of a spectrum at a point (t_0, f_0) in the TF-plane is equal to the magnitude of a filter output and this filter is such that it passes only signals around t_0 and with frequencies around f_0, e.g. a narrow bandpass with center frequency f_0 that is "switched on" only in a certain period of time around t_0. Additionally to this very primitive but intuitive explanation of the notion of a "spectrum", we will give a precise mathematical definition of a (very) special example of a spectrum, the so called Wigner-Ville spectrum (WVS) for the stochastic setting and the Wigner distribution (WD) for the deterministic setting, below.

The other category of TF-methods does not use absolute times and frequencies, but rather describes the inner or relative structure of the random process $X(t)$/deterministic function $x(t)$. More specifically it investigates the relationship of $X(t)/x(t)$ with a time-shifted (by delay τ) and frequency-shifted (by doppler frequency shift ν) version $X(t-\tau)e^{j2\pi\nu t}/x(t-\tau)e^{j2\pi\nu t}$ of itself. We will call this second category the "correlative-methods". However we use only one specific member of this category, namely the so called expected ambiguity function (EAF) for the stochastic setting and the so called ambiguity function (AF) for the deterministic setting.

Both categories have their pros and cons in their usage for analyzing a random process $X(t)$ /deterministic function $x(t)$ but of course these two categories have intimate relationships that should by exploited.

In the end of this chapter we additionally present another important tools for TF-signal processing, namely the concept of "Weyl-Heisenberg" sets or Gabor Frames and the concept of local cosine bases (LCB). These two concepts are not directly related to the two categories of analysis tools mentioned above but however, play a central role in the theory of time-frequency signal analysis and synthesis and are heavily used in the course of this thesis.

2.2 Wigner Ville Spectrum and Wigner Distribution

The Wigner-Ville spectrum (WVS) of a process $X(t)$, which we will denote by $\overline{W}_X(t,f)$, is a function of time and frequency i.e., its domain is the TF-plane, and takes on real values. It is a function of the random process $X(t)$ and defined via the kernel $r_X(t_1,t_2)$ of the corresponding correlation operator $\mathbf{R}_X$:

$$\overline{W}_X(t,f) \triangleq \int_\tau r_X\left(t+\frac{\tau}{2}, t-\frac{\tau}{2}\right) e^{-j2\pi f\tau} d\tau. \tag{2.1}$$

[2]The energy of a signal cannot be exactly concentrated at a single point at the TF-plane as this is forbidden by the uncertainty principle [40].

In fact, the WVS defined by this equation fulfills the properties that a spectrum intuitively should have. We list the major properties of the WVS:

- **Real-valuedness.** $\overline{W}_X(t,f)$ can be shown to take on only real values. However, in contrast to the stationary case (where a spectrum is represented by the power spectral density (PSD) of the process) the WVS can also take on negative values. This behavior is clearly in contrast to the interpretation of the WVS as an energy distribution over the TF-plane.[3]

- **TF-covariance.** The WVS of the process $X(t-\tau_0)e^{2\pi t f_0}$ is equal to $\overline{W}_X(t-\tau_0, f-f_0)$.

- **Quadratic Form.** The quadratic form $\langle \mathbf{R}_X u, v\rangle$ is equal to $\langle \overline{W}_X, W_{u,v}\rangle$. Here $W_{u,v}$ denotes the cross-Wigner distribution of u and v (for the exact definition of the cross-Wigner distribution and its properties we refer to [40]).

- **Fourier Duality.** The WVS $\overline{W}_X(t,f)$ and the EAF $\bar{A}_X(\tau,\nu)$, defined in Section 2.3, form a 2D-Fourier pair.

- **"Perfect" Time-Localization.** If the process $X(t)$ is zero (at least with probability 1) outside a time interval around t_0: $[t_0-\frac{T}{2}, t_0+\frac{T}{2}]$ then the WVS $\overline{W}_X(t,f)$ is zero for all $t \notin [t_0-\frac{T}{2}, t_0+\frac{T}{2}]$.

- **"Perfect" Frequency-Localization.** If the process $X(t)$ has no frequency components (at least with probability 1) outside a frequency interval around f_0: $[f_0-\frac{B}{2}, f_0+\frac{B}{2}]$ then the WVS $\overline{W}_X(t,f)$ is zero for all $f \notin [f_0-\frac{B}{2}, f_0+\frac{B}{2}]$.

- **Marginal Properties.** The WVS satisfies some important marginal properties. If we integrate $\overline{W}_X(t,f)$ over frequency f, then we get the instantaneous mean power of $X(t)$:

$$\int_{f=-\infty}^{+\infty} \overline{W}_X(t,f)df = \mathrm{E}\{|X(t)|^2\}. \tag{2.2}$$

  Finally if we integrate over the time t we get the power of the respective frequency component[4]:

$$\int_{t=-\infty}^{+\infty} \overline{W}_X(t,f)dt = \mathrm{E}\{|\hat{X}(f)|^2\}. \tag{2.3}$$

  Finally, combining these two properties we have that the integral of $\overline{W}_X(t,f)$ over the whole TF-plane yields the mean energy $\bar{E}_X$ of the process:

$$\int_{t=-\infty}^{+\infty}\int_{f=-\infty}^{+\infty} \overline{W}_X(t,f)df\,dt = \mathrm{E}\{\|X\|_2^2\} \triangleq \bar{E}_X. \tag{2.4}$$

[3] Unfortunately it can be shown that it is not possible to construct a quadratic time-frequency covariant representation of a process, that is real valued and non-negative. This result is sometimes called "Wigner - Theorem" [35].

[4] $\hat{X}(f)$ denotes the random process, that is obtained deterministically from $X(t)$ by applying a Fourier transformation to each realization $x(t)$ of $X(t)$.

- **Unitarity.** The WVS $\overline{W}_X(t,f)$ of a process $X(t)$ obeys:

$$\|\overline{W}_X(t,f)\|_2^2 = \|\mathbf{R}_X\|_2^2. \tag{2.5}$$

  This is a consequence of the definition of the WVS and Plancherel's Theorem for Fourier transforms [23].

To summarize, the WVS of a random process $X(t)$, denoted by $\overline{W}_X(t,f)$ is a function of two variables, time t and frequency f. It is assigned to $X(t)$ in such a way that it fulfills the properties that we demand from a spectrum, e.g. to commute with time/frequency shifts of the process $X(t)$ (TF-covariance). The WVS has an outstanding role among all possible definitions of a "spectrum". One indication of that special role are the "perfect" localization properties as stated above.

The WVS is a stochastic implementation of a spectrum. Its deterministic "brother" is the Wigner distribution (WD) of a function $x(t)$ (which is assumed to be in $L^2(\mathbb{R})$, i.e., it is square integrable with respect to the Lesbesgue measure). The WD of a function $x(t)$ will be denoted by $W_x(t,f)$. Conceptually the WD is in a tight relationship to the WVS. One manifestation of this fact is, that under mild conditions the WVS $\overline{W}_X(t,f)$ of a random process $X(t)$ can be written as the expectation of the WD $W_x(t,f)$ taken over all realizations $x(t)$ of the random process $X(t)$. Note that $W_x(t,f)$ is a random quantity because the signal $x(t)$ is a (randomly fluctuating) realization of a random process. Conversely the WVS $\overline{W}_X(t,f)$ is a deterministic quantity, namely a *parameter* of the random process $X(t)$ (just as the variance of an arbitrary scalar random variable is a deterministic parameter).

We now state the exact definition of the WD $W_x(t,f)$ of a (deterministic) function $x(t)$:

$$W_x(t,f) \triangleq \int_\tau x\left(t+\frac{\tau}{2}\right) x^*\left(t-\frac{\tau}{2}\right) e^{-j2\pi f\tau} d\tau. \tag{2.6}$$

Already from this expression the similarity of the WD to the WVS is obvious.

As for the WVS we state some important properties and facts for the WD. We will only detail the properties which differ fundamentally from the respective property of the WVS:

- **Real-valuedness.** $W_x(t,f) \in \mathbb{R}$ for all signals $x(t) \in L^2(\mathbb{R})$.
- **TF-covariance.** $x(t-\tau)e^{j2\pi\nu t} \Rightarrow W_x(t-\tau, f-\nu)$.
- **Fourier Duality.** The WD $W_x(t,f)$ and the AF $A_x(\tau,\nu)$, defined in Section 2.3, form a 2D-Fourier pair.
- **"Perfect" Time-Localization.**
- **"Perfect" Frequency-Localization.**

- **Marginal Properties.** The WD satisfies some important marginal properties. If we integrate $W_x(t,f)$ over frequency f, then we get the instantaneous power of $x(t)$:

$$\int_{f=-\infty}^{+\infty} W_x(t,f)df = |x(t)|^2. \tag{2.7}$$

Finally if we integrate over the time t we get the instantaneous power of the respective frequency component:[5]

$$\int_{t=-\infty}^{+\infty} W_x(t,f)dt = |\hat{x}(f)|^2. \tag{2.8}$$

Finally, combining these two properties we have that the integral of $W_x(t,f)$ over the whole TF-plane yields the mean energy $E_x \triangleq \int_t |x(t)|^2 dt = \|x\|_2^2$ of the function $x(t)$:

$$\int_{t=-\infty}^{+\infty}\int_{f=-\infty}^{+\infty} W_x(t,f)df\,dt = E_x. \tag{2.9}$$

- **"Flandrins Conjecture".** A conjecture of P. Flandrin [28] states that:

$$\int\int_C W_x(t,f)dtdf \leq \|x\|_2^2 \tag{2.10}$$

for all signals $x(t) \in L^2(\mathbb{R})$ and convex sets C. This inequality essentially mens that over a convex set $C \in \mathbb{R}^2$ the positive and negative values of $W_x(t,f)$ cancel each other to an extent that the integral over C does not exceed the integral over the whole plane.

2.3 Expected Ambiguity Function and Ambiguity Function

A fully dual concept to the WVS/WD is the expected ambiguity function(EAF)/ambiguity function(AF) of a process $X(t)$/a function $x(t)$, which we will denote by $\bar{A}_X(\tau,\nu)/A_x(\tau,\nu)$. We already mentioned that in contrast to the WVS/WD, the EAF/AF analyzes the "inner" or "correlative" structure of the process $X(t)$/function $x(t)$.

Again, we start with the stochastic setting and discuss the EAF. The EAF is based on correlations of the process $X(t)$ with time- and frequency shifted versions of itself:

$$\bar{A}_X(\tau,\nu) = \mathrm{E}\{\langle X\left(t+\frac{\tau}{2}\right), X\left(t-\frac{\tau}{2}\right)e^{j2\pi\nu t}\rangle\}. \tag{2.11}$$

According to this expression, the EAF compares in a stochastic way (via the expectation of the inner product) the process $X(t)$ itself, with a time- and frequency shifted version of itself. The formal definition of the EAF $\bar{A}_X(\tau,\nu)$ of a random process $X(t)$ is again based on the kernel $r_X(t_1,t_2)$ of the correlation operator:

$$\bar{A}_X(\tau,\nu) \triangleq \int_t r_X\left(t+\frac{\tau}{2}, t-\frac{\tau}{2}\right)e^{-j2\pi\nu t}dt. \tag{2.12}$$

[5] $\hat{x}(f)$ denotes the Fourier transform of the function $x(t)$.

We list some fundamental properties of the EAF:

- **Maximum at Origin.** The EAF satisfies the following inequality:

$$|\bar{A}_X(\tau,\nu)| \leq \bar{A}_X(0,0) = \bar{E}_X \tag{2.13}$$

  where $\bar{E}_X$ denotes the mean energy of $X(t)$.

- **Perfect Concentration Property of White Stationary Noise.** If $X(t)$ is a white stationary noise (with correlation function $r_X(t_1,t_2) = \eta\delta(t_1 - t_2)$ then its EAF $\bar{A}_X(\tau,\nu)$ is given by:

$$\bar{A}_X(\tau,\nu) = \eta\delta(\tau)\delta(\nu). \tag{2.14}$$

  Here, η is a scalar constant that has the interpretation of a power spectral density[6]. Because the mean energy is given by the EAF-value at the origin $\bar{E}_X = \bar{A}_X(0.0)$, we conclude that for a stationary white process $X(t)$, the mean energy is necessarily infinite. We note that within this work we formally only consider random processes with finite mean energy $\bar{E}_X < \infty$ and of course this excludes a white stationary process $X(t)$. However, this process can be viewed as the limit of sequence of finite energy processes with EAF supported within a rectangle of decreasing support. A physical realization of such a process would be to filter a white stationary noise with a linear system $\mathbf{H}$ that introduces only small delays and doppler shifts but has a finite operator norm[7]. It can be shown that the output of the filter is a finite energy process that has a small EAF-support.

- **Hermitian Symmetry.** The EAF satisfies:

$$\bar{A}_X(\tau,\nu) = \bar{A}_X^*(-\tau,-\nu) \tag{2.15}$$

- **Quadratic Form.** Similar as for the WVS also the EAF allows to express the quadratic form associated with $\mathbf{R}_X$:

$$\langle \mathbf{R}_X v, u\rangle = \mathrm{E}\{\langle X,u\rangle\langle X,v\rangle^*\} = \langle \bar{A}_X, A_{u,v}\rangle = \int_\tau \int_\nu \bar{A}_X(\tau,\nu) A_{u,v}^*(\tau,\nu) d\tau d\nu. \tag{2.16}$$

  Here, u and v are deterministic functions in $L^2(\mathbb{R})$ and $A_{u,v}(\tau,\nu)$ denotes the cross ambiguity function defined as:

$$A_{u,v}(\tau,\nu) \triangleq \int_t u\left(t+\frac{\tau}{2}\right) v^*\left(t-\frac{\tau}{2}\right) e^{-j2\pi\nu t} dt. \tag{2.17}$$

[6] In fact, because $r_X(t_1,t_2)$ only depends on the difference $t_1 - t_2$ we can compute the PSD as the Fourier transform of $r_X(\tau) = \eta\delta(\tau)$ which gives a constant spectrum with height η.

[7] Typically, a mobile radio channel fulfills these assumptions.

- **Innovation System.** The EAF of a process $X(t)$ that is obtained at the output of a linear system $\mathbf{H}$ which is excited with white stationary noise is given as:

$$\bar{A}_X(\tau,\nu) = S_{\mathbf{HH}^*}(\tau,\nu). \tag{2.18}$$

  Here, $S_{\mathbf{HH}^*}$ denotes the spreading function of the concatenation of $\mathbf{H}$ with its adjoint operator $\mathbf{H}^*$ (see [40] for a detailed discussion of the spreading function). This relationship implies that if the system $\mathbf{H}$ introduces only small delays and doppler shifts, then $X(t)$ has an EAF that is well concentrated around the origin in the (τ,ν)-plane. This fact can be used to generate underspread random processes ("innovation system representation").

As already mentioned the EAF has a tight relationship to the WVS. In fact, for a process $X(t)$, the 2D-functions $\bar{A}_X(\tau,\nu)$ and $\overline{W}_X(t,f)$ form a Fourier pair:

$$\bar{A}_X(\tau,\nu) = \int_t \int_f \overline{W}_X(t,f) e^{-j2\pi(\nu t - \tau f)} dt df. \tag{2.19}$$

The EAF will be the key tool for defining and analyzing a special class of non-stationary processes $X(t)$, namely the class of underspread processes. In the following chapter we will first give an informative definition of underspread processes using the EAF. Additionally we will use parameters that are calculated out of the EAF (weighted moments of the magnitude) to state precise quantitative results for underspread processes.

We now discuss the deterministic counterpart of the EAF, namely the AF. The AF $A_x(\tau,\nu)$ of a function $x(t)$ is defined via:

$$A_x(\tau,\nu) \triangleq \int_t x\left(t+\frac{\tau}{2}\right) x^*\left(t-\frac{\tau}{2}\right) e^{-j2\pi\nu t} dt. \tag{2.20}$$

We list the main properties/facts of/about the AF. Again, we omit discussions of properties if they are almost identical to the properties of the EAF with the same name:

- **Maximum at Origin.**

$$|\bar{A}_x(\tau,\nu)| \leq \bar{A}_x(0,0) = E_x \triangleq \|x\|_2^2 \tag{2.21}$$

- **Radar Uncertainty Principle.** The shape of the AF A_x of *any* function $x(t)$ is constrained by:

$$\int_\tau \int_\nu |A_x(\tau,\nu)|^2 d\tau d\nu = \left[A_x(0,0)\right]^2 = E_x^2. \tag{2.22}$$

  This inequality essentially states that the AF cannot be concentrated too much.

- **Hermitian Symmetry.** The AF satisfies:

$$A_x(\tau,\nu) = A_x^*(-\tau,-\nu) \tag{2.23}$$

- **Fourier Duality.** The AF $A_x(\tau,\nu)$ and the WD $W_x(t,f)$ of the *same* function $x(t)$ form a 2D-Fourier pair:

$$A_x(\tau,\nu) = \mathcal{F}_{t\to\nu}\mathcal{F}_{f\to-\tau}W_x(t,f) = \int_t\int_f W_x(t,f)e^{-j2\pi(\nu t-\tau f)}dtdf. \tag{2.24}$$

Note, that instead of the property "perfect concentration of white stationary noise" of the EAF, here we have the "uncertainty principle" for the AF which prohibits a perfect concentration of the AF. This is due to the fact that white stationary noise is a purely random construction that has no analogue in the deterministic setting. As a consequence of this discrepancy we also have a fundamental difference in the dual domain, represented by the WVS and the WD. The WVS can be arbitrarily smooth whereas the WD of a function is prohibited by the radar uncertainty principle to be approximately constant over an arbitrary large domain in the TF-plane because the spreads of the AF $A_x(\tau,\nu)$ and the WD $W_x(t,f)$ are related reciprocally.

2.4 Weyl Symbol and Spreading Function

The deterministic concepts of the Wigner distribution and the ambiguity function and theis stochastic counterparts Wigner-Ville spectrum and expected ambiguity function can be formally merged within a more general framework.

This framework is given by the concept of linear operators. We can represent a deterministic function $x(t)$ by the rank 1 operator $\mathbf{C}_x \triangleq x\otimes x$, whose kernel $h_{\mathbf{C}_x}$ is given as $h_{\mathbf{C}_x}(t,t') = x(t)x^*(t')$. On the other hand we can represent the second order statistic of a random process $X(t)$ by the correlation operator $\mathbf{R}_X$ whose kernel $h_{\mathbf{R}_X}$ is the autocorrelation function $r_X(t,t') \triangleq \mathrm{E}\{X(t)X^*(t')\}$ of the process.

Now we formally define the Weyl symbol $L_{\mathbf{C}}(t,f)$ and the spreading function $S_{\mathbf{C}}(\tau,\nu)$ of a linear operator $\mathbf{C}$ and show how it is related to the WD,WVS as well as the AF and EAF.

The Weyl symbol $L_{\mathbf{C}}(t,f)$ of a linear operator $\mathbf{C}$ with kernel $h_{\mathbf{C}}(t,t')$ is a 2D function of time t and frequency f which is given as:

$$L_{\mathbf{C}}(t,f) \triangleq \int_\tau h_{\mathbf{C}}\left(t+\frac{\tau}{2},t-\frac{\tau}{2}\right)e^{-j2\pi f\tau}d\tau. \tag{2.25}$$

As can be seen directly from this definition the WVS $\overline{W}_X(t,f)$ of a random process $X(t)$ is equal to the Weyl symbol $L_{\mathbf{R}_X}(t,f)$ of the correlation operator $\mathbf{R}_X$:

$$L_{\mathbf{R}_X}(t,f) = \overline{W}_X(t,f). \tag{2.26}$$

Furthermore, given a deterministic signal $x(t)$ the Weyl - symbol $L_{x\otimes x}(t,f)$ of the operator $x\otimes x$ is equal to the WD $W_x(t,f)$ of $x(t)$:

$$L_{x\otimes x}(t,f) = W_x(t,f) \tag{2.27}$$

Because of these relationships, most of the properties of the WD and the WVS induce corresponding properties of the Weyl symbol.

The spreading function $S_{\mathbf{C}}(\tau,\nu)$ of a linear operator $\mathbf{C}$ with kernel $h_{\mathbf{C}}(t,t')$ is a 2D function of delay τ and doppler frequency ν which is given as:

$$S_{\mathbf{C}}(\tau,\nu) \triangleq \int_t h_{\mathbf{C}}\left(t+\frac{\tau}{2}, t-\frac{\tau}{2}\right) e^{-j2\pi\nu t} dt. \tag{2.28}$$

As can be seen directly from this definition, the EAF $\bar{A}_X(\tau,\nu)$ of a random process $X(t)$ is equal to the spreading function $S_{\mathbf{R}_X}(\tau,\nu)$ of the correlation operator R_X:

$$S_{\mathbf{R}_X}(\tau,\nu) = \bar{A}_X(\tau,\nu). \tag{2.29}$$

Furthermore, given a deterministic signal $x(t)$, the spreading function $S_{x\otimes x}(\tau,\nu)$ of the operator $x \otimes x$ is equal to the AF $A_x(\tau,\nu)$ of $x(t)$:

$$S_{x\otimes x}(\tau,\nu) = A_x(\tau,\nu). \tag{2.30}$$

Because of these relationships, most of the properties of the AF and the EAF induce corresponding properties of the spreading function.

2.5 Weyl-Heisenberg sets and Gabor Frames

A Weyl-Heisenberg (WH) set is a set of functions $\{g_{k,l}(t)\}_k$, indexed by two integers k and l, that is generated by applying time- and frequency shifts to a single prototype function[8] denoted by $g(t) \in L^2(\mathbb{R})$ (in this thesis almost always a Gaussian function is used for the prototype of a WH set):

$$g_{k,l}(t) = g(t-kT)e^{j2\pi lFt} \qquad \begin{array}{l} T \text{ ... time step} \\ F \text{ ... frequency step} \\ g(t) \text{ ... window function} \end{array}$$

Formally we can identify a WH set by a triple $\mathcal{G}$, $\mathcal{G} = (g(t), T, F)$ consisting of the prototype function and the time- and frequency steps T, F. We will denote a WH set by the calligraphic symbol corresponding to the letter used for its prototype. Therefore we denote the WH set $(g(t), T, F)$ by $\mathcal{G}$.

Closely related to the concept of WH sets is the concept of Gabor frames. A Gabor frame is a special kind of frame. A frame, in turn, is the generalization of a basis for a Hilbert space. Loosely speaking a frame is a set of vectors, such that if we are given all the inner products of a

[8] Throughout this work we will always assume the window function $g(t)$ and the dual window function $\tilde{g}(t)$ of any WH set to be normalized, such that $\|g\|_2 = \|\tilde{g}\|_2 = 1$.

specific vector x_0 of $\mathcal{H}$ with the elements of this set, then we are able to recover x_0 from the inner products and moreover this recovery can be implemented in a stable way.

To make this ideas more precise we give the formal definition of a frame for a Hilbert space $\mathcal{H}$ (which in our work is almost always identical to $L^2(\mathbb{R})$):

Definition 2.5.1. *A frame for a Hilbert space $\mathcal{H}$ is a, general infinite, countable sequence of elements out of $\mathcal{H}$, denoted by $\mathcal{B}$:*

$$\mathcal{B} = \{g_k\}_k, \quad g_k \in \mathcal{H} \tag{2.31}$$

such that the following inequality holds for all $x \in \mathcal{H}$:

$$A\|x\|_2^2 \leq \sum_k |\langle x, g_k\rangle|^2 \leq B\|x\|_2^2. \tag{2.32}$$

Here, A and B are positive and real-valued constants and are called the "frame-bounds". If $A = B$ then the frame is called tight.

A Gabor frame is a special kind of frame. It is a frame that is also a WH set, i.e., the elements g_k of a Gabor Frame are related to each other via (discrete) time- and frequency shifts.

If we are given a WH set $\mathcal{G} = (g, T, F)$, what are conditions that the elements of $\mathcal{G}$, i.e, the time- and frequency shifted versions $g_{k,l}(t)$ of the prototype functions form a frame for $L^2(\mathbb{R})$? Surprisingly, these conditions are very intuitive and not too restrictive. If e.g. $g(t) \in L^2(\mathbb{R})$ is well localized in the TF-plane, i.e., the WD $W_g(t, f)$ of $g(t)$ has a small effective support and if the lattice constants T, F of the WH set $\mathcal{G}$ are not too large then $\mathcal{G}$ is a frame for $L^2(\mathbb{R})$. Of course, this definition is far from mathematical exactness. Without going into detail (that is beyond the scope of this work) we give the precise conditions only for the specific prototype function $g_{\text{Gaussian}}(t) = e^{-\frac{t^2}{2}}$ because this choice is almost always used within this thesis.

Theorem 2.5.1. *The WH set $\mathcal{G} = (g(t), T, F)$ with the Gaussian prototype:*

$$g(t) = e^{-\pi t^2/2} \tag{2.33}$$

is a frame for $L^2(\mathbb{R})$ iff the lattice constants T, F of $\mathcal{G}$ satisfy

$$TF < 1. \tag{2.34}$$

For a proof and a more detailed discussion of this theorem we refer to[9] [10, 35].

We would like to note that it is easy to verify that if a certain prototype function $g(t)$ and lattice constants T,F are shown to yield a WH set $\mathcal{G} = (g(t), T, F)$ that is a frame for $L^2(\mathbb{R})$ with bounds A and B then a prototype $g'(t)$ that is obtained from $g(t)$ via scaling, i.e.,

$$g'(t) = \frac{1}{|a|} g(at) \quad a \in \mathbb{R} \tag{2.35}$$

[9] A very short and elegant proof for the necessity of the condition (2.34) can be found in [29].

together with the new lattice constants $T' = \frac{T}{a}$ and $F' = Fa$ yield a WH set $\mathcal{G}' = (g'(t), T', F')$ that also is a frame for $L^2(\mathbb{R})$ with the same frame bounds A and B.

The concept of WH sets and Gabor frames can be adapted to the discrete time setting very easily by sampling the individual continuous-time functions.

2.6 The Physical Spectrum – Gabor Analysis meets TF-Spectrum

We already introduced the WVS as representative for TF spectra of nonstationary random processes. Of course there are a lot more definitions for TF spectra. For our purposes one additional definition of a TF spectrum is interesting. The so called "Physical Spectrum" of a nonstationary random process $X(t)$, denoted by $\mathrm{PS}_X^{(g)}(t,f)$, is in some sense the bridge between the concepts of TF spectra and Gabor frames/analysis. As the notation already indicated the physical spectrum is parameterized by a function $g(t)$. The exact definition of the physical spectrum $\mathrm{PS}_X^{(g)}(t,f)$ is as follows:

$$\mathrm{PS}_X^{(g)}(t,f) \triangleq \mathrm{E}\left\{\left|\int_{t'} X(t')g^*(t'-t)e^{-j2\pi ft'}dt'\right|^2\right\} = \mathrm{E}\left\{\left|\langle X(t'), g(t-t')e^{j2\pi ft'}\rangle\right|^2\right\}. \qquad (2.36)$$

From the last expression we conclude that the physical spectrum $\mathrm{PS}_X^{(g)}(t,f)$ is nothing else than the mean power of the Gabor coefficient of $x(t)$ at point (t,f) in the TF plane using $g(t)$ as the prototype for the analyzing WH set. It can be shown straightforwardly [40] that the physical spectrum $\mathrm{PS}_X^{(g)}(t,f)$ can be written as a convolution of the WVS $\overline{W}_X(t,f)$ of the same process with the mirrored WD $W_g(-t,-f)$ of the function $g(t)$:

$$\mathrm{PS}_X^{(g)}(t,f) = \int_{t'}\int_{f'} \overline{W}_X(t',f')W_g(t'-t,f'-f)dt'df'. \qquad (2.37)$$

2.7 Local Cosine Bases

The expansion in terms of a Gabor frame has two drawbacks. Firstly, the atoms of the expansion (the time-frequency shifted prototype) are in general not orthogonal which makes the inverse transformation difficult. Secondly it can be shown that the expansion of a process in terms of a Gabor frame with a Gaussian prototype (which presupposes $TF < 1$) is not well suited for compressed sensing because loosely speaking the expansion atoms are too "similar" (the similarity is measured via the inner products between the atoms). The only, but very important reason why we use the concept of Gabor expansions and Gabor frames at all within this thesis is the fact that underspread process can be effectively decorrelated by means of Gabor expansions while at the same time allowing efficient hardware implementations of the Gabor analysis through a sampled filterbank.

A way to mitigate the two problems of Gabor frames is to use an expansion of the signal/process of interest into an orthonormal basis (ONB) for $L^2(\mathbb{R})$, whose elements have still some degree of TF-concentration. One specific example for such an ONB is the so called local cosine basis (LCB) [35].

Local cosine bases are constructed according to the following steps:

- First, the real line $\mathbb{R}$ (which represents the time axis in our context) is separated into consecutive, non overlapping intervals:

$$\mathbb{R} = \bigcup [a_p, a_{p+1}]. \tag{2.38}$$

  The length $a_{p+1} - a_p$ of the interval $[a_p, a_{p+1}]$ will be denoted by l_p.

- To each interval $[a_p, a_{p+1}]$, we associate a window function $g_p(t)$ with support $[a_p - \eta_p, a_{p+1} + \eta_{p+1}]$. The extension lengths η_p should be such that $l_p \geq \eta_p + \eta_{p+1}$ holds, i.e., the support of $g_p(t)$ overlaps only with the support of the neighboring windows $g_{p-1}(t)$ and $g_{p+1}(t)$. The windows $g_p(t)$ have to be designed such that the following symmetry holds:

$$g_p(t) = g_{p-1}(2a_p - t) \tag{2.39}$$

  and finally the windows have to cover the time axis uniformly, i.e.:

$$\forall t, \quad \sum_{p=-\infty}^{+\infty} |g_p(t)|^2 = 1 \tag{2.40}$$

  .

Then it can be shown [35, 36] that the set of functions:

$$\left\{ \phi_{p,k}(t) = g_p(t) \sqrt{\frac{2}{l_p}} \cos \left[\frac{\pi(k + \frac{1}{2})}{l_p} (t - a_p) \right] \right\} \tag{2.41}$$

is an orthonormal basis of $L^2(\mathbb{R})$.

Another advantage of local cosine bases is their representability by binary trees. In fact, for suitable chosen interval lengths, a local cosine basis can be represented by a binary tree, where each node of the tree corresponds to a certain time interval and the two descendants of each node correspond to a splitting of this specific time interval into two intervals of half the length of the original interval. The tree-like representation is used for fast implementations of adaptive CS schemes, discussed in Chapter 4.

Chapter 3

Underspread Processes

3.1 Introduction

From a theoretical point of view, stationary random processes are clearly the "nice" random processes. Stationary random processes allow a very elegant and intuitive description of the second order statistic in a "frequency"-domain by the so called power spectral density (PSD). With the help of the PSD a lot of problems in estimation theory are radically simplified. A very prominent example is the Wiener Filter, where the usage of the PSD leads to simple point wise addition and divisions instead of operator inversions.

Unfortunately, for general non-stationary random processes we don't have any tool of comparable simplicity and usefulness as the PSD for the stationary case. However, if we place certain constraints on the process, more precisely on the EAF of the process, then we are able to define a time-varying spectrum that is very similar in usage and properties to the PSD.

In this chapter we will first give a precise definition of these constraints, that define the class of underspread processes. Then we will present some properties of underspread processes that are necessary for our thesis.

The two most important properties of underspread process that are relevant for us are:

- First, the second order statistic or the WVS of an underspread process can be conveniently estimated by using a filter bank as a front-end, i.e., the estimator only uses coefficients computed with a suitable analyzing WH-set (not necessarily a Gabor frame).
- Second, for the class of underspread operators there inherently exist good estimators for the WVS that additionally allow a simple theoretical analysis. This is due to the fact that the WVS $\overline{W}_X(t,f)$ of an underspread process $X(t)$ is a smooth function over the TF-plane.

After the introductional sections for underspread processes, we present a simple heuristic design

for a WVS estimator using a sampled filter bank as a frontend. The concept underlying the design of this estimator is strongly inspired by [41].

3.2 Definition of Underspread Processes

Underspread processes are non-stationary random processes whose components, separated by τ in time and ν in frequency direction can be considered effectively uncorrelated unless τ and ν are very mall. The meaning of this statement is illustrated in Figure 3.1, where for an underspread process $X(t)$, the components $S_1(t)$ and $S_2(t)$ are effectively uncorrelated. In order to get

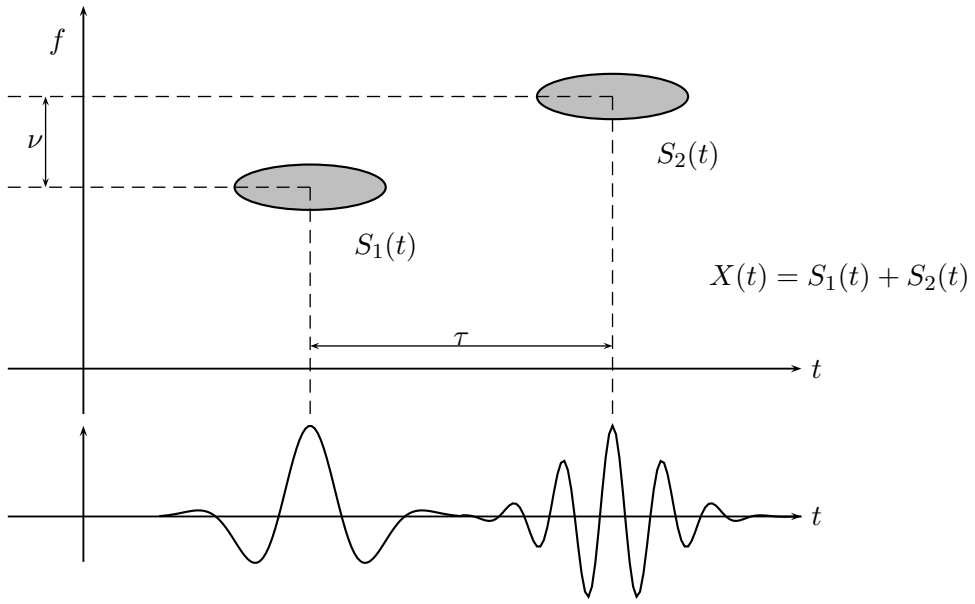

Figure 3.1: An underspread process has a limited time-frequency correlation horizon

quantitative results for underspread processes we also have to introduce a quantitative measure of "underspreadness" of a process $X(t)$. A convenient way to introduce such a measure is to consider the expected ambiguity function $\bar{A}_X(\tau,\nu)$ of the process $X(t)$. The value $\bar{A}_X(\tau,\nu)$ corresponds to the correlation of the components of $X(t)$ which are separated by τ in time and ν in frequency direction. Obviously the underspreadness of $X(t)$ can be measured by the spread of $|\bar{A}_X|$. The spread of $|\bar{A}_X(\tau,\nu)|$, in turn, can be measured by weighted integrals of $|\bar{A}_X(\tau,\nu)|$:

$$m_{\boldsymbol{X}}^{(\phi)} \triangleq \frac{\int_\tau \int_\nu \phi(\tau,\nu)|\bar{A}_X(\tau,\nu)|d\tau d\nu}{\int_\tau \int_\nu |\bar{A}_X(\tau,\nu)|d\tau d\nu} \tag{3.1}$$

$$M_{\boldsymbol{X}}^{(\phi)} \triangleq \left[\frac{\int_\tau \int_\nu \phi(\tau,\nu)^2|\bar{A}_X(\tau,\nu)|^2 d\tau d\nu}{\int_\tau \int_\nu |\bar{A}_X(\tau,\nu)|^2 d\tau d\nu}\right]^{1/2} \tag{3.2}$$

The quantities $m_{\boldsymbol{X}}$ are parameterized by the real-valued and non-negative function $\phi(\tau,\nu)$ which has the task to penalize components of $|\bar{A}_X(\tau,\nu)|$ that are located far away from the origin in the (τ,ν)-plane. Therefore, it is common to require that $\phi(\tau,\nu) \geq \phi(0,0) = 0$. The two definitions are closely related, in fact they only differ in the underlying measure (norm). Whereas $m_X^{(\phi)}$ corresponds to the $\|\cdot\|_1$-norm, the quantity $M_X^{(\phi)}$ corresponds to the $\|\cdot\|_2$-norm. An important choice for $\phi(\tau,\nu)$ are the members of the family of functions that is given by the following generic expression:

$$\phi(\tau,\nu) = |\tau|^k|\nu|^l, k,l \in \mathbb{N}. \tag{3.3}$$

For this specific weighting functions, the resulting integrals $m_{\boldsymbol{X}}^{(\phi)}$ and $M_{\boldsymbol{X}}^{(\phi)}$ are called "moments" and are denoted by $m_{\boldsymbol{X}}^{(k,l)}$ and $M_{\boldsymbol{X}}^{(k,l)}$.

We are now in the position to define the class of underspread random processes:

Underspread processes are those non-stationary random processes for which $m_X^{(\phi)}$ and $M_X^{(\phi)}$ are sufficiently small (e.g. $\ll 1$).

For mathematical results that rely on underspreadness, the quantities $m_{\boldsymbol{X}}^{(\phi)}$ and $M_{\boldsymbol{X}}^{(\phi)}$ are the only relevant properties of the process $X(t)$. A special class of underspread processes is given by those processes with an EAF that is exactly supported within a small rectangle in the (τ,ν)-plane. For this processes the following approximate properties are fulfilled exactly (e.g. the sampling of the spectrum is lossless). However this special case is of limited relevance for practical applications, as pointed out in [40].

3.3 Sampling the Spectrum

The definition of underspread processes implies that the EAF $\bar{A}_X(\tau,\nu)$ of an underspread process $X(t)$ is well concentrated on a small area around the origin in the (τ,ν)-plane. Now, because the WVS $\overline{W}_X(t,f)$ of $X(t)$ is the 2D-Fourier transform of the EAF $\bar{A}_X(\tau,\nu)$, this implies that for underspread processes it should be possible to sample the WVS $\overline{W}_X(t,f)$ on a rectangular lattice $\{(kT,lF)|k,l \in \mathbb{Z}\}$ in the TF-plane without loosing much information about $\overline{W}_X(t,f)$. More precisely, if we perform a reconstruction with a reconstruction kernel $\psi(t,f)$:

$$\widehat{W}_X(t,f) = \sum_{k,l} \overline{W}_X(kT,lF)\psi(t-kT,f-lF) \tag{3.4}$$

to obtain a reconstructed version $\widehat{W}_X(t,f)$ of the original WVS $\overline{W}_X(t,f)$ then the deviation of $\widehat{W}_X(t,f)$ from $\overline{W}_X(t,f)$ should be small. If the EAF $\bar{A}_X(\tau,\nu)$ of $X(t)$ is exactly supported within a rectangle, then the sample values are an exact representation of the WVS $\overline{W}_X(t,f)$. However for a general underspread process $X(t)$, an exact reconstruction of $\overline{W}_X(t,f)$ from its sample values $\overline{W}_X(kT,lF)$ will be impossible. In that case we can only compute an approximate

reconstruction $\widehat{W}_X(t,f)$ that should be close to $\overline{W}_X(t,f)$. It is convenient to use a reconstruction scheme, that preserves the sample values, i.e., $\widehat{W}_X(kT,lF) = \overline{W}_X(kT,lF)$. A specific method to achieve this goal is to use the reconstruction kernel $\psi(t,f) = \frac{1}{TF}\mathrm{sinc}\big(\frac{\pi t}{T}\big)\mathrm{sinc}\big(\frac{\pi f}{F}\big)$. For this specific reconstruction scheme, the following error bound holds [40]:

Theorem 3.3.1. *For any random process $X(t)$ and any sampling period T and F, the difference*

$$\Delta_{\mathrm{Sampling}}(t,f) \triangleq \widehat{W}_X(t,f) - \overline{W}_X(t,f) \tag{3.5}$$

is bounded as

$$\frac{|\Delta_{\mathrm{Sampling}}(t,f)|}{\|\bar{A}_X\|_1} \leq 4\left(m_{\boldsymbol{X}}^{(1,0)}F + m_{\boldsymbol{X}}^{(0,1)}T\right), \qquad \frac{\|\Delta_{\mathrm{Sampling}}(t,f)\|_2}{\|\boldsymbol{R}_X\|_2} \leq 4\left(M_{\boldsymbol{X}}^{(1,0)}F + M_{\boldsymbol{X}}^{(0,1)}T\right). \tag{3.6}$$

If one gives up the preservation of the sample values, it is possible to perform an optimization in the sense of minimum deviation between $\hat{W}_X(t,f)$ and $\overline{W}_X(t,f)$ (considered as 2D-real valued functions of t and f). The fundamental observation for this approach is that the reconstruction error is caused by aliasing of the EAF $\bar{A}_X(t,f)$ because sampling the WVS corresponds to a periodization of the EAF (completely analogous to the conventional 1D - case). In order to avoid this aliasing we could first filter the WVS $\overline{W}_X(t,f)$ to obtain $\widetilde{W}_X(t,f)$ such that the 2D-Fourier transform (which is a "pseudo" EAF, because $\widetilde{W}_X(t,f)$ is not necessarily the WVS of any random process) is exactly contained within the rectangle $\mathcal{G} = [-\frac{1}{2F},\frac{1}{2F}] \times [-\frac{1}{2T},\frac{1}{2T}]$ in the (τ,ν)-plane. Moreover, within this rectangle the values of the Fourier transform of $\widetilde{W}_X(t,f)$ should be equal to the EAF $\bar{A}_X(\tau,\nu)$ of the process $X(t)$. It can be shown that this is accomplished by smoothing the WVS $\overline{W}_X(t,f)$ with the kernel $\psi(t,f) = \frac{1}{TF}\mathrm{sinc}(\frac{\pi t}{T})\mathrm{sinc}(\frac{\pi f}{F})$. Afterwards we sample the function $\widetilde{W}_X(t,f)$. Again we note that $\widetilde{W}_X(t,f)$ is also only a "pseudo"-WVS, because it is not necessarily the WVS of any random process. But we are not interested in that, we only want to get a discrete sequence of number (called sample values) that allow us to reconstruct the WVS $\overline{W}_X(t,f)$ of $X(t)$ with small error. In this scheme, we take this discrete sequence of sample values not directly out of $\overline{W}_X(t,f)$ but rather out of the smoothed 2D-function $\widetilde{W}_X(t,f)$. For this scheme, the reconstruction error (when using the same reconstruction kernel as above for the sampling sequence $\widetilde{W}_X(kT,lF)$) can be bounded as follows [40]:

Theorem 3.3.2. *For any random process $X(t)$ and any sampling period T and F, the difference*

$$\Delta'_{\mathrm{Sampling}}(t,f) \triangleq \widetilde{W}_X(t,f) - \overline{W}_X(t,f) \tag{3.7}$$

is bounded as

$$\frac{|\Delta'_{\mathrm{Sampling}}(t,f)|}{\|\bar{A}_X\|_1} \leq 2\left(m_{\boldsymbol{X}}^{(1,0)}F + m_{\boldsymbol{X}}^{(0,1)}T\right), \qquad \frac{\|\Delta'_{\mathrm{Sampling}}(t,f)\|_2}{\|R_X\|_2} \leq 2\left(M_{\boldsymbol{X}}^{(1,0)}F + M_{\boldsymbol{X}}^{(0,1)}T\right). \tag{3.8}$$

We see that the bounds are lower (tighter) than in (3.6), therefore the latter sampling method tends to be superior in terms of the error magnitude to the previous one. However, the drawback of the second method is that before sampling a smoothing has to be applied on the WVS $\overline{W}_X(t,f)$ (not on the signal itself) and this task is computational expensive in general.

3.4 Approximate Diagonalization

A process $X(t)$ is called decorrelated, if we have found a representation of $X(t)$ by a set of uncorrelated random variables (RVs), denoted by A_k, that are *linearly* obtained from $X(t)$. The A_k are a complete representation of $X(t)$, i.e., we can perfectly reobtain $X(t)$ from the A_k.

On the other hand, if we have an orthonormal basis $\{u_k\}_k$ for our signal space $L^2(\mathbb{R})$ then a complete representation of $X(t)$ would be the following sequence of inner products:

$$B_k = \langle X, u_k \rangle. \tag{3.9}$$

The process $X(t)$ is reobtained as follows:

$$X_k(t) = \sum_k B_k u_k(t). \tag{3.10}$$

This rather simple relationships are due to the (deterministic) orthonormality of the set $\{u_k\}_k$. However, the computation of the B_k is not necessarily a decorrelation of $X(t)$ because the RVs B_k may be correlated.

Fortunately, it can be shown that for every random process $X(t)$ (with the mild restriction that every realization $x(t)$ is in $L^2(\mathbb{R})$) we can find a specific orthonormal basis $\{u_k\}_k$ for which the B_k obtained by (3.9) are perfectly uncorrelated:

$$\mathrm{E}\{B_k B_l^*\} = \langle \mathbf{R}_X u_l, u_k \rangle = P_{B_k} \delta_{k-l}. \tag{3.11}$$

Here, the first equality is a direct consequence of the definition of the correlation operator $\mathbf{R}_X$ (in fact the equality: $\mathrm{E}\{\langle X, u_k \rangle \langle X, u_l \rangle^*\} = \langle \mathbf{R}_X u_l, u_k \rangle$ may be used as a definition for a correlation operator $\mathbf{R}_X$). More specifically the $\{u_k\}_k$ are the eigenfunctions of the correlation operator $\mathbf{R}_X$ and the mean powers P_{B_k} equal the real-valued and non negative eigenvalues[1] λ_k of $\mathbf{R}_X$

$$P_{B_k} = \lambda_k. \tag{3.12}$$

Beside the decorrelation, the set of eigenvectors $\{u_k\}$ fulfills the following orthogonality relation:

$$\langle \mathbf{R}_X u_k, u_l \rangle = \lambda_k \delta_{k-l} \tag{3.13}$$

[1] Because $\mathbf{R}_X$ is a positive semi-definite self-adjoint linear operator and we assume that it has finite HS-norm, it follows that $\mathbf{R}_X$ has a set of eigenvectors that form an orthonormal basis of $L^2(\mathbb{R})$ and a corresponding sequence of real-valued (and moreover non-negative) eigenvalues.

where the λ_k are the real-valued eigenvalues of $\mathbf{R}_X$ that corresponds to the eigenfunction u_k. For a given operator $\mathbf{R}_X$ any set of vectors $\{u_k\}_k$ which fulfill these equations is called a diagonalizing set of vectors. The $\{u_k\}_k$ diagonalize the operator $\mathbf{R}_X$. On the other hand we have shown that the $\{u_k\}_k$ also yield a decorrelation of the process $X(t)$. Therefore the term "decorrelation" of a process $X(t)$ can be used as a pseudonym for a "diagonalization" of the correlation operator $\mathbf{R}_X$.

The decorrelation of a random process $X(t)$ using the eigenvalues and eigenfunctions (eigenvectors) of the correlation operator $\mathbf{R}_X$ is not necessarily the only possible decorrelation, i.e., there may exist other uncorrelated sequences B_k that are a complete representation of $X(t)$ but are not obtained via the eigenfunctions of $\mathbf{R}_X$. However, this specific choice for the decorrelation has an outstanding position because of the "double" orthogonality (deterministic orthogonality of the expansion vectors/functions and stochastic orthogonality of the expansion coefficients) and is sometimes termed the "$Karhunen-Loeve$" - transformation (KLT). Another name of this scheme is "Hotelling" transformation. All these names correspond effectively to an eigenvalue/eigenvector decomposition of $\mathbf{R}_X$. In the case of stationary processes, these eigenvectors are known in advance, namely they are given by the complex sinusoids $u_f(t) = e^{j2\pi ft}$ where this set is now continuously parameterized by $f \in \mathbb{R}$. Unfortunately for non-stationary processes the eigenvectors of the correlation operator are in general not structured with respect to time and frequency. One of the big desirable properties of an underspread process $X(t)$ now is that it allows an approximate decorrelation, or an approximate diagonalization of the correlation operator $\mathbf{R}_X$, with a set of vectors that are strongly structured with respect to the TF-plane. More specifically, underspread processes are effectively decorrelated by so called Weyl-Heisenberg (WH) sets.

A WH set is a set of functions[2] $\{g_{k,l}\}_{k,l}$that is obtained by time- and frequency shifting a prototype function $g(t)$

$$g_{k,l}(t) = g(t - kT)e^{j2\pi lFt}. \tag{3.14}$$

Because of this structure signal processing schemes relying on Weyl Heisenberg sets allow in general the usage of computational efficient "FFT-like" implementations in real digital signal processing hardware [39].

A WH-set can be identified by the triple $\mathcal{G} = (g(t), T, F)$, consisting of the prototype function $g(t)$ (e.g. a Gaussian function), the time step T and the frequency step F. We will show below that the sequence $C_{k,l}$ obtained by:

$$C_{k,l} = \langle X, g_{k,l} \rangle \tag{3.15}$$

is approximately uncorrelated if the process $X(t)$ is underspread. Assuming only that the realizations of $X(t)$ are in $L^2(\mathbb{R})$, for a decorrelation of $X(t)$ the $C_{k,l}$ have also to be a complete

[2]Note that we are now using two indices k, l instead of one single index k as above, but this difference is only for notational purposes. In the end we are interested in a sequence of decorrelating/diagonalizing vectors (e.g. denoted by $\{u_k\}$ or $\{g_{k,l}\}$) and not in how we index or label them.

representation of $X(t)$, i.e., $X(t)$ must be reobtainable from the sequence $C_{k,l}$. This is the case in particular if the WH-set $\mathcal{G}$ is a frame for $L^2(\mathbb{R})$ (cf. Chapter 2). As already mentioned in Chapter 2, if $g(t)$ is a Gaussian (this will be the main choice for $g(t)$ within this thesis) than $\mathcal{G}$ is a frame for $L^2(\mathbb{R})$ if $TF < 1$ [35] (although for $TF = 1$ the WH-set still yields a complete representation of $X(t)$, it can be shown that this representation is not invertible in a stable way).

To summarize, an underspread process $X(t)$ is completely represented by the sequence of RVs B_k given by (3.15). Moreover, these RVs are effectively uncorrelated [40]:

$$\mathrm{E}\{C_{k,l}C^*_{k',l'}\} = \langle \mathbf{R}_X g_{k,l}, g_{k',l'}\rangle \approx P_{C_{k,l}}\delta_{k'-k}\delta_{l'-l}. \tag{3.16}$$

Here, $P_{C_{k,l}}$ denotes the stochastic/mean power of $C_{k,l}$:

$$P_{C_{k,l}} \triangleq \mathrm{E}\{|C_{k,l}|^2\}. \tag{3.17}$$

The exact values of the correlations between the coefficients $B_{k,l}$ can be expressed according to Section 2.3 as

$$\mathrm{E}\{C_{k,l}C^*_{k',l'}\} = \langle \mathbf{R}_X g_{k',l'}, g_{k,l}\rangle = \langle \bar{A}_X, A_{g_{k,l},g_{k',l'}}\rangle \tag{3.18}$$

where the cross AF $A_{g_{k,l},g_{k',l'}}$ of $g_{k,l}(t)$ and $g_{k',l'}(t)$ can be shown to be given as

$$A_{g_{k,l},g_{k',l'}} = e^{j2\pi\tau\frac{l+l'}{2}F}e^{-j2\pi\frac{k+k'}{2}T\nu}e^{-j2\pi\frac{k+k'}{2}F(l'-l)}A_g(\tau-(k-k')T,\nu-(l-l')F). \tag{3.19}$$

Here, $A_g(\tau,\nu)$ denotes auto-ambiguity function of the prototype $g(t)$ used for the analyzing WH-set.

Using (3.18) and (3.19) one can derive a quantitative result that shows how the "uncorrelatness" of the $C_{k,l}$ is related to the EAF $\bar{A}_X(\tau,\nu)$ and how the powers $P_{C_{k,l}}$ are related to the values of the WVS $\overline{W}_X(t,f)$ of $X(t)$.

Theorem 3.4.1. (Matz [40]) *For any random process X(t) and any Weyl-Heisenberg set $\{g_{k,l}(t)\}$, the difference*

$$\Delta_g[k,l;k',l'] \triangleq \langle R_X g_{k,l}, g_{k',l'}\rangle - \overline{W}_X(kT,lF)\delta_{kk'}\delta_{ll'} \tag{3.20}$$

is bounded as

$$\frac{|\Delta_g[k,l;k',l']|}{\|\bar{A}_X\|_1} \le m_X^{\phi^{(k-k',l-l')}} \tag{3.21}$$

with $\phi^{(k,l)}(\tau,\nu) = |\delta_{k0}\delta_{l0} - A_g(\tau+kT,\nu+lF)|$.

Here, $A_g(\tau,\nu)$ denotes the auto-ambiguity function of the prototype function $g(t)$ as defined in Chapter 2 and $\overline{W}_X(t,f)$ denotes the WVS of $X(t)$. One important detail of this theorem is, that the ℓ_1-norm $\|\bar{A}_X\|_1 \triangleq \int_\tau\int_\nu |\bar{A}_X(\tau,\nu)|d\tau d\nu$ of $\bar{A}_X$ is used and this quantity is not directly related

to the mean energy $\bar{E}_X$ of the process, which is given by the value of the EAF at the origin in the (τ,ν)-plane: $\bar{E}_X = \bar{A}_X(0,0)$.

We want to begin the discussion of the Theorem 3.4.1 by graphically illustrating the two cases: $(k,l) \neq (k',l')$ and $(k,l) = (k',l')$.

In the case $(k,l) = (k',l')$, Theorem 3.4.1 states that if the process $X(t)$ is sufficiently underspread, the powers of the coefficients $B_{k,l}$ are close to the sampling values of the WVS $\overline{W}_X(t,f)$ at the points (kT, lF) in the TF-plane that correspond to the WH-set member $g_{k,l}(t)$ that is associated with $B_{k,l}$. For the discussion we assume that the prototype $g(t)$ is a Gaussian: $g(t) = c \cdot e^{-\pi \cdot \frac{t^2}{2T_0^2}}$ with the characteristic time T_0 (sometimes the parameter T_0^2 is called "variance") and a normalization constant c. It can be shown that in that case also the ambiguity function $A_g(\tau,\nu)$ is also a (2D-) Gaussian:

$$A_g(\tau,\nu) = c^2 \int_t g\left(t+\frac{\tau}{2}\right) g^*\left(t-\frac{\tau}{2}\right) e^{-j2\pi\nu t} dt \tag{3.22}$$

$$= c^2 \int_t e^{-\pi \frac{(t+\frac{\tau}{2})^2}{2T_0^2}} e^{-\pi \frac{(t-\frac{\tau}{2})^2}{2T_0^2}} e^{-j2\pi\nu t} dt \tag{3.23}$$

$$= c^2 \int_t e^{-\pi \frac{t^2+\frac{\tau^2}{4}}{T_0^2}} e^{-j2\pi\nu t} dt \tag{3.24}$$

$$= c^2 e^{-\pi \frac{\tau^2}{4T_0^2}} \mathcal{F}_{t\to\nu}\left\{ e^{-\pi \frac{t^2}{T_0^2}} \right\} \tag{3.25}$$

$$= c^2 T_0 e^{-\pi \frac{\tau^2}{4T_0^2}} e^{-\pi \frac{\nu^2}{1/T_0^2}}. \tag{3.26}$$

We see from the last expression that the more the prototype $g(t)$ is concentrated (i.e., T_0 is very small), the more the ambiguity function $A_g(\tau,\nu)$ is concentrated in τ-direction but conversely the less concentrated it is along the ν-direction. However the joint spread in the (τ,ν)-plane, which may be quantified by weighted integrals as they are used for the classification of underspread processes, is invariant of the parameter T_0.

For this specific choice for $g(t)$, we plotted the bound in Theorem 3.4.1 for the case $(k,l) = (k',l')$: $(|1 - A_g(\tau,\nu)|)$ along the τ-axis for $\nu = 0$ in Figure 3.2.

We conclude from Figure 3.2 that the value of the upper bound $m_X^{\phi^{(k-k',l-l')}}$ in Theorem 3.4.1 is small if the area of the effective overlapping region (i.e., the region where the respective functions have large values in magnitude) of $\bar{A}_X(\tau,\nu)$ and $|1 - A_g(\tau,\nu)|$ is small. This is the case if e.g. $\bar{A}_X(\tau,\nu)$ is strongly concentrated around the origin in the (τ,ν)-plane and $A_g(\tau,\nu)$ is sufficiently flat around the origin in the (τ,ν)-plane (the constant c in (3.22) is chosen such that $A_g(0,0) = 1$). However the effective area of "flatness" around the origin of the ambiguity function $A_g(\tau,\nu)$ is limited for any deterministic function $g(t)$ by the uncertainty principle of the Wigner distribution $W_g(t,f)$ in the dual domain (TF-plane).

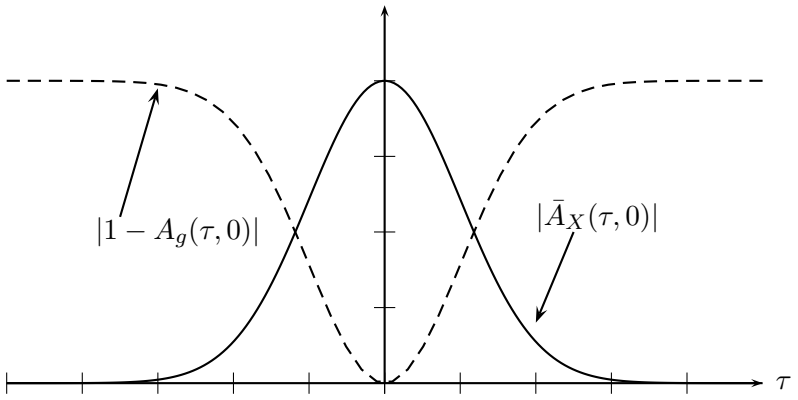

Figure 3.2: Illustration for the bound in Theorem 3.4.1.

For the second case $k \neq k'$ or $l \neq l'$, the weighting function ϕ in the bound in Theorem 3.4.1 is equal to $|A_g(\tau + (k-k')T, \nu + (l-l')F)|$. We illustrated corresponding functions in the (τ, ν)-plane in Figure 3.3. From this Figure it is clear that a small correlation between $B_{k,l}$ and $B_{k,l}$ is only possible if the shifted AF $A_g(\tau - (k'-k)T, \nu - (l'-l)F)$ of $g(t)$ is very small within the effective support of $\bar{A}_X(\tau, \nu)$. In particular it requires that $A_g(\tau, \nu)$ decays fast within the effective support of $\bar{A}_X(\tau, \nu)$ and that the lattice constants T and F are not too small. The stronger it is concentrated the closer are the $B_{k,l}$ to being uncorrelated. In this scenario the precise shape of $A_g(\tau, \nu)$, i.e., the properties of the prototype pulse $g(t)$ are rather irrespective. Conversely, if the effective support of $A_X(\tau, \nu)$ is not extremely small, then of course also the concentration of $A_g(\tau, \nu)$ has to be considered in more detail. We note that for the concentration of $A_g(\tau, \nu)$ there is a fundamental limit given by the uncertainty principle of the deterministic ambiguity function $A_g(\tau, \nu)$ as presented in Chapter 2.

If $X(t)$ is normalized such that $\|\bar{A}_X\|_1$ is equal to e.g. 1 ($\|\bar{A}_X\|_1$=1) and we use for the analyzing WH-set $\mathcal{G} = (g, T, F)$ a Gabor frame with a Gaussian prototype $g(t) = e^{-\pi t^2/T_0^2}$ (the time constant T_0 is a free design parameter that allows to adapt $g(t)$ to the EAF $\bar{A}_X(\tau, \nu)$), which implies $TF < 1$, then in the case $(k, l) \neq (k', l')$ the bound on $\Delta_g[k, l; k', l']$ cannot be arbitrarily small because the AF $A_g(\tau, \nu)$ of the Gaussian prototype $g(t)$ cannot decay arbitrarily fast within a rectangle of area ≈ 1 (corresponding to the elementary cell of the WH-set lattice (kT, lF)). Indeed, the Gaussian prototype is (in some sense) the optimum choice for $g(t)$ and even this prototype always yields a finite, non-zero, value of the AF $A_g(\tau, \nu)$ within a rectangle of area ≈ 1 centered around the origin of the (τ, ν)-plane[3].

[3]Because for a Dirac type EAF the upper bounds on the cross correlations between different Gabor coefficients

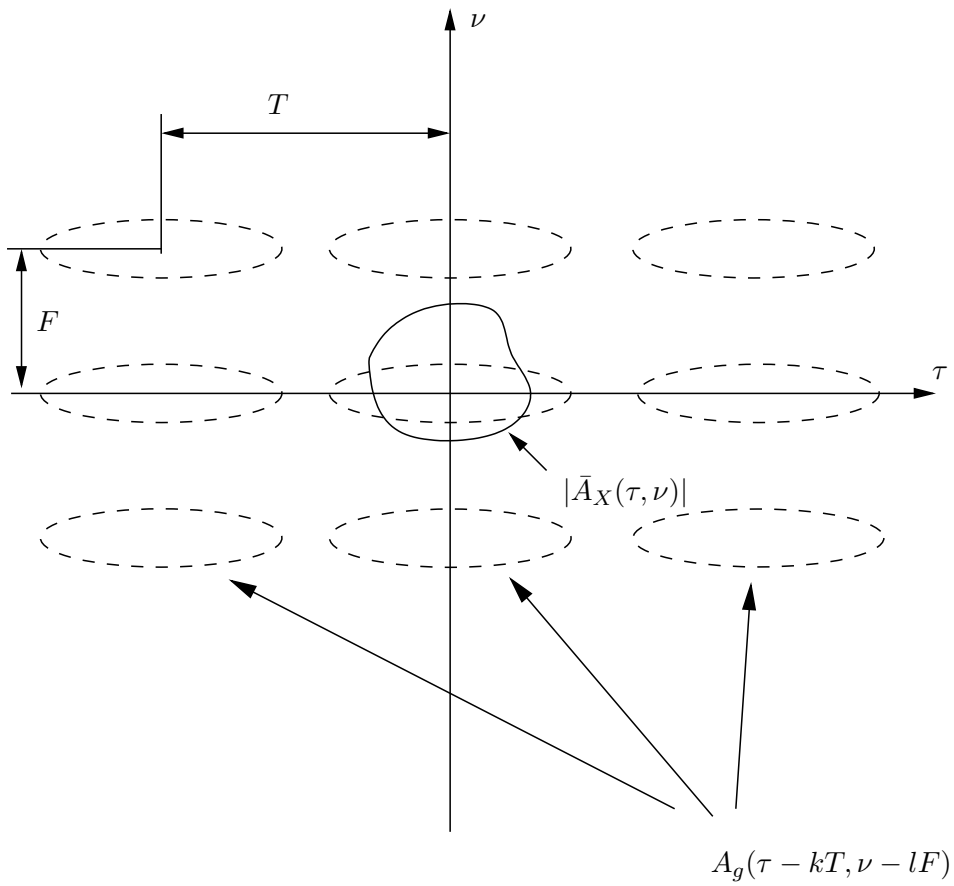

Figure 3.3: Illustration of the bound in Theorem 3.4.1 in the (τ, ν)-plane.

However, because we have normalized $X(t)$ such that $\|\bar{A}_X\|_1 = 1$ we have that for a small support of $\bar{A}_X$, the value of $\bar{A}_X(\tau,\nu)$ at the origin $\bar{A}_X(0,0)$ is very large (inversely proportional to the effective support of $\bar{A}_X(\tau,\nu)$) and this implies that the mean energy $\bar{E}_X$ of the process $X(t)$ is large. In contrast to the mean energy, the powers $P_{B_{k,l}}$ do generally *not* scale inversely with the effective support of the EAF $\bar{A}_X(\tau,\nu)$ because the effective support of the WVS $\overline{W}_X(t,f)$ scales inversely proportional with the effective support of the EAF due to the Fourier correspondence between $\overline{W}_X(t,f)$ and $\bar{A}_X(t,f)$ such that for decreasing support of the EAF the energy is spread over a larger region in the TF-plane.

We may conclude, that for a process with fixed ℓ_1 norm $\|\bar{A}_X\|_1$ of the EAF $\bar{A}_X(\tau,\nu)$ even an arbitrary small effective support of the EAF $\bar{A}_X(\tau,\nu)$ does *not* imply that the correlation coefficient:

$$\rho_{k,l;k',l'} \triangleq \frac{|\mathrm{E}\{C_{k,l}C^*_{k',l'}\}|}{\sqrt{P_{C_{k,l}}P_{C_{k',l'}}}} \tag{3.27}$$

are arbitrarily small (close to 0) if one uses a Gabor frame with $TF < 1$ and a Gaussian prototype. This can also be explained by the equation (3.18). If we assume that the EAF is a small sharp peak - approximating a Dirac pulse - centered at the origin of the (τ,ν)-plane, then we see from the expression (3.18) that the correlations between $C_{k,l}$ and $C_{k',l'}$ are effectively determined by the values of $A_g(\tau,\nu)$ evaluated at the points $((k-k')T,(l-l')F)$ in the (τ,ν)-plane. In particular the decorrelation between $C_{k,l}$ and $C_{k+1,l}$ relative to the mean power of $B_{k,l}$ is effectively given by the decay of $A_g(\tau,\nu)$ from the origin to the point $(T,0)$ in the (τ,ν)-plane. If we assume that we use an oversampled Gabor frame with $TF < 1$ and a Gaussian prototype, which implies that the TF shifted versions of $g(t)$ are not orthogonal the values $A_g(\tau,\nu)$ evaluated at the points kT, lF for $(k,l) \neq (0,0)$ do not vanish. Because on the other hand the decay of $A_g(\tau,\nu)$ is constrained by the radar uncertainty principle (cf. Section 2.3), there is in general an inherent limitation of the uncorrelatness of adjacent Gabor coefficients if we use an oversampled Gabor frame ($TF < 1$). However, we could use the critical sampling rate $TF = 1$ to get an orthonormal frame which would imply that the values $A_g(kT,lF)$ are exactly zero and yielding therefore an optimal decorrelation of the B_k's but this choice is rarely used because the *Balian-Low-Theorem* states that *every* frame at the critical sampling rate has a very poor TF-localization property. E.g., the frame generated by modulating time-shifted rectangular windows is a frame with $TF = 1$ and the Balian-Low-

depends effectively only on the values $A_g(kT,lF)$, i.e., the AF evaluated at a rectangular grid it would suggest to chose a prototype $g(t)$ and lattice constant T,F such that these values vanish. These could be satisfied (in order to still get a complete WH-set) only for the critical sampling rate $TF = 1$ which in turn implies very poor TF-localization properties of the resulting Gabor frame. In this thesis we are dealing only with well TF-localized WH-sets, i.e., the prototype of the analysis WH-set will mainly be chosen to be a Gaussian function. However the problem of finding a prototype function $g(t)$ and lattice constants T,F such that the cross correlations between the Gabor coefficients are minimized is studied in [31, 32]

Theorem states that no other frame at $TF = 1$ has a fundamental better TF-localization than this specific frame.

To further illustrate this we calculate the magnitude of the correlation between a fixed Gabor coefficient C_{k_0,l_0} and the neighbors C_{k_0+k,l_0+l} for $k = -3..3$ and $l = -3..3$. In Figure 3.4 the EAF of the process is shown. Obviously the effective support of the EAF is very small, i.e., it is a strongly underspread process. The analyzing Gabor frame used a Gaussian prototype $g(t) = e^{-\pi t^2}$

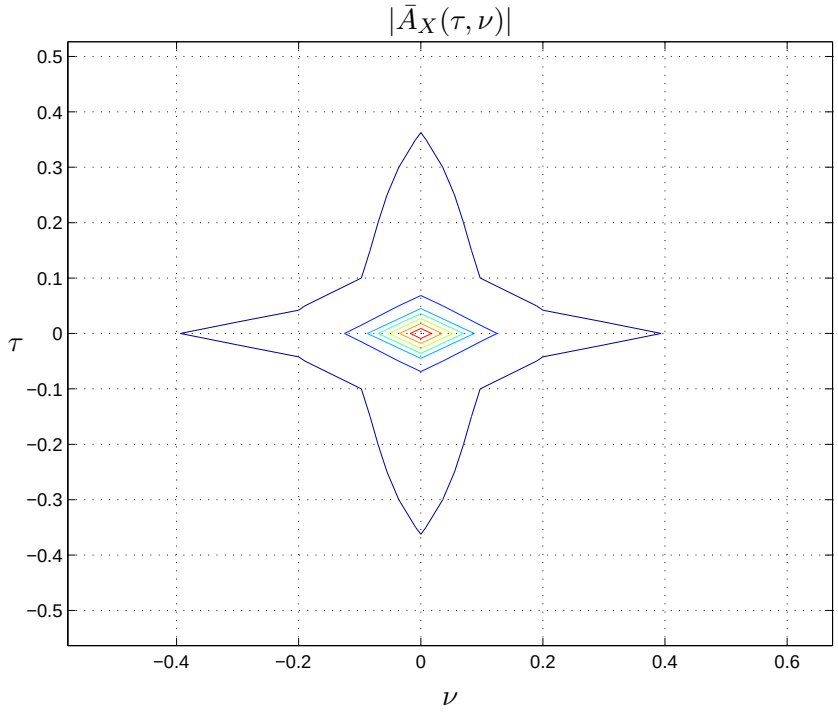

Figure 3.4: Contour plot of the magnitude of the expected ambiguity function $|\bar{A}_X(\tau,\nu)|$ of an strongly underspread process $X(t)$. The maximum (at the origin) is 1 and the lowest contour level is at 0.01.

and the lattice constants $T = \frac{19}{20}$ and $F = 1$. Table 3.4 lists the correlation of $C_{k,l}$ with $C_{0,0}$ for $k = -3...3$ and $l = -3...3$ normalized to the mean power $P_{C_{0,0}}$ of $C_{0,0} = \langle X, g_{0,0} \rangle$. It can be seen that the relative correlations of the adjacent Gabor coefficients ($k = 1, l = 0$ or $l = 1, k = 0$) is in the order of 0.2 and therefore not negligible although the process $X(t)$ is rather strongly underspread.

The existence of this inherent restriction for the Gaussian prototype, limiting the degree of uncorrelatness of different Gabor coefficients $C_{k,l}$ of the underspread process $X(t)$ is only observed for the case $(k,l) \neq (k',l')$ in Theorem (3.4.1). In the complementary case, $(k,l) = (k',l')$, such

$k \setminus l$	-3	-2	-1	0	1	2	3
-3	0	0	0	0	0	0	0
-2	0	0	0	0.003	0	0	0
-1	0	0	0.04	0.23	0.04	0	0
0	0	0.001	0.19	1	0.19	0.001	0
1	0	0	0.04	0.23	0.04	0	0
2	0	0	0	0.003	0	0	0
3	0	0	0	0	0	0	0

Table 3.1: Correlations between $C_{k,l}$ and $C_{0,0}$ normalized to $P_{C_{0,0}}$ for a strongly underspread process.

an inherent restriction seems not to exist, i.e., the powers $P_{C_{k,l}}$ of the Gabor coefficients $C_{k,l}$ are arbitrary close to the corresponding sample values of the WVS $\overline{W}_X(t,f)$ if the process $X(t)$ is sufficiently underspread.

However, for the case $(k,l) \neq (k',l')$ we have that the correlations between $B_{k,l}$ and $C_{k',l'}$ will generally decay fast[4] with increasing $|k-k'|$ and $|l-l'|$. The degree of the decay will be essentially determined by the shape of the AF $A_g(\tau,\nu)$ of the prototype $g(t)$. For the Gaussian prototype, this means that the correlations between $C_{k,l}$ and $C_{k',l'}$ decay exponentially fast with increasing $|k-k'|$ and $|l-l'|$.

If we stack a certain number of coefficients $C_{k,l}$ into a random vector $\mathbf{c}$, than the magnitude of the off-diagonal elements of the correlation matrix $\mathbf{R_c}$ of $\mathbf{c}$ will decay exponentially with increasing distance from the main diagonal of the matrix $\mathbf{R_c}$.

3.5 A Simple WVS Estimator

In this section we want discuss a very simple heuristic design for an estimator of the WVS $\overline{W}_X(t,f)$ of an underspread process $X(t)$. The estimator will be denoted by $\widetilde{W}_X(t,f)$ and is a random quantity, more specifically a 2D-function of time and frequency that is assigned to each realization of the underspread process $X(t)$.

In the following we assume that the estimator uses a sampled filter bank as a front end. From a theoretical point of view this means that we have access to $X(t)$ only via the inner products $C_{k,l} = \langle X(t), u_{k,l}(t) \rangle$ of the process with a analyzing Weyl-Heisenberg set $\{u_{k,l}(t)\}$ which can be represented by the triple $(g(t),T,F)$ consisting of the prototype or window $g(t)$ (which will be a

[4]In fact, this fast decay of the expansion coefficients has been used in [36] to define the class of local stationary processes which can be considered as a special subclass of underspread processes.

Gaussian in our context) and the lattice constants T and F. The overall structure of our estimator is shown in Figure 3.5. We note that for this estimator we will use undersampled WH-sets, i.e., $TF > 1$. Although this means that the Gabor coefficients are no complete representation of the realizations, this choice is advantageous for two reasons:

- It results in a compression because we have less Gabor coeffiecients that are located within the effective support of $\overline{W}_X(t, f)$ in the TF-plane and moreover, it is not nececessary to use a complete WH-set (i.e., $TF < 1$) because we are interested in the WVS of $X(t)$ and not in a complete representation of $X(t)$ itself. Due to the assumption that $X(t)$ is underspread we can sample the WVS at a grid with $TF > 1$ without loosing much information.

- For $TF > 1$ the Gabor coefficients can be regarded as effectively uncorrelated. This approximation is the better fulfilled the larger the product TF is. The (approximate) uncorelatness of the Gabor coefficients $C_{k,l}$ will greatly simplify the following derivations.

For our estimator design we will exploit two results deduced from the previous sections of this chapter:

- Firstly, we exploit the fact that the variances of $C_{k,l}$ are approximately equal to the values of the WVS $\overline{W}_X(t, f)$ at the points (kT, lF) in the (t, f)-plane.

- Secondly, the coefficients $C_{k,l}$ are approximately uncorrelated if the lattice constants T and F are not too small. Moreover, in order to simplify the calculation we assume that the $C_{k,l}$ are exactly uncorrelated unless otherwise stated throughout this section.

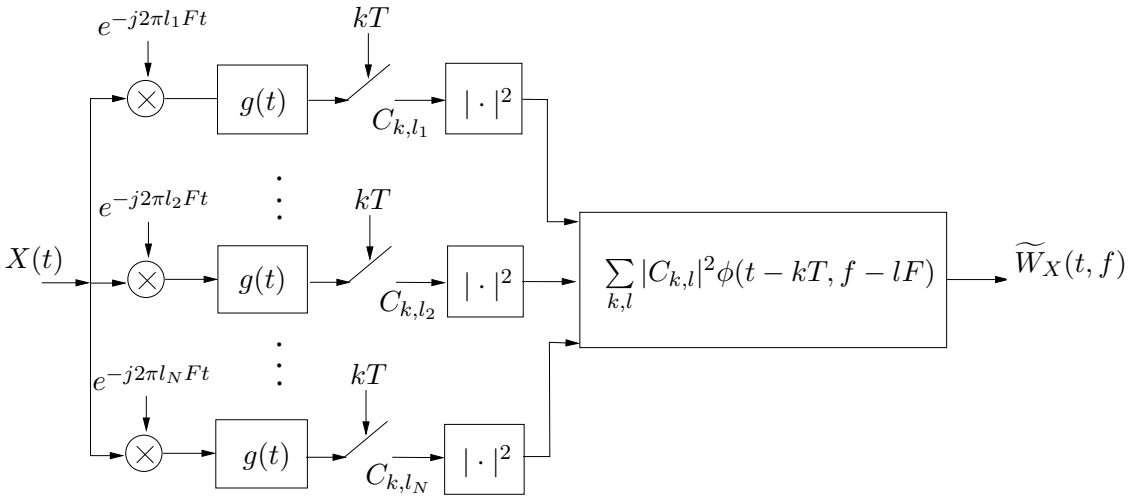

Figure 3.5: Block diagram of the proposed WVS estimator.

More precisely, the estimator $\widetilde{W}_X(t,f)$ is constrained to have the following form, i.e.,

$$\widetilde{W}_X(t,f) = \sum_{k,l} |C_{k,l}|^2 \phi(t-kT, f-lF) \tag{3.28}$$

where the real-valued function $\phi(t-kT, f-lF)$ denotes a reconstruction kernel. For the choice of the reconstruction kernel $\phi(t,f)$, we use the the mean square error (MSE)

$$\varepsilon_{\text{simple}} \triangleq \mathrm{E}\{\|\overline{W}_X(t,f) - \widetilde{W}_X(t,f)\|_2^2\} \tag{3.29}$$

as the objective to be minimized.

Because we want to estimate the WVS $\overline{W}_X(t,f)$, which is a deterministic parameter (in contrast to the WVS, the estimated WVS $\widetilde{W}_X(t,f)$ is a random quantity), we can split the MSE into a bias and a variance term:

$$\varepsilon_{\text{simple}} = B^2 + V^2 \tag{3.30}$$

with the (global) bias[5] term

$$B^2 \triangleq \|\mathrm{E}\{\widetilde{W}_X(t,f)\} - \overline{W}_X(t,f)\|_2^2 \tag{3.31}$$

and the (global) variance term

$$V^2 \triangleq \mathrm{E}\{\|\widetilde{W}_X(t,f) - \mathrm{E}\{\widetilde{W}_X(t,f)\}\|_2^2\}. \tag{3.32}$$

We can develop the bias term as follows:

$$\begin{aligned}
B^2 &= \|\mathrm{E}\{\sum_{k,l} |C_{k,l}|^2 \phi(t-kT, f-lF) - \overline{W}_X(t,f)\}\|_2^2 && (3.33)\\
&= \|\sum_{k,l} \mathrm{E}\{|C_{k,l}|^2\} \phi(t-kT, f-lF) - \overline{W}_X(t,f)\|_2^2 && (3.34)\\
&\approx \|\sum_{k,l} \overline{W}_X(kT,lF) \phi(t-kT, f-lF) - \overline{W}_X(t,f)\|_2^2 && (3.35)\\
&= \|\mathcal{F}_{t\to\nu, f\to\tau} \left\{ \sum_{k,l} \overline{W}_X(kT,lF) \phi(t-kT, f-lF) - \overline{W}_X(t,f) \right\} \|_2^2 && (3.36)\\
&= \| \left(\sum_{k,l} \frac{1}{TF} \bar{A}_X(\tau - \frac{k}{F}, \nu - \frac{l}{T}) \right) \Phi(\tau,\nu) - \bar{A}_X(\tau,\nu)\|_2^2 && (3.37)\\
&\approx \|\frac{1}{TF} \bar{A}_X(\tau,\nu)\Phi(\tau,\nu) - \bar{A}_X(\tau,\nu)\|_2^2 && (3.38)\\
&= \int_\tau \int_\nu |\bar{A}_X(\tau,\nu)|^2 |1 - \frac{1}{TF}\Phi(\tau,\nu)|^2 d\tau d\nu, && (3.39)
\end{aligned}$$

where $\Phi(\tau,\nu)$ denotes the 2D-Fourier transform of the reconstruction kernel $\phi(t,f)$ and we used the following facts:

[5] strictly speaking we would have to use the name "squared bias term"

- the form of the estimator is fixed by $\sum_{k,l} |C_{k,l}|^2 \phi(t - kT, f - lF)$,
- the expectation operator $\mathrm{E}\{\cdot\}$ commutes with linear operations,
- the variances (which equal the mean powers because we consider non-zero processes exclusively) are approximately equal to corresponding sample values of the WVS $\overline{W}_X(t,f)$ for an underspread process $X(t)$,
- the Fourier transform conserves norms because it is a unitary operator,
- the estimator $\widetilde{W}_X(t,f)$ can be written as $\widetilde{W}_X(t,f) = \Big(\sum_{k,l} C_{k,l}\delta(t-kT)\delta(f-lF)\Big) ** \phi(t,f)$.
- the following identities:

$$
\begin{aligned}
&\mathcal{F}_{t\to-\nu,f\to\tau}\left\{\sum_{k,l}\overline{W}_X(kT,lF)\phi(t-kT,f-lF)\right\} = \\
&= \mathcal{F}_{t\to-\nu,f\to\tau}\left\{\left(\sum_{k,l}\overline{W}_X(kT,lF)\cdot\delta(t-kT)\delta(f-lF)\right) *_t *_f \phi(t,f)\right\} \\
&= \mathcal{F}_{t\to-\nu,f\to\tau}\left\{\left(\sum_{k,l}\overline{W}_X(t,f)\cdot\delta(t-kT)\delta(f-lF)\right) *_t *_f \phi(t,f)\right\} \\
&= \left[\bar{A}_X(\tau,\nu) *_\tau *_\nu \Phi^{T,F}_{\mathrm{comb}}(\tau,\nu)\right]\cdot\Phi(\tau,\nu) \\
&= \frac{1}{TF}\sum_{k,l}\bar{A}_X(\tau-\frac{k}{F},\nu-\frac{l}{T})\cdot\Phi(\tau,\nu)
\end{aligned}
\tag{3.40}
$$

  where $\Phi^{T,F}_{\mathrm{comb}} \triangleq \frac{1}{TF}\sum_{k,l}\delta(\tau-\frac{k}{F})\delta(\nu-\frac{l}{T}) = \mathcal{F}_{t\to-\nu,f\to\tau}\left\{\sum_{k,l}\delta(t-kT)\delta(f-lF)\right\}$.

- for suitable chosen lattice constants T and F, the EAF $\bar{A}_X(\tau,\nu)$ is effectively supported within the rectangle $[-\frac{1}{2F},\frac{1}{2F}]\times[-\frac{1}{2T},\frac{1}{2T}]$ in the (τ,ν) plane.
- the definition of the (induced) quadratic norm of 2D-functions.

The final (underspread) approximation of the bias term is therefore:

$$B^2 \approx \int_\tau\int_\nu |\bar{A}_X(\tau,\nu)|^2 |1-\frac{1}{TF}\Phi(\tau,\nu)|^2 d\tau d\nu. \tag{3.41}$$

It remains to develop the variance term V^2:

$$\begin{aligned}
V^2 &= \mathrm{E}\{\| \sum_{k,l} |C_{k,l}|^2 \phi(t-kT, f-lF)\|_2^2\} - \| \sum_{k,l} \mathrm{E}\{|C_{k,l}|^2\}\phi(t-kT, f-lF)\|_2^2 \\
&= \int_t \int_f \sum_{k,l} \sum_{k',l'} \\
&\mathrm{E}\{C_{k,l} C_{k,l}^* C_{k',l'} C_{k',l'}^*\}\phi(t-kT, f-lF)\phi(t-k'T, f-l'F) \\
&- \left(\sum_{k,l} \mathrm{E}\{|C_{k,l}|^2\}\phi(t-kT, f-lF) \right)^2 dtdf \\
&= \int_t \int_f \sum_{k,l} \sum_{k',l'} (\mathrm{E}\{|C_{k,l}|^2\}\mathrm{E}\{|C_{k',l'}|^2\} \\
&+ \delta_{k-k'}\delta_{l-l'} \mathrm{E}\{|C_{k,l}|^2\}^2)\phi(t-kT, f-lF)\phi(t-k'T, f-l'F) \\
&- \left(\sum_{k,l} \mathrm{E}\{|C_{k,l}|^2\}\phi(t-kT, f-lF) \right)^2 dtdf \\
&= \int_t \int_f \sum_{k,l} \mathrm{E}\{|C_{k,l}|^2\}^2 \phi(t-kT, f-lF)\phi(t-kT, f-lF) dtdf \\
&= \sum_{k,l} \mathrm{E}\{|C_{k,l}|^2\}^2 \cdot \|\phi(t,f)\|_2^2 \\
&\approx \sum_{k,l} \overline{W}_X^2(t-kT, f-lF) \cdot \|\phi(t,f)\|_2^2 \\
&\approx \frac{1}{TF} \|\mathbf{R}_X\|_2^2 \cdot \|\phi(t,f)\|_2^2 \\
&= \frac{1}{TF} \|\mathbf{R}_X\|_2^2 \cdot \|\Phi(\tau,\nu)\|_2^2
\end{aligned} \tag{3.42}$$

where, we used the following facts:

- The relationship $\mathrm{var}\{A\} = \mathrm{E}\{A^2\} - \mathrm{E}\{A\}^2$, valid for any scalar random variable A.
- The interchangeability of expectation and summation.
- Isserli's formula for fourth-order moments of zero mean multivariate gaussian random variables [33]. If x_1, x_2, x_3, x_4 are zero mean and circular complex gaussian random variables (i.e., in particular $\mathrm{E}\{x_k x_l\} = 0$ for $k, l \in \{1,2,3,4\}$) then:

$$\mathrm{E}\{x_1 x_2^* x_3 x_4^*\} = \mathrm{E}\{x_1 x_2^*\} \cdot \mathrm{E}\{x_3 x_4^*\} + \mathrm{E}\{x_1 x_4^*\} \cdot \mathrm{E}\{x_3 x_2^*\}. \tag{3.43}$$

- The definition of the (induced) norm of a function $\phi(t,f)$.
- the approximate equivalence of the variances of $C_{k,l}$ with sample values of the WVS.

- One can show the following identity, valid for every 2D-function $\vartheta(t,f)$ whose fourier transform $\theta(\tau,\nu)$ is supported within the rectangle $[-\frac{1}{2F_0},\frac{1}{2F_0}]\times[-\frac{1}{2T_0},\frac{1}{2T_0}]$ in the (τ,ν)-plane:

$$\vartheta(t,f)=\sum_{k,l}\vartheta(kT_0,lF_0)\psi(t-kT_0,f-lF_0) \tag{3.44}$$

  where the set of 2D-functions $\{\psi(t-kT_0,f-lF_0)\}$ is an orthogonal set and each element has a squared norm of: $\|\psi(t-kT_0,f-lF_0)\|_2^2=T_0F_0$. Therefore we conclude the following equivalence:

$$\begin{aligned}\|\phi(t,f)\|_2^2&=\sum_{k,l}\sum_{k',l'}\phi(kT_0,lF_0)\phi^*(k'T_0,l'F_0)\langle\psi(t-kT_0,f-lF_0),\psi(t-k'T_0,f-l'F_0)\rangle\\&=T_0F_0\sum_{k,l}|\phi(kT_0,lF_0)|^2\end{aligned} \tag{3.45}$$

  which leads to the following relation, that is relevant for our derivation:

$$\sum_{k,l}|\phi(kT_0,lF_0)|^2=\frac{1}{T_0F_0}\|\phi(t,f)\|_2^2. \tag{3.46}$$

- The relation $\|R_X\|_2^2=\|\overline{W}_X\|_2^2$ [40] which is due to the unitarity of the mapping $R_X\mapsto\overline{W}_X$.

To summarize, the final approximation of the variance term V^2 is:

$$V^2\approx\frac{1}{TF}\|\mathbf{R}_X\|_2^2\cdot\|\Phi(\tau,\nu)\|_2^2. \tag{3.47}$$

From the approximate expressions for the variance- and the bias term of the estimator $\widetilde{W}_X(t,f)$ is obvious that there exists a "bias-variance" tradeoff:

- In order to have a bias term B^2 close to zero, we have to use a reconstruction kernel $\phi(t,f)$ whose (2D) Fourier transform $\Phi(\tau,\nu)$ is equal to TF on the effective support of $\bar{A}_X(\tau,\nu)$.
- On the other hand, if we want to have a small variance V^2, then the effective support of $\Phi(\tau,\nu)$ should be very small, even smaller than the effective support of $\bar{A}_X(\tau,\nu)$.

The argument now is, as pointed out in [41], that for an underspread process the variance term for an *unbiased* ($B^2=0$) estimator will be small, because the unbiased estimator has a reconstruction kernel whose Fourier transform $\Phi(\tau,\nu)$ has to be supported only on the effective support of $\bar{A}_X(\tau,\nu)$ and exactly this effective support is small for an underspread process $X(t)$. Therefore we chose the reconstruction kernel $\phi(t,f)$ such that the support of $\Phi(\tau,\nu)$ is approximately identical with the effective support of $\bar{A}_X(\tau,\nu)$, more specifically:

$$\Phi(\tau,\nu)=\begin{cases}TF, & \text{for } (\tau,\nu)\in\text{effective support of } \bar{A}_X(\tau,\nu)\\ 0, & \text{elsewhere}\end{cases} \tag{3.48}$$

which, using (3.30),(3.47) and $B = 0$ yields the following approximate expression for the $\varepsilon_{\text{simple}}$:

$$\varepsilon_{\text{simple}} \approx \|R_X\|_2^2 TF\mathcal{A}(\textbf{effective support of } \bar{A}_X). \tag{3.49}$$

where $\mathcal{A}(\mathcal{G}) \triangleq \int_{(\tau,\nu)\in\mathcal{G}} d\tau d\nu$. We see that the error will be smaller for decreasing lattice constants T, F of the analyzing WH-set (implemented by the sampled filterbank).

So far we have determined only the effective support of $\Phi(\tau, \nu)$. It remains to choose T and F. For fixed HS-norm of the correlation operator we see from the approximate expressions for the bias and variance term, that for a unbiased estimator, i.e., $\Phi(\tau, \nu) = TF$ on the effective support of $\bar{A}_X(\tau, \nu)$ and zero elsewhere, the variance term V^2 is directly proportional to the product TF. Therefore it is desirable to use small values for the lattice constants T,F of the analyzing Weyl Heisenberg set $\mathcal{G} = (g(t), T, F)$ in order to get a small variance for the unbiased estimator. However, one of the assumptions at the beginning of our derivation was that the analysis coefficients $C_{k,l}$ are effectively uncorrelated. As we observed in a previous section, this requires that the lattice constants T,F are not too small, i.e., a choice $TF < 1$ will clearly violate the assumptions underlying our derivation and therefore is not allowed. As indicated by Theorem 3.4.1 the exact lower bound on the lattice constants depends on the effective support of the EAF $\bar{A}_X(\tau, \nu)$ and the shape of the prototype $g(t)$.

We note that a fundamental difference of the WVS estimator proposed here to the one proposed in [41] is that our estimator is not TF-shift covariant, i.e., if we move from the process $X(t)$ to the process $X(t - \tau)$ then it is in general not the case that $\widetilde{W}_{X(t-\tau)}(t, f) = \widetilde{W}_X(t - \tau, f)$ and the same holds for frequency shifts (modulations).

Beside the relative simple actual implementation of the proposed estimator $\widetilde{W}_X(t, f)$ via an filter bank we see that our design only used the effective support of $\bar{A}_X(\tau, \nu)$ as an a priori knowledge and not the complete second order statistic as it is required for the estimator design scheme proposed in [52].

Finally, we note that because of the Fourier correspondence between the kernel $r_X(t, t') = \mathrm{E}\{X(t)X(t')^*\}$ of the correlation operator $\mathbf{R}_X$ and the WVS $\overline{W}_X(t, f)$ we can estimate the autocorrelation function $r_X(t, t')$ of $X(t)$ (which is identical to the kernel of $\mathbf{R}_X$) by replacing the postprocessing step

$$\sum_{k,l} |C_{k,l}|^2 \phi(t - kT, f - LF) \tag{3.50}$$

of the WVS estimator by the following operation

$$\sum_{k,l} |C_{k,l}|^2 \phi_r(t - kT/2, t - kT/2) e^{j2\pi lF(t-t')} \tag{3.51}$$

where the function $\phi_r(t, t')$ is given by

$$\phi_r(t, t') = \int_f \phi\left(\frac{t + t'}{2}, f\right) e^{j2\pi f(t-t')} df. \tag{3.52}$$

The resulting estimator $\tilde{r}_X(t,t')$ for the autocorrelation function is given as

$$\sum_{k,l} |\langle X(t), g_{k,l}(t)\rangle|^2 \phi_r(t-kT/2, t-kT/2) e^{j2\pi lF(t-t')}. \tag{3.53}$$

Defining the mean squared estimation error e_r as

$$e_r = \mathrm{E}\{\|\tilde{r}_X(t,t') - r_X(t,t')\|_2^2\} \tag{3.54}$$

we can directly take over all results of the above error analysis for the estimator $\widetilde{W}_X(t,f)$ by recognizing that the corresponding norms are conserved by the mappings $\widetilde{W}_X(t,f) \mapsto \tilde{r}_X(t,t')$ and $\overline{W}_X(t,f) \mapsto r_X(t,t')$. Especially if we have found an optimum estimator $\widetilde{W}_{X,opt}(t,f)$ of the WVS $\overline{W}_X(t,f)$ then the specific autocorrelation estimator $\tilde{r}_{X,opt}(t,f)$ that corresponds to $\widetilde{W}_{X,opt}(t,f)$ via the relation (3.52) will also be optimal in the sense of the mean squared error.

Chapter 4

Compressed Sensing

4.1 Introduction

As the name already indicates, "Compressed Sensing" (CS) deals with sensing strategies that inherently use a compression of the raw data. Let us illustrate a setting that is typical for CS:

We have a signal/object of interest, denoted by $\mathbf{x}$. In the literature this signal is almost always modeled as a deterministic finite-dimensional vector $\mathbf{x} \in \mathbb{C}^n$ (n denotes the signal dimension, for typical CS-applications n is in the order of thousands) but a generalization to a random object (vector) is possible. However, unfortunately, we have no direct access to $\mathbf{x}$. All we know about $\mathbf{x}$ is a certain number of very few linear measurements. The basic problem considered in CS is the recovery of the signal $\mathbf{x}$ from these incomplete and in some cases corrupted (by additive noise) measurements.

In this section we will first give a formal description of the CS-setting. Then we discuss the main quantitative concepts for CS that allow to investigate precisely under what conditions an accurate recovery of the signal vector $\mathbf{x}$ from the linear measurements is possible.

4.2 Basic Data Model

Let us formalize the content of the discussion of a basic CS-setting/scenario given in the introduction. We will do this by means of the following data model:

$$\mathbf{z} = \mathbf{M}\mathbf{x} + \mathbf{w}. \tag{4.1}$$

Here,

- $\mathbf{z} \in \mathbb{C}^m$ is the observed (random) measurement vector,
- $\mathbf{x} \in \mathbb{C}^n$ is the unknown signal vector to be estimated/recovered,

- $\mathbf{w} \in \mathbb{C}^m$ is the random noise vector, further specified below,
- and finally, $\mathbf{M} \in \mathbb{C}^{m \times n}$ is a known measurement matrix.

Each row of $\mathbf{M}$ represents a single linear measurement that is taken on the signal of interest $\mathbf{x}$. Typically the number of measurements is much lower than the dimension of the vector space $\mathbb{C}^n$ to which $\mathbf{x}$ belongs. This implies that $\mathbf{M}$ has much more columns than rows ($m \ll n$). From linear algebra it follows that without any further assumptions on the signal $\mathbf{x}$ it is impossible to recover $\mathbf{x}$ from the measurements $\mathbf{z}$, even in the noiseless ($\mathbf{w} = 0$) case. Therefore the measurements $\mathbf{z}$ are called an "incomplete" information about $\mathbf{x}$. However, in CS we explicitly introduce a constraint/assumption on $\mathbf{x}$. Namely, we assume that $\mathbf{x}$ has only few coefficients that are effectively non-vanishing (or in other words: most of the elements of $\mathbf{x}$ are effectively zero). If a vector $\mathbf{x}$ has this property then it is called "sparse". More precisely we call a vector $\mathbf{x}$ "exactly S-sparse" with a number $S \in \mathbb{N}$ if it has at most S entries that are non-zero. This can be denoted fomally with the help of the ℓ_0-norm ($\|\cdot\|_0$) by

$$\|\mathbf{x}\|_0 = w_{\mathrm{H}}(\mathbf{x}) = S. \tag{4.2}$$

Here, S denotes the sparsity of $\mathbf{x}$ and $w_{\mathrm{H}}(\cdot)$ denotes the hamming weight [25]. The name "ℓ_0-norm" with the corresponding notation $\|\cdot\|_0$, for the number of nonzeros of a vector is sometimes misleading because the number of nonzeros does not fulfill the axioms of a norm for a linear vector space (e.g. for the space $\mathbb{C}^n$). However, this sloppy naming is virtually used everywhere in the literature and therefore we use it also within this thesis. However, in practical applications the signal vectors will in general not be ideally sparse but approximately. The degree of sparseness, given a specific order S, may be measured by the norm of its "tail", i.e., the norm of the vector $\mathbf{x} - \mathbf{x}_S$, where $\mathbf{x}_S$ denotes the vector that is obtained from $\mathbf{x}$ by setting every coordinates to zero except the S largest coefficients (coordinates), e.g. if $\mathbf{x} = \begin{bmatrix} 4 & 3 & 2 & 1 & 1 \end{bmatrix}^T$ and $S = 3$ then $\mathbf{x}_S = \begin{bmatrix} 4 & 3 & 2 & 0 & 0 \end{bmatrix}^T$.

4.3 Recovery

A central question considered in CS deals with the exact conditions such that one can recover $\mathbf{x}$ from the incomplete measurements $\mathbf{z}$ with small error and how large these errors are exactly. We will answer this question for two recovery algorithms (BP and (R)OMP) which will be presented below. Obviously those conditions will mainly depend on the measurement matrix $\mathbf{M}$. It is in some sense the "window" through which we observe the signal vector $\mathbf{x}$ and if it is "dirty" then we can expect that an accurate identification of $\mathbf{x}$ will not be possible.

From a theoretical point of view the optimal recovery scheme, at least in the noiseless case ($\mathbf{w} = 0$) is the "brute-force"-method. This method consists of seeking the sparsest vector $\hat{\mathbf{x}}$ that

agrees with the measurements $\mathbf{z}$:

$$(P_0) \qquad \hat{\mathbf{x}}_0 = \arg\min_{\mathbf{x}'} \|\mathbf{x}'\|_0 \quad \text{subject to} \quad \mathbf{M}\mathbf{x}' = \mathbf{z}. \tag{4.3}$$

where $\|\mathbf{x}\|_0$ denotes the the number of non-zeros of $\mathbf{x}$. Under certain conditions, as explained below in more detail, it can be shown that $\hat{\mathbf{x}}$ coincides with $\mathbf{x}$. However, this optimization is not tractable because for its solution one has to consider all possible patterns of non-zeros in a vector $\mathbf{x} \in \mathbb{C}^n$ and this search space is obviously too large for practical implementations. Therefore, in practice, other methods for recovery are employed. Of course from a performance point of view they are suboptimum but they need much less computational resources.

One of the key results in CS is that for most practical scenarios the performance loss of the suboptimum (but tractable) methods is very small. However, the recovery via the optimization problem (P_0) can be used as a benchmark, i.e., we may compare the results of other recovery schemes to the result of (P_0) $\hat{\mathbf{x}}_0$ and use the difference between these two solutions as a measure of performance.

In the literature, the vast majority of proposed recovery schemes, i.e., methods to recover $\mathbf{x}$ from $\mathbf{z}$ belong to one of the two following categories:

- convex optimization methods;
- greedy methods.

It seems that all other methods are essentially variants or combinations of the key ideas behind these two categories.

4.4 Basic Ingredients for CS

4.4.1 Spark

Definition 4.4.1. (Donoho, Elad [14]) *Given a matrix $\mathbf{A} \in \mathbb{C}^{m\times n}$ where $n > m$, we define $\sigma =$ Spark($\mathbf{A}$) as the smallest natural number such that there exits a subset of σ columns from $\mathbf{A}$ that are linearly dependent.*

As mentioned in [14], although there is an obvious relationship between the spark of a matrix and its rank[1] (e.g. $\sigma \leq \text{Rank}(\mathbf{A})$), a fundamental difference is that the determination of the rank of a given matrix $\mathbf{A}$ is a process which takes maximally a number of steps equal to the size of the larger matrix dimension. Conversely, the determination of the spark of the matrix $\mathbf{A}$ requires a combinatorial process whose complexity scales exponentially with the size of the matrix $\mathbf{A}$.

[1]The rank of a matrix $\mathbf{A} \in \mathbb{C}^{m\times n}$ is defined as the maximum number of linearly independent columns of $\mathbf{A}$.

However, the notion of the spark of a matrix gives us the formal tool to formulate a uniqueness theorem elegantly. As can be easily proven the following holds:

Theorem 4.4.1. *A representation* $\mathbf{y} = \mathbf{A}\mathbf{x}$ *of the vector* $\mathbf{y}$ *by the coefficient vector* $\mathbf{x}$ *is necessarily the sparsest possible for* $\mathbf{y}$ *if* $\|\mathbf{x}\|_0 < \text{Spark}(\mathbf{A})/2$.

Proof. Assume that there are two different coefficient vectors $\mathbf{x}_0$, $\mathbf{x}_1$ with $\|\mathbf{x}_{0,1}\|_0 < \text{Spark}(\mathbf{A})/2$ and $\mathbf{y} = \mathbf{A}\mathbf{x}_0 = \mathbf{A}\mathbf{x}_1$. Then the difference coefficient vector $\mathbf{x}_0 - \mathbf{x}_1$, which is not equal the zero vector because we assumed $\mathbf{x}_1$ and $\mathbf{x}_0$ to be different, obeys obviously $\|\mathbf{x}_0 - \mathbf{x}_1\|_0 < \text{Spark}(\mathbf{A})$ and $\mathbf{A}(\mathbf{x}_0 - \mathbf{x}_1) = 0$. In other words, we have found a subset of less then Spark($\mathbf{A}$) columns out of A, which are linearly dependent. But this is in contradiction to the definition of Spark($\mathbf{A}$). □

In other words, Theorem 4.4.1 states that if we fix a matrix $\mathbf{A}$ and observe a vector $\mathbf{y}$, which is generated by $\mathbf{x}$ through $\mathbf{y} = \mathbf{A}\mathbf{x}$, then there exists at most one $\mathbf{x}$ which has fewer non-zeros than Spark($\mathbf{A}$)/2. This theorem gives us the absolute minimum theoretical requirements for the measurement matrix $\mathbf{M}$ in (4.1) that is necessary for a unique recovery. In other words, the spark of the measurement matrix $\mathbf{M}$ is an absolute fundamental limit of how sparse a signal $\mathbf{x}$ must be in order to uniquely recover it from a small set of linear measurements $\mathbf{z}$. However, in practical applications of CS the spark is rarely used. For practical applications other concepts, that quantify the "CS-performance" of the measurement matrix $\mathbf{M}$ more gradually, like the restricted isometry property (RIP) or the coherence, as discussed below, are better suited.

Finally we want to translate the result stated in Theorem 4.4.1 to our CS-setting, i.e., we adapt it to our basic data model (4.1):

Theorem 4.4.2. *Referring to the data model* (4.1) *and assuming a noiseless situation* ($\mathbf{w} = 0$), *if the signal vector* $\mathbf{x}$ *satisfies*

$$\|\mathbf{x}\|_0 < \text{Spark}(\mathbf{M})/2 \tag{4.4}$$

then the solution $\hat{\mathbf{x}}_0$ *of* (P_0) *coincides with the signal vector* $\mathbf{x}$ *and this solution is moreover unique.*

4.4.2 Coherence/Cumulative Coherence

A useful quantity assigned to a measurement matrix $\mathbf{M}$ describing the performance of $\mathbf{M}$ in the context of CS-recovery is the coherence. The definition of the coherence is given in [55]:

Definition 4.4.2. *The coherence* μ *of a matrix* $\mathbf{M}$ *is defined as the maximum absolute inner product between two distinct columns of* $\mathbf{M}$

$$\mu \triangleq \max_{j \neq k} |\langle \mathbf{M}(:,j), \mathbf{M}(:,k) \rangle|. \tag{4.5}$$

Here we have adopted the MATLAB-programming notation. Thereby we denote the k-th column of matrix A by "$A(:,k)$". A fully equivalent definition of the coherence can be given via the Grammian $\mathbf{G} = \mathbf{M}^H\mathbf{M}$ of $\mathbf{M}$:

$$\mu = \max_{i \neq j} |\mathbf{G}_{ij}|. \tag{4.6}$$

As proved in [14], the coherence μ and the spark of a measurement matrix $\mathbf{M}$ satisfy the inequality:

$$\text{Spark}(\mathbf{M}) > \frac{1}{\mu}. \tag{4.7}$$

Closely related to the coherence is the concept of the cumulative coherence $\mu_1(k)$ of a matrix $\mathbf{M}$ [55]. It is defined as

$$\mu_1(k) \triangleq \max_{|\Lambda|=k, j \notin \Lambda} \sum_{i \in \Lambda} |\langle \mathbf{M}(:,i), \mathbf{M}(:,j) \rangle|. \tag{4.8}$$

Here, k is an integer in the range from 1 to the number of columns of $\mathbf{M}$ (which is denoted by n throughout this thesis if $\mathbf{M}$ denotes a matrix that is used for constructing CS measurements).

4.4.3 Restricted Isometry Property/Restricted Isometry Condition

This concept has been introduced by Candes et.al. in order to quantify the CS-performance of a measurement matrix. In particular they define:

Definition 4.4.3. *The local isometry constant $\delta_\Lambda = \delta_\Lambda(\mathbf{M})$ of a matrix $\mathbf{M} \in \mathbb{C}^{m \times n}$ for the index set $\Lambda \subset \{1, 2, ..., n\}$ is defined as the smallest real number satisfying*

$$(1 - \delta_\Lambda)\|\mathbf{x}\|_2^2 \leq \|\mathbf{M}_\Lambda \mathbf{x}\|_2^2 \leq (1 + \delta_\Lambda)\|\mathbf{x}\|_2^2 \quad \textit{for all vectors } \mathbf{x} \textit{ with } \text{supp}(\mathbf{x}) = \Lambda \tag{4.9}$$

where $\mathbf{M}_\Lambda$ is the sub matrix of $\mathbf{M}$ containing all columns of $\mathbf{M}$ whose indexes are in the index set Λ. Subsequently, for a given number $S \in \{1, 2, ..., n\}$ which will be called the sparsity degree, the global restricted isometry constant of $\mathbf{M}$ is defined as

$$\delta_S = \delta_S(\mathbf{M}) \triangleq \sup_{|\Lambda|=S} \delta_\Lambda(\mathbf{M}). \tag{4.10}$$

Trivially the restricted isometry property (RIP) - constant δ_S for $S > m$ cannot be smaller than 1 because any subset of more then m columns out of $\mathbf{M}$ must be linearly dependent. Furthermore δ_1 is equal to 0 if every column of $\mathbf{M}$ has unit norm. Another important property of the RIP constants is that they are nondecreasing with respect to the sparsity degree S, i.e., $\delta_S \leq \delta_{S+1}$.

The defining condition (4.9) for the local isometry constant δ_Λ is equivalent to the requirement that the eigenvalues λ_k of the matrix $\mathbf{M}_\Lambda^H \mathbf{M}_\Lambda$ obey

$$(1 - \delta_\Lambda) \leq \lambda_k \leq (1 + \delta_\Lambda). \tag{4.11}$$

Here $\mathbf{M}_\Lambda$ again denotes the matrix which is obtained by selecting those columns of $\mathbf{M}$ which are indexed by Λ. Unfortunately the RIP constant is only a sufficient condition for good CS performance [11]. If we know that a specific measurement-matrix has good/low RIP constants then we know that it yields good CS performance. Otherwise if we get bad/large RIP-constants, this means not necessarily that the corresponding measurement matrix yields poor CS-performance. A crude estimate for the RIP constants is given by the following upper bound using the coherence and babel function μ_1 [49]:

$$\delta_S \leq \mu_1(S-1) \leq (S-1)\mu. \tag{4.12}$$

The drawback of this upper bound is, that a large value of μ (typically μ can be verified easily) does not imply a large value of the RIP-constant δ_S. Otherwise, if we knew that μ is small, than we know that δ_S is also small.

Restricted Isometry Condition

The main tool in our thesis for measuring the CS-recovery performance of a measurement matrix $\mathbf{M}$ will be a slightly modified version of the restricted isometry property, the so called *"Restricted Isometry Condition"* (RIC) introduced in [45]:

Definition 4.4.4. Restricted Isometry Condition. *A matrix $\mathbf{M} \in \mathbb{C}^{m\times n}$ satisfies the Restricted Isometry Condition (RIC) with parameters $(k, \varepsilon) \in [1, n] \times [0, 1]$ if*

$$(1-\varepsilon)\|\mathbf{x}\|_2 \leq \|\mathbf{M}\mathbf{x}\|_2 \leq (1+\varepsilon)\|\mathbf{x}\|_2 \quad \textit{for all } k\textit{-sparse vectors } \mathbf{x}. \tag{4.13}$$

We note that the RIC is essentially the same as the RIP, except that the inequalities are stated in terms of the norms of the vectors and not in terms of the squared norms as in (4.9).

4.4.4 The Johnson-Lindenstrauss Lemma or the Concentration of Measure

The determination of the RIP constants directly according to its definition (by searching over every possible subset of columns out of $\mathbf{M}$), yields an unpractical algorithm with exponential complexity. A way out of this difficulty may be given by an interesting link of CS to a well known result on Banach spaces.

The so called "*Johnson-Lindenstrauss*"-Lemma [1] essentially states that for every set of points in a high-dimensional vector space there always exists a mapping, which maps the original points into a lower-dimensional vector space such that the relative distances between the points are approximately conserved. This property is closely related to the RIP and the techniques developed for the derivation of the Johnson-Lindenstrauss Lemma can be used for the determination of the RIP for specific types of measurement matrices [3, 49]. More specifically, these methods work for

random measurement matrices, i.e., the measurement matrix $\mathbf{M}$ in our basic data model (4.1) is regarded as a specific realization of a random matrix $\underline{\mathbf{M}}$ with an associated probability density function (pdf) $f_{\underline{\mathbf{M}}}(\mathbf{M})$.

4.4.5 Random Measurement Matrices

The performance of the recovery schemes (BP or OMP) depends crucially on the measurement matrix $\mathbf{M}$. As discussed further above, the relevant quantity for the recovery performance of the BP is the RIP-constant of the measurement matrix $\mathbf{M}$ corresponding to the sparsity degree S of the signal vector $\mathbf{x}$. The question now is, how to construct a measurement matrix $\mathbf{M} \in \mathbb{C}^{m \times n}$ that yields good/small RIP constants and additionally possess a small compression factor "m/n". Unfortunately, until now only random matrices yield satisfactory performance. This is analogous to coding theory, where one can show that an optimal coding scheme uses a random mapping and good deterministic coding schemes (like Turbo Codes) essentially rely on imitating the "non-structure" of random codes [25].

Three Popular Choices For the Measurement Matrix M

In the literature three choices for the random measurement matrix $\mathbf{M}$ are popular:

- **Gaussian ensemble.** The entries of $\mathbf{M}$ are i.i.d. normally distributed.
- **Bernoulli ensemble.** The entries of $\mathbf{M}$ are i.i.d. Bernoulli distributed.
- **Sampled unitary matrix.** The measurement matrix $\mathbf{M}$ is obtained by selecting uniformly at random the rows of a unitary matrix $\mathcal{U}$. A very popular choice for the unitary matrix is the DFT matrix. Mathematically speaking, $\mathbf{M}$ is obtained by selecting the rows of a unitary matrix $\mathcal{U}$ that are indexed by a random set $\Omega \subset \{1, .., n\}$ of size m.

  The reason for choosing mainly a DFT matrix for $\mathcal{U}$ twofold. Firstly, it can be shown that the DFT matrix is optimum with respect to the compression performance, i.e., in order to achieve the same performance fewer rows of the DFT matrix are required than for any other unitary matrix. Secondly, the special (deterministic) structure of a DFT matrix allows very fast algorithms to be used for real-world implementations.

As mentioned above, although random measurement matrices yield the best performance regarding compression factor and accuracy, for a fast implementation of the CS recovery schemes in hardware a rich (deterministic) structure of the measurement matrix $\mathbf{M}$ is very desirable. Therefore there has been a great effort [12,20] to find other constructions beside the randomly sampled DFT matrix

that yield random measurement matrices that also have a rich (deterministic) structure in order to get fast algorithms (like the FFT for the randomly sampled DFT matrix).

For the actual recovery performance, a main criterion is the RIP or RIC introduced above. Fortunately a lot of results have been obtained regarding the RIP/RIC of the random measurement matrices listed above. The Gaussian ensemble and the Bernoulli ensemble can be considered as specific instances of a subgaussian random matrix. According to [45] a measurement matrix is called subgaussian if its entries are i.i.d. subgaussian[2] random variables. For subgaussian and sampled unitary matrices the following result regarding the RIC is presented in [45]:

Theorem 4.4.3. (Measurement matrices satisfying the RIC). *Consider an $m \times n$ measurement matrix $\mathbf{M}$ and let $n \geq 1$, $\varepsilon \in (0, 1/2)$, and $\delta \in (0, 1)$.*

1. *If $\mathbf{M}$ is a subgaussian matrix, then with probability $1 - \delta$ the matrix $\frac{1}{\sqrt{m}}\mathbf{M}$ satisfies the RIC with parameters (k, ε) provided that*

$$m \geq \frac{Ck}{\varepsilon^2} \ln \frac{n}{\varepsilon^2 k}. \tag{4.14}$$

2. *If $\mathbf{M}$ is a sampled unitary matrix, then with probability $1 - \delta$ the matrix $\sqrt{\frac{n}{m}}\mathbf{M}$ satisfies the RIC with parameters (k, ε) provided that*

$$m \geq C \frac{k \ln n}{\varepsilon^2} \ln \left(\frac{k \ln n}{\varepsilon^2} \right) \ln^2 n. \tag{4.15}$$

In both cases, the constant C depends only on the confidence level δ and on the type of the measurement matrix $\mathbf{M}$.

Another result for the RIC of a measurement matrix that either is a Gaussian or Bernoulli ensemble is presented in [3]:

Theorem 4.4.4. *Let $\mathbf{M} \in \mathbb{C}^{m \times n}$ be a random measurement matrix that either is a Gaussian (with entries that are distributed i.i.d. $\mathcal{N}(0, \frac{1}{m})$) or a Bernoulli ensemble (with entries that are distributed i.i.d. in $\{-\frac{1}{\sqrt{m}}, \frac{1}{\sqrt{m}}\}$ with equal probabilities). Then $\mathbf{M}$ satisfies the RIC with parameter (k, ε) with a probability exceeding*

$$1 - 2 \left(\frac{12}{\varepsilon} \right)^k e^{-c_0(\varepsilon/2) \cdot m} \tag{4.16}$$

with the function $c_0(x) = \frac{x^2}{4} - \frac{x^3}{6}$.

For the RIC of the sampled unitary matrix the following result has been presented in [53]:

[2] A random variable X is subgaussian if its tail distribution is dominated by that of the standard Gaussian random variable.

Theorem 4.4.5. *Suppose the random measurement matrix* $\mathbf{M} \in \mathbb{C}^{m\times n}$ *is given by selecting* m *rows uniformly at random out of a unitary matrix* $\mathcal{U}$ *and normalizing the columns so that they have unit Euclidian norm, then* $\mathbf{M}$ *will satisfy the RIC with parameter* (k, ε) *with small* ε *(close to zero) with overwhelming*[3] *probability if*

$$m \geq C(\ln n)^4 \mu^2 k \tag{4.17}$$

where the constant C *depends on the desired probability that the RIC holds and on* ε*. The constant* μ *in* (4.17) *is defined by* $\mu = \sqrt{n}\max_{i,j}|\mathcal{U}_{ij}|$ *and is equal to* 1 *if* $\mathcal{U}$ *is a DFT matrix.*

We note that the results of the RIP/RIC performance of random measurement matrices seem to show a big gap between theoretical and empirical methods. Indeed, the most theoretical results are upper bounds that in general seem to be very far from being "tight". However, the tightest results seem to exist only for the Gaussian ensemble [50].

Uniform vs. Nonuniform Results

Another important aspect regarding results on CS (more specifically, the results regarding the recovery performance of a specific scheme like Basis Pursuit) is whether they are of "uniform" or "non-uniform" type [48]. In the following, we will make the meaning of this terms clear. A "uniform" result is a property of a deterministic measurement matrix (maybe a single realization of a random measurement matrix) together with a recovery algorithm (e.g. BP or OMP) which holds for arbitrary signal vectors $\mathbf{x}$, i.e., once we have found a "good" (deterministic) measurement matrix $\mathbf{M}$ for a recovery scheme, then this measurement matrix has a good performance for all possible signal vectors $\mathbf{x}$.

For further purposes it is important to note that when we use a random measurement matrix it may happen that for each realization of the measurement matrix we also get a different realization of the coefficient vector $\mathbf{x}$ (in particular when using CS for statistical signal processing).

Exactly this situation can also be used for judging a result (regarding CS performance) "uniform" or "non-uniform". A result is called uniform if its statement is valid for an arbitrary dependence of the coefficient vector $\mathbf{x}$ on the realization of the measurement matrix $\mathbf{M}$. On the other hand if a result is only "non-uniform" it means that the stated CS-recovery performance can only be achieved for a *fixed* signal vector $\mathbf{x}$ and a random measurement matrix $\mathbf{M}$.

However, the two most important performance results for CS recovery (one for the BP and one for the ROMP) within this thesis are uniform results.

[3] "overwhelming" means that the probability that $\mathbf{M}$ does not satisfy the RIC decreases exponentially with the number m of selected rows.

4.4.6 Deterministic Measurement Matrices

The best deterministic construction of measurement matrices known to the author is presented in [11]. Their approach is based on finite fields. Unfortunately the guaranteed theoretical performance of the measurement matrices constructed with the method presented there is rather poor. More specifically, the number of required non-vanishing coefficients of the signal vector is much higher for deterministic constructions of the measurement matrix than for random constructions. Alternatively, deterministic constructions need a lot more measurements to yield the same recovery accuracy as when using random measurement matrices.

4.5 Main CS-Recovery Strategies

4.5.1 Basis Pursuit

The key tool for CS in our thesis will be the Basis Pursuit (BP). Although the name is somewhat similar to Matching Pursuit (MP) and Orthogonal Matching Pursuit (OMP), there are fundamental differences. However BP and OMP can be used for the recovery of the signal $\mathbf{x}$ from the incomplete and corrupted measurements $\mathbf{z}$ of our fundamental data model (4.1).

Within this work Basis Pursuit (BP) refers to *any* scheme or algorithm that solves the following *convex* optimization problem:

$$\hat{\mathbf{x}} = \arg\min_{\mathbf{x}' \in \mathbb{C}^n} \|\mathbf{x}'\|_1 \quad \text{subject to} \quad \|\mathbf{M}\mathbf{x}' - \mathbf{z}\|_2 \leq \epsilon. \tag{4.18}$$

The theoretical justification for the using of this minimization as an approach to recover $\mathbf{x}$ from $\mathbf{z}$ is the following theorem, which is a slightly modified version of Theorem 2 presented[4] in [18]

Theorem 4.5.1. (Stability of the Basis Pursuit.) *Consider the basic data model for CS* (4.1) *with bounded noise* $\|\mathbf{w}\| \leq \epsilon$*, suppose that* $\mathbf{x}$ *is an arbitrary vector in* $\mathbb{C}^n$*, and let* $\mathbf{x}_S$ *be the masked vector corresponding to the* S ($S \in \{1, 2..., n\}$) *largest* (*with respect to absolute values*) *coefficients/coordinates of* $\mathbf{x}$ (*in absolute value*)*. Under the assumption that measurement matrix* $\mathbf{M}$ *satisfies the RIC with parameters* $(5 \cdot S, \varepsilon)$ *whereby* $\varepsilon < \frac{1}{3}$*, the solution* $\hat{\mathbf{x}}$ *of the optimization problem* (4.18) *obeys:*

$$\|\hat{\mathbf{x}} - \mathbf{x}\|_2 \leq C_{1,S}\epsilon + C_{2,S}\frac{\|\mathbf{x} - \mathbf{x}_S\|_1}{\sqrt{S}}. \tag{4.19}$$

For reasonable values of ε *the constants in* (4.19) *are well behaved; e.g.* $C_{1,S} \approx 30$ *and* $C_{2,S} \approx 7$ *for* $\varepsilon \leq \frac{1}{5}$.

[4] It had been already observed in [47] that the original statement of this theorem which was stated only for the real valued setting can be immediately restated for the complex valued setting because the proof presented there did not rely on real-valuedness.

This result is extremely useful for the following reasons:

- It is valid for *arbitrary* vectors in $\mathbb{C}^n$, not only for ideally sparse vectors.
- The size of the error $\|\hat{\mathbf{x}}-\mathbf{x}\|$ splits nicely into two additive terms. The first term corresponds to the error induced by the noise $\mathbf{w}$ and the second term is due to the non sparsity of the original signal vector $\mathbf{x}$. The non-sparsity of the signal $\mathbf{x}$ influences the recovery error exclusively via the ℓ_1-norm of the tail $\|\mathbf{x}-\mathbf{x}_S\|_1$ where $\mathbf{x}_S$ is obtained from $\mathbf{x}$ by setting all coefficient to zero except the S largest.
- It shows that the recovery error $\|\hat{\mathbf{x}}-\mathbf{x}\|$ scales only linearly with the magnitude of the error term ϵ.
- It is a *deterministic* statement which implies that this is a uniform result if $\mathbf{M}$ is a random matrix, i.e., if we have found a single realization of $\mathbf{M}$ that fulfills the RIC condition of the theorem, then the recovery is accurate for *every* (sparse) signal vector $\mathbf{x}$.

The proof presented here, is a slightly modified and more detailed version of that presented in [18].

Proof. Throughout the proof we will use the following notations: Let $\mathbf{a}$ denote a vector in $\mathbb{C}^n$ and let $\mathcal{I} \subseteq \{1, 2..., n\}$ denote an index set. Then we denote by $\mathbf{a}_{\mathcal{I}}$ the vector that is obtained from $\mathbf{a}$ by zeroing all coefficients except those that are indexed by $\mathcal{I}$. Given an index set $\mathcal{I} \subseteq \{1, 2..., n\}$ we denote by $\mathcal{I}^c$ the complementary set within $\{1, 2...., n\}$. Given two sets T_k and T_l we denote by $T_{k,l}$ their union.

Let $T_0 \subseteq \{1, 2...., n\}$ denote the index set of the S largest coefficients of $\mathbf{x}$. We partition the complementary set T_0^C into sets $T_1, T_2...., T_J$ of equal size $|T_j| = M, j \geq 1$ (except the last one T_J), by decreasing order of magnitude, i.e,

$$k \in T_j, l \in T_i \quad i \leq j \Rightarrow |\mathbf{x}_{(k)}| \leq |\mathbf{x}_{(l)}|. \tag{4.20}$$

Then we decompose the solution $\hat{\mathbf{x}}$ of (4.18) as: $\hat{\mathbf{x}} = \mathbf{x} + \mathbf{h}$. Since $\mathbf{x}$ is feasible for (4.18) it must hold that $\|\hat{\mathbf{x}}\|_1 \leq \|\mathbf{x}\|_1$ and therefore

$$\|\mathbf{x}\|_1 \geq \|\hat{\mathbf{x}}\|_1 = \|\mathbf{x}_{T_0} + \mathbf{h}_{T_0}\|_1 + \|\mathbf{x}_{T_0^C} + \mathbf{h}_{T_0^C}\|_1 \geq \|\mathbf{x}_{T_0}\|_1 - \|\mathbf{h}_{T_0}\|_1 - \|\mathbf{x}_{T_0^C}\|_1 + \|\mathbf{h}_{T_0^C}\|_1 \tag{4.21}$$

where we used (4.57). It follows that

$$\|\mathbf{h}_{T_0^C}\|_1 \leq \|\mathbf{h}_{T_0}\|_1 + 2\|\mathbf{x}_{T_0^C}\|_1. \tag{4.22}$$

For the remainder we make use of the following observation: The k-th largest value $|\mathbf{h}_{T_0^C}|_{(k)}$ of $\mathbf{h}_{T_0^C}$ satisfies

$$|\mathbf{h}_{T_0^C}|_{(k)} \leq \frac{\|\mathbf{h}_{T_0^C}\|_1}{k} \tag{4.23}$$

and therefore[5]

$$\|\mathbf{h}_{T_{0,1}^C}\|_2^2 \leq \|\mathbf{h}_{T_0^C}\|_1^2 \sum_{k=M+1}^{N} \frac{1}{k^2} \leq \frac{\|\mathbf{h}_{T_0^C}\|_1^2}{M}. \tag{4.24}$$

The last inequality follows from

$$\sum_{k=M+1}^{N} \frac{1}{k^2} \leq \int_M^{\infty} \frac{1}{x^2} dx = \frac{1}{M}. \tag{4.25}$$

We can conclude, by setting $\rho = \frac{S}{M}$ and using (4.22) as well as the relation $\|\mathbf{h}_{T_0}\|_1 \leq \sqrt{S}\|\mathbf{h}_{T_0}\|_2$

$$\|\mathbf{h}_{T_{01}^C}\|_2 \leq \frac{\|\mathbf{h}_{T_0^C}\|_1}{\sqrt{M}} \leq \frac{\|\mathbf{h}_{T_0}\|_1 + 2\|\mathbf{x}_{T_0^C}\|_1}{\sqrt{M}} \leq \sqrt{\rho}\left(\|\mathbf{h}_{T_0}\|_2 + \frac{2\|\mathbf{x}_{T_0^C}\|_1}{\sqrt{S}}\right) \tag{4.26}$$

which implies, using the triangle inequality for norms and the obvious fact that $\|\mathbf{h}_{T_{01}}\|_2 \geq \|\mathbf{h}_{T_0}\|_2$

$$\|\mathbf{h}\|_2 \leq (1+\sqrt{\rho})\|\mathbf{h}_{T_{0,1}}\|_2 + 2\sqrt{\rho}\cdot\eta, \quad \eta \triangleq \|\mathbf{x}_{T_0^C}\|_1/\sqrt{S}. \tag{4.27}$$

Now we observe that by construction, the magnitude of each coefficient in T_{j+1} is less or equal than the average of the magnitudes in T_j, i.e.,

$$|(\mathbf{h}_{T_{j+1}})_k| \leq \frac{\|\mathbf{h}_{T_j}\|_1}{M}. \tag{4.28}$$

Then we have:

$$\|\mathbf{h}_{T_{j+1}}\|_2 = \sqrt{\sum_{k\in T_{j+1}} |\left(\mathbf{h}_{T_{j+1}}\right)_k|^2} \leq \sqrt{M \cdot \frac{\|\mathbf{h}_{T_j}\|_1^2}{M^2}} = \frac{\|\mathbf{h}_{T_j}\|_1}{\sqrt{M}} \tag{4.29}$$

which implies:

$$\sum_{j\geq 2} \|\mathbf{h}_{T_j}\|_2 \leq \sum_{j\geq 1} \frac{\|\mathbf{h}_{T_j}\|_1}{\sqrt{M}} = \frac{\|\mathbf{h}_{T_0^c}\|_1}{\sqrt{M}}. \tag{4.30}$$

Combining (4.30) and (4.26) yields:

$$\sum_{j\geq 2} \|\mathbf{h}_{T_j}\|_2 \leq \frac{\|\mathbf{h}_{T_0^c}\|_1}{\sqrt{M}} \leq \sqrt{\rho}\cdot(\|\mathbf{h}_{T_0}\|_2 + 2\eta) \tag{4.31}$$

which implies using the RIC with parameters $((S+M),\varepsilon)$ for $\mathbf{M}$, (4.57) and the fact that $\|\mathbf{h}_{T_0}\|_2 \leq$

[5] $\mathbf{h}_{T_{0,1}} = \mathbf{h}_{T_0 \cup T_1}$

$\|\mathbf{h}_{T_{01}}\|_2$:

$$\begin{aligned}\|\mathbf{Mh}\|_2 = \|\mathbf{Mh}_{T_{0,1}} + \sum_{j\geq 2}\mathbf{Mh}_{T_j}\|_2 &\geq \|\mathbf{Mh}_{T_{0,1}}\|_2 - \left\|\sum_{j\geq 2}\mathbf{Mh}_{T_j}\right\|_2 \\ &\geq \|\mathbf{Mh}_{T_{0,1}}\|_2 - \sum_{j\geq 2}\|\mathbf{Mh}_{T_j}\|_2 \\ &\geq (1-\varepsilon)\|\mathbf{h}_{T_{0,1}}\|_2 - (1+\varepsilon)\sum_{j\geq 2}\|\mathbf{h}_{T_j}\|_2 \\ &\geq (1-\varepsilon)\|\mathbf{h}_{T_{0,1}}\|_2 - (1+\varepsilon)\sqrt{\rho}\left(\|\mathbf{h}_{T_{0,1}}\|_2 + 2\eta\right) \\ &\geq \|\mathbf{h}_{T_{0,1}}\|_2\left((1-\varepsilon) - (1+\varepsilon)\sqrt{\rho}\right) - 2\sqrt{\rho}(1+\varepsilon)\eta.\end{aligned} \tag{4.32}$$

Since $\|\mathbf{Mh}\| \leq 2\epsilon$ because of:

$$\|\mathbf{Mh}\| = \|\mathbf{M}(\mathbf{x}-\hat{\mathbf{x}})\| = \|\mathbf{Mx}-\mathbf{z}+\mathbf{z}-\mathbf{M}\hat{\mathbf{x}}\| \leq \|\mathbf{Mx}-\mathbf{z}\| + \|\mathbf{M}\hat{\mathbf{x}}-\mathbf{z}\| \leq 2\epsilon \tag{4.33}$$

we conclude:

$$\|\mathbf{h}_{T_{0,1}}\|_2 \leq \frac{2}{(1-\varepsilon)-(1+\varepsilon)\sqrt{\rho}}[\epsilon + \sqrt{\rho}(1+\varepsilon)\eta] \tag{4.34}$$

For the specific choice $M = 4S$ the theorem now follows from (4.27)

$$\|\hat{\mathbf{x}}-\mathbf{x}\|_2 = \|\mathbf{h}\|_2 \leq \epsilon(1+\sqrt{\rho})\frac{2}{(1-\varepsilon)-(1+\varepsilon)\sqrt{\rho}} + \eta 2\sqrt{\rho}\left[1 + \frac{(1+\varepsilon)}{(1-\varepsilon)-(1+\varepsilon)\sqrt{\rho}}\right] \tag{4.35}$$

because the condition on ε required by the theorem and $M = 4S$ guarantees that the denominator $(1-\varepsilon)-(1+\varepsilon)\sqrt{\rho}$ is positive. The explicit expressions for the constants of the theorem are found to be:

$$C_{1,S} = (1+\sqrt{\rho})\frac{2}{(1-\varepsilon)-(1+\varepsilon)\sqrt{\rho}} \tag{4.36}$$

and

$$C_{2,S} = 2\sqrt{\rho}\left[1 + \frac{(1+\varepsilon)}{(1-\varepsilon)-(1+\varepsilon)\sqrt{\rho}}\right]. \tag{4.37}$$

□

The main differences between Theorem 4.5.1 and the result presented in [18] are:

- The result presented here is valid for arbitrary vectors in $\mathbb{C}^n$ whereas [18] considers only the real valued setting.
- We use the RIC and not the RIP.
- The numerical values of the constants $C_{1,S}$ and $C_{2,S}$ are different (because we use the RIC instead of the RIP).

4.5.2 Orthogonal Matching Pursuit and Variants

Orthogonal Matching Pursuit (OMP) [55] is an iterative algorithm that given an input vector $\mathbf{z} \in \mathbb{C}^m$ and a matrix $\mathbf{M} \in \mathbb{C}^{m \times n}$ where usually $m \ll n$ tries to find those m columns of $\mathbf{M}$ that matches best the input vector $\mathbf{z}$, i.e, the least square approximation of $\mathbf{z}$ using the matrix consisting of the already selected columns of $\mathbf{M}$ yields a small approximation error. A characteristic of OMP is that it selects only one new column of $\mathbf{M}$ during each iteration. Trivially, if $\mathbf{M}$ has full rank (which will be assumed to hold for all measurement matrices in this thesis) OMP is guaranteed to yield an exact representation of $\mathbf{z}$ after m steps.[6] It is a improved derivative of the so called "Matching-Pursuit" algorithm introduced in [37]. Throughout this section, unless stated otherwise, we will consider the noiseless case $\mathbf{w} = 0$ of our basic data model (4.1) for CS.

We will use OMP as a main representative of the class of greedy methods. A greedy method is a recursive scheme that tries to improve the approximation of a given input signal under certain constraints at each stage. Under certain conditions (to be explained below in detail) these greedy methods can be shown to be very fast and relatively accurate. However, the theoretical results for greedy methods do not attain the same quality as the results for Basis Pursuit at the moment. On the other hand, the computational cost of greedy methods is in general considerably lower than that of convex optimization methods like Basis Pursuit[7].

In the CS context, OMP identifies the specific columns of $\mathbf{M}$ and the associated coefficients that describe the given measurements $\mathbf{z}$ in an optimum (with respect to the number of selected columns) way. The algorithm is called "greedy" because of its behavior. It is a recursive scheme that selects a single column out of $\mathbf{M}$ during each recursion. Moreover it can be shown that OMP never selects the same column twice. Therefore, OMP is guaranteed to stop after a number of steps that is equal to the number of columns n of the measurement matrix $\mathbf{M}$.

There have been investigated extensions of the OMP scheme, which are mainly based on further assumptions regarding the signal model. Using a scheme called "Tree Orthogonal Matching Pursuit" (TOMP) [34] the authors assume not only sparsity of the coefficients vector in the reconstruction problem. Their additional assumption is that the significant nonzero coefficients w.r.t. to a proper wavelet dictionary can be represented as a sparse tree. This tree-like structure enables the authors to design a derivative of OMP, called TOMP, that outperforms conventional OMP in specific scenarios.

[6] However, when using OMP for Compressed Sensing we are not interested in an arbitrary exact representation of the input (the input vector for OMP is the context of CS equal to the measurement vector $\mathbf{z}$). Within CS we want to get the locations (indices) and values of the coefficients belonging to the sparsest possible representation. In general the number of iterations that are used is smaller than m, i.e., the dimension of the input vector.

[7] However, improvements in the development of fast algorithms for the solution of convex optimization problems and increasing available computing resources make this argument a little bit less important.

Another interesting derivative of OMP is the so called "Stagewise-Orthogonal Matching Pursit" presented in [16].

In this section we summarize some results regarding the performance of OMP for the recovery problem (4.1), but first we give the exact definition of OMP:

1. OMP begins by setting the residual $\mathbf{r}$ (which is the difference of the current approximation and the input signal vector) equal to the input measurements $\mathbf{z}$ and making the initial approximation $\mathbf{a}_0 = 0$ of the input signal $\mathbf{z}$. Furthermore it initializes the set of selected indices at step k, denoted by λ_k, to $\lambda_0 = \{\}$.

2. At step k, OMP chooses the column with index λ out of the measurement matrix $\mathbf{M}$, denoted by $m = \mathbf{M}(:, \lambda)$, that yields the maximum correlation with the residual $\mathbf{r}_{k-1}$ at step k:

$$\lambda = \arg \max_{n \in (1 \ldots N)} |\langle \mathbf{r}_{k-1}, \mathbf{M}(:, n) \rangle|. \tag{4.38}$$

   The chosen column index λ is added to the set of selected column indices:

$$\lambda_k = \lambda_{k-1} \cup \{\lambda\}. \tag{4.39}$$

3. Then, OMP computes the coefficient vector $\mathbf{c}_k$ of the kth approximation $\mathbf{a}_k \triangleq \mathbf{M}\mathbf{c}_k$ by a least square scheme:

$$\mathbf{c}_k = \arg \min_{\mathbf{c}} \|\mathbf{z} - \mathbf{M}\mathbf{c}\|_2 \quad \text{subject to} \quad \text{supp}(\mathbf{c}) \subseteq \lambda_k. \tag{4.40}$$

4. The last step of the kth iteration is to update the residual:

$$\mathbf{r}_k = \mathbf{z} - \mathbf{a}_k. \tag{4.41}$$

5. The algorithm stops after the kth step if the residual is below a predefined small threshold and outputs the estimated coefficient vector $\hat{\mathbf{x}} = \mathbf{c}_k$.

After n steps, where n is number of columns of the measurement matrix $\mathbf{M}$, the algorithm necessarily yields a residual r equal to zero[8], i.e., the approximation $\mathbf{a}_k$ is equal to the input $\mathbf{z}$.

The computational cost for OMP depends mainly on the step involving the least square minimization (4.40). A fast execution of this step is possible if the measurement matrix $\mathbf{M}$ entails a

[8]This presupposes that $\mathbf{M}$ is full rank. This condition is assumed to be fulfilled by a measurement matrix $\mathbf{M}$ throughout this thesis.

special structure, e.g., if it is obtained by taking rows out of a discrete Fourier transform matrix $\mathbb{F}_n$.[9]

Conditions for accurate recovery of $\mathbf{x}$ from $\mathbf{z}$ within a certain (small) number of iterations of OMP are available via the coherence μ and the cumulative coherence μ_1 of the measurement matrix $\mathbf{M}$. As a first result we present the following theorem, adopted from [15]:

Theorem 4.5.2. *Considering the basic data model:*

$$\mathbf{z} = \mathbf{M}\mathbf{x} + \mathbf{w} \tag{4.43}$$

with a bounded noise $\|\mathbf{w}\|_2 \leq \varepsilon$*, suppose that*

$$\|\mathbf{x}\|_0 \leq \frac{1+\mu}{2\mu} - \frac{1}{M} \cdot \frac{\varepsilon}{|\,(\mathbf{x})_L\,|} \tag{4.44}$$

where $(\mathbf{x})_L$ *denotes the* L*th largest element of* $\mathbf{x}$*, then*

- $\hat{\mathbf{x}}_{\mathrm{OMP}}$ *has the correct sparsity pattern, i.e.,*

$$\mathrm{supp}(\hat{\mathbf{x}}_{OMP}) = \mathrm{supp}(\mathbf{x}); \tag{4.45}$$

- *the error is small:*

$$\|\hat{\mathbf{x}}_{\mathrm{OMP}} - \mathbf{x}\|_2^2 \leq \frac{\varepsilon^2}{1-\mu(L-1)}. \tag{4.46}$$

  Here, $\hat{\mathbf{x}}_{\mathrm{OMP}}$ *denotes the coefficients vector* $\mathbf{c}_k$ *of the* k*-th approximant* $\mathbf{a}_k$ *calculated by the first OMP recursion for which the residual* $\mathbf{r}_k$ *satisfies* $\|\mathbf{r}_k\| \leq \varepsilon$ *and* $\mu = \mu(\mathbf{M})$ *denotes the coherence of the measurement matrix* $\mathbf{M}$*.*

We note that there are a lot of other theoretical results for the performance of OMP and related recovery schemes. But it seems that Theorem 4.5.2 presented here, is best suited for our setting. One key property of this result is, that it allows to consider also approximately sparse signal vectors $\mathbf{x}$ in an indirect fashion, namely via incorporating the smaller coefficients (i.e., the tail) of $\mathbf{x}$ in the noise term $\mathbf{w}$ of our basic data model (4.1).

However this result has a big drawback: The condition (4.44) used in the Theorem is a "hard" one, i.e., if the norm of the noise term $\mathbf{w}$ in the basic data model is not below a specific threshold

[9] The Fourier matrix $\mathbb{F}_n \in \mathbb{C}^{n\times n}$ is defined as

$$\mathbb{F}_n \triangleq \frac{1}{\sqrt{n}} \cdot \begin{bmatrix} 1 & 1 & \cdots & 1 \\ 1 & e^{-j2\pi\frac{1}{n}} & \cdots & e^{-j2\pi\frac{(n-1)}{n}} \\ \vdots & \vdots & \ddots & \vdots \\ 1 & e^{-j2\pi\frac{(n-1)}{n}} & \cdots & e^{-j2\pi\frac{(n-1)(n-1)}{n}} \end{bmatrix} \tag{4.42}$$

then this theorem does not apply at all. This is a big difference to the central statement (Theorem 4.5.1) that we use for the Basis Pursuit - performance. There we observe a gradually degradation of the performance if the norm of the noise becomes larger. Moreover, Theorem 4.5.1 handles approximate sparse signals directly, whereas Theorem 4.5.2 presupposed ideally sparse signals, because it uses a condition on the ℓ_0-norm.

Some other results concerning the recovery performance of OMP are given in [55]:

Theorem 4.5.3. *Assume that the measurement matrix $\mathbf{M} \in \mathbb{C}^{m \times n}$ satisfies*

$$k < \frac{1}{8\sqrt{2}} \mu^{-1} - 1 \tag{4.47}$$

where μ denotes the coherence of $\mathbf{M}$. For an arbitrary measurement vector $\mathbf{z}$, OMP generates an k-term approximant $\mathbf{a}_k$ that satisfies:

$$\|\mathbf{z} - \mathbf{a}_k\|_2 \leq 8\sqrt{k} \|\mathbf{z} - \mathbf{a}_{opt}\|_2 \tag{4.48}$$

where $\mathbf{a}_{opt}$ is an optimal k-term approximation of $\mathbf{z}$.

Considering our data model (4.1) this theorem means that if we consider the noiseless case and the signal $\mathbf{x}$ is sufficiently sparse, then a_m coincides with the *unique* solution of (P_0) in Section 4.3. The application of this theorem is limited because the theorem assumes ideally sparse signals, whereas in practice one always is confronted with "effective" sparse signals, i.e., most components of the vector are "effectively" zero and not exactly. For this general setting the following theorem is useful [55]:

Theorem 4.5.4. *Assume that $\mu_1(d) < \frac{1}{2}$ where d is a natural number and $\mu_1(d)$ is the cumulative coherence of the measurement matrix $\mathbf{M} \in \mathbb{C}^{m \times n}$. The column indices of $\mathbf{M}$ that are contained in the best d-term approximation of $\mathbf{z}$ are collected to the set Λ_{opt} with $|\Lambda_{opt}| = d$. Suppose that $\mathbf{a}_k$ is an arbitrary linear combination of columns of $\mathbf{M}$ whose indices are in Λ_{opt}. At step $k+1$, OMP will recover another column of $\mathbf{M}$ whose index is in Λ_{opt} provided that*

$$\|\mathbf{z} - a_k\|_2 > \sqrt{1 + \frac{d[1 - \mu_1(d)]}{[1 - 2\mu_1(d)]^2}} \|\mathbf{z} - \mathbf{a}_{opt}\|_2. \tag{4.49}$$

Here, $\mathbf{a}_{opt}$ denotes the best d-term approximation of $\mathbf{z}$:

$$\mathbf{a}_{opt} = \sum_{\ell \in \Lambda_{opt}} \mathbf{c}_\ell \mathbf{M}(:, \ell). \tag{4.50}$$

The (technical) proof of this theorem can be found in [55]. This theorem helps us not directly because it gives results concerning the best d-term approximation $\mathbf{a}_{opt}$ of $\mathbf{z}$. But we would be interested in statements concerning the signal vector $\mathbf{x}$. Therefore we have to analyze the relationship between $\mathbf{a}_{opt}$ (the best d-term representation of $\mathbf{z}$) and $\mathbf{x}$.

For simplicity, we will do this analysis for the noiseless case $\mathbf{w} = 0$. As a first step, we use the fact that the best d-term approximation of $\mathbf{z}$ cannot be larger away from $\mathbf{z}$ than the specific d-term approximation a_d that results in setting all coefficients of $\mathbf{x}$ to zero, except the d largest (this coefficient vector will be denoted by $\mathbf{x}_d$):

$$\|\mathbf{a}_{\text{opt}} - \mathbf{z}\|_2 \leq \|\mathbf{M}\mathbf{x}_d - \mathbf{z}\|_2. \tag{4.51}$$

This simple inequality allows us to reformulate Theorem 4.5.3 and Theorem 4.5.4.

Corollary 4.5.5. *Assume that the measurement matrix $\mathbf{M} \in \mathbb{C}^{m\times n}$ has a coherence μ and consider d with $d < \frac{1}{8\sqrt{2}}\frac{1}{\mu} - 1$. For an arbitrary input $\mathbf{z}$, OMP generates an d-term approximant $\mathbf{a}_d$ that satisfies*

$$\|\mathbf{x} - \mathbf{a}_d\|_2 \leq 8\sqrt{d}\|\mathbf{M}\mathbf{x}_d - \mathbf{z}\|_2, \tag{4.52}$$

where $\mathbf{x}_m$ denotes the vector that is obtained from $\mathbf{x}$ by setting all coefficients except the m largest to zero.

Corollary 4.5.6. *Assume that $\mu_1(d) < \frac{1}{2}$ where d is a natural number and $\mu_1(d)$ is the cumulative coherence of the measurement matrix $\mathbf{M} \in \mathbb{C}^{m\times n}$. The column indices of $\mathbf{M}$ that are contained in the best d-term approximation of $\mathbf{z}$ are collected to the set Λ_{opt} with $|\Lambda_{opt}| = d$. Suppose that $\mathbf{a}_k$ is an arbitrary linear combination of columns of $\mathbf{M}$ whose indices are in Λ_{opt}. At step $k+1$, OMP will recover another column of $\mathbf{M}$ whose index is in Λ_{opt} provided that*

$$\|\mathbf{z} - \mathbf{a}_k\|_2 > \sqrt{1 + \frac{d[1-\mu_1(d)]}{[1-2\mu_1(d)]^2}}\|\mathbf{z} - \mathbf{M}\mathbf{x}_d\|_2. \tag{4.53}$$

Here, $\mathbf{x}_d$ denotes the vector that is obtained from $\mathbf{x}$ by setting all coefficients except the d largest to zero.

Following the arguments in [55], Theorem 4.5.4 implies the following statement:

Corollary 4.5.7. *Assume that $d \leq \frac{1}{3}\frac{1}{\mu}$, or more generally, that $\mu_1(d) \leq \frac{1}{3}$. Then OMP generates d-term approximants that satisfy*

$$\|\mathbf{z} - \mathbf{a}_d\|_2 \leq \sqrt{1+6d}\|\mathbf{z} - \mathbf{M}\mathbf{x}_d\|_2. \tag{4.54}$$

The shortcoming of Corollary 4.5.5 – 4.5.7 is the fact that they only make statements about the distance between $\mathbf{a}_d$ and the measurement vector $\mathbf{z}$, but we are interested in the deviations of the coefficient vector $\mathbf{c}_d$ corresponding to $\mathbf{a}_d$ and the original signal vector $\mathbf{x}$.

Fortunately, as we will demonstrate in the following, we can make use of the concept of restricted isometry, i.e., the RIP and RIC (both introduced above) of the measurement matrix $\mathbf{M}$, to show that the OMP yields a small difference between the coefficient vector $\mathbf{c}_d$ and $\mathbf{x}$ as well.

Theorem 4.5.8. *Consider the basic data model for CS in the noiseless case ($\mathbf{w} = 0$). We assume that the measurement matrix $\mathbf{M} \in \mathbb{C}^{m \times n}$ satisfies the RIP for the degree $S = 2d$ with a RIP constant δ_{2d}. Given an d-term approximation $\mathbf{a}_d$, i.e, $\mathbf{a}_d = \mathbf{M}\mathbf{c}_d$ with some d-sparse coefficient vector $\mathbf{c}_d$ corresponding to the observed measurement $\mathbf{z}$ ($\mathbf{z} = \mathbf{M}\mathbf{c}_d$), we can bound the distance between $\mathbf{c}_d$ and the signal vector $\mathbf{x}$ as follows:*

$$\|\mathbf{x} - \mathbf{c}_d\|_2 \leq (\|\mathbf{z} - \mathbf{a}_d\|_2 + \|\mathbf{M}\mathbf{x}_{\mathcal{I}^c}\|_2) \frac{1}{\sqrt{1 - \delta_{2d}}} + \|\mathbf{x}_{\mathcal{I}^c}\|_2 \tag{4.55}$$

where $\mathbf{x}_{\mathcal{I}^c}$ denotes the vector which is obtained by setting the coefficients corresponding to the index set $\mathcal{I}$ in $\mathbf{x}$ to zero. The index set $\mathcal{I}$ consists of those indices which are either in the support of the d largest coefficients of $\mathbf{x}$ or in the support of $\mathbf{c}_d$: $\mathcal{I} = \operatorname{supp}(\mathbf{x}_d) \cup \operatorname{supp}(\mathbf{c}_d)$.

The reasons why we introduce the specific index set $\mathcal{I}$ in the theorem are:

- We anticipate that the support of the d largest coefficients of $\mathbf{x}$ approximately coincide with the support of $\mathbf{c}_d$.
- We expect that the coefficients of $\mathbf{x}$ that are not contained within the d largest coefficients are very small, because $\mathbf{x}$ is assumed to be sparse.

Proof. The proof of the theorem begins with the application of the following two inequalities valid for the 2-norm $\|\cdot\|_2$:

$$\|\mathbf{u} + \mathbf{v}\|_2 \leq \|\mathbf{u}\|_2 + \|\mathbf{v}\|_2 \tag{4.56}$$

and

$$\|\mathbf{u} - \mathbf{v}\|_2 \geq \|\mathbf{u}\|_2 - \|\mathbf{v}\|_2. \tag{4.57}$$

Now we can deduce the following:

$$\begin{aligned} \|\mathbf{z} - \mathbf{a}_d\|_2 &= \|\mathbf{M}\mathbf{x}_{\mathcal{I}} + \mathbf{M}\mathbf{x}_{\mathcal{I}^C} - \mathbf{M}\mathbf{c}_d\|_2 \\ &= \|\mathbf{M}(\mathbf{x}_{\mathcal{I}} - \mathbf{c}_d) + \mathbf{M}\mathbf{x}_{\mathcal{I}^C}\|_2 \geq \|\mathbf{M}(\mathbf{x}_{\mathcal{I}} - \mathbf{c}_d)\|_2 - \|\mathbf{M}\mathbf{x}_{\mathcal{I}^C}\|_2 \\ &\geq \|\mathbf{x}_{\mathcal{I}} - \mathbf{c}_d\|_2 \sqrt{1 - \delta_{2d}} - \|\mathbf{M}\mathbf{x}_{\mathcal{I}^C}\|_2. \end{aligned} \tag{4.58}$$

The proof is finalized by another application of the triangle inequality:

$$\begin{aligned} \|\mathbf{x} - \mathbf{c}_d\|_2 &= \|\mathbf{x}_{\mathcal{I}} + \mathbf{x}_{\mathcal{I}^C} - \mathbf{c}_d\|_2 \\ &\leq \|\mathbf{x}_{\mathcal{I}} - \mathbf{c}_d\| + \|\mathbf{x}_{\mathcal{I}^C}\|_2 \\ &\leq \frac{1}{\sqrt{1 - \delta_{2d}}} (\|\mathbf{z} - \mathbf{a}_d\|_2 + \|\mathbf{M}\mathbf{x}_{\mathcal{I}^C}\|_2) + \|\mathbf{x}_{\mathcal{I}^C}\|_2. \end{aligned} \tag{4.59}$$

□

This theorem can obviously made a little bit more precise if one considers the exact size of $\mathcal{I}$ instead of $2m$, but we will not do this. By combining the Theorem 4.5.8 with Theorem 4.5.7 we arrive at our key result for the theoretical performance of OMP in the CS recovery setting:

Theorem 4.5.9. *Assume that $d \leq \frac{1}{3}\frac{1}{\mu}$, or more generally, that $\mu_1(d) \leq \frac{1}{3}$ where μ and μ_1 denote the coherence and cumulative coherence of the measurement matrix $\mathbf{M} \in \mathbb{C}^{m\times n}$ respectively. Furthermore we assume that $\mathbf{M}$ satisfies the RIP for $S = 2d$ with a RIP constant δ_{2d}. Then OMP generates an d-term approximant a_d with an associated coefficient vector c_d that satisfies*

$$\|\mathbf{x} - \mathbf{c}_d\| \leq \left(\sqrt{1+6d}\|\mathbf{z} - \mathbf{M}\mathbf{x}_d\|_2 + \|\mathbf{M}\mathbf{x}_{\mathcal{I}^c}\|_2\right)\frac{1}{\sqrt{1-\delta_{2d}}} + \|\mathbf{x}_{\mathcal{I}^c}\|_2 \tag{4.60}$$

where $\mathbf{x}_{\mathcal{I}^c}$ denotes the vector which is obtained by setting the coefficients corresponding to the index set $\mathcal{I}$ in $\mathbf{x}$ to zero. The index set $\mathcal{I}$ consists of those positions which are either in the support of the m largest coefficients of $\mathbf{x}$ or in the support of c_m.

ROMP - Regularized Orthogonal Matching Pursuit

Although the recovery via OMP has some advantages, including the execution speed and transparency of the algorithm, it lacks of theoretical performance guarantees that are as strong and useful as the main Theorem 4.5.1 for BP. Note that the best known results regarding the recovery performance of OMP are non-uniform. In fact, it has been shown in [48] that in general it is impossible to derive uniform results for OMP. A more practical drawback of the results for OMP presented above is that they mainly rely on the (commulative) coherence of the measurement matrix $\mathbf{M}$ and it seems that the coherence as a performance parameter is not as detailed analyzed in the literature as the RIP/RIC.

Therefore it would be beneficial to have an OMP variant that on one hand can be characterized by the RIP/RIC of the measurement matrix and secondly yields uniform results similarily to Theorem 4.5.1.

Fortunately, such an modified version has already been proposed under the name *Regularized Orthogonal Matching Pursuit* (ROMP) [44, 45]. As shown in [44] the ROMP algorithm perfectly fulfills the two desired properties:

Theorem 4.5.10. (Stability of ROMP under signal perturbations). *Suppose that the measurement vector $\mathbf{z}$ is given by $\mathbf{z} = \mathbf{M}\mathbf{x} + \mathbf{w}$ where $\mathbf{w}$ is some error vector. Assume a measurement matrix $\mathbf{M} \in \mathbb{C}^{m\times n}$ satisfies the RIC with parameters $(8k, \varepsilon)$ for $\varepsilon = \frac{0.01}{\sqrt{\ln n}}$. Consider an arbitrary vector $\mathbf{x}$ in $\mathbb{R}^n$. Then ROMP produces a good approximation $\hat{\mathbf{x}}$ to $\mathbf{x}$, i.e.,*

$$\|\hat{\mathbf{x}} - \mathbf{x}\|_2 \leq 160\sqrt{\ln 2k}\left(\|\mathbf{w}\|_2 + \frac{\|\mathbf{x} - \mathbf{x}_k\|_1}{\sqrt{k}}\right), \tag{4.61}$$

where $\mathbf{x}_k$ is obtained from $\mathbf{x}$ by zeroing all coefficients except the k largest.

In contrast to the performance result for BP presented above the result for ROMP is only valid for the real valued setting. However, one can easily transform any complex valued data model for CS into a real valued one for which the same sparsity properties are valid [53].

We now state the exact definition of ROMP:

1. **Initialize.** Given the measurement vector $\mathbf{z} \in \mathbb{R}^n$ and a sparsity level k we initialize the index set $I = \{\}$ and the residual $\mathbf{r} = \mathbf{z}$. We repeat the following steps until the residual $\mathbf{r}$ is sufficiently small.

2. **Identify.** Choose a set J of the k biggest coordinates in magnitude of the vector $\mathbf{u} = \mathbf{M}^H\mathbf{r}$, or all of its nonzero coordinates, whichever set is smaller.

3. **Regularize.** Among all subsets $J_0 \subset J$ with comparable coordinates, i.e,

$$|\mathbf{u}_i| \leq 2|\mathbf{u}_j| \quad \text{for all} \quad i, j \in J_0, \tag{4.62}$$

   choose J_0 with the maximal energy $\|\mathbf{u}|_{J_0}\|_2$.

4. **Update.** Add the set J_0 to the index set: $I \leftarrow I \cup J_0$, and update the residual:

$$\mathbf{r} = \mathbf{z} - \mathbf{M}\mathbf{y} \quad \text{with} \quad \mathbf{y} = \arg \min_{\text{supp}(v)=I} \|\mathbf{z} - \mathbf{M}\mathbf{v}\|_2. \tag{4.63}$$

5. Go back to the **Identify** step unless $\mathbf{r} = 0$.

We note that the "Regularize" step of ROMP does not imply combinatorial complexity, but actually can be done in linear time. More specifically, as shown in [45], the "Regularize" step has a computational complexity of $\mathcal{O}(k)$. A difference to the BP is that ROMP needs to know the sparsity degree S in advance because this is the sparsity level k used as an input for the ROMP algorithm. The BP itself does not need this information for its implementation. However, its performance also depends strongly on the sparsity of the signal vector $\mathbf{x}$ and the sparsity degree S for which the measurement matrix $\mathbf{M}$ satisfies the RIC.

StOMP - Stage Wise Orthogonal Matching Pursuit

Another derivative of OMP has been proposed in [16]. Their approach called *stagewise orthogonal matching pursuit* (StOMP) is based on a iterative scheme that uses a matched filter with thresholding of the output, a projection and a subtraction stage during each iteration. A big difference to OMP is that StOMP may select more than 1 column of $\mathbf{M}$ per stage. It is shown that in some cases StOMP is considerably faster than BP while yielding a recovery accuracy comparable to BP. Moreover, it is found that in some cases StOMP is even faster than ordinary OMP.

TOMP - Tree Based Orthogonal Matching Pursuit

As already mentioned above, the authors of [34] propose a modification of OMP that incorporates a second assumption on the signal vector $\mathbf{x}$ beside the sparsity assumption. They assume that $\mathbf{x}$ can be represented efficiently by a sparse tree with respect to a multi scale dictionary (e.g. based on wavelets). It is shown with the help of numerical studies that TOMP outperforms OMP if the signal $\mathbf{x}$ is a samples version of piecewise smooth signal.

4.5.3 Adaptive Recovery Schemes

So far we considered a fixed, though possibly random, measurement matrix $\mathbf{M}$. In particular the recovery algorithms use a fixed matrix $\mathbf{M}$ to compute an estimation of $\mathbf{x}$ from the measurements $\mathbf{z}$. However, in some cases the signal vector $\mathbf{x}$ itself can be represented by $\mathbf{x} = \mathbf{\Psi c}$, where the regular matrix $\mathbf{\Psi}$ represents a specific basis of $\mathbb{C}^n$ and $\mathbf{c}$ is the coefficient vector for $\mathbf{x}$ w.r.t this specific basis. Now, if the vector $\mathbf{c}$ is much more sparse than the signal vector $\mathbf{x}$ then it would be wiser to write the measurements as $\mathbf{z} = \mathbf{M'c}$ where the new measurement matrix $\mathbf{M'}$ is given by $\mathbf{M'} = \mathbf{M\Psi}$. With this new measurement matrix and corresponding generation model for $\mathbf{z}$ we can use conventional recovery schemes to recover the coefficient vector $\mathbf{c}$. This recovery can be expected to be more accurate than the original recovery of $\mathbf{x}$ from $\mathbf{z}$, if the sparsity of $\mathbf{c}$ is significantly lower then $\mathbf{x}$ and the new measurement matrix $\mathbf{M'}$ has approximately the recovery capabilities as the original measurement matrix $\mathbf{M}$ (which intuitively can be expected to be true, if $\mathbf{\Psi}$ represents an orthonormal basis, i.e., $\mathbf{\Psi}$ is a unimodular matrix).

The problem of finding an appropriate "sparsifying" basis matrix $\mathbf{\Psi}$ is investigated in [2, 46]. While in [46] one searches for the best dictionary over a predefined collection of dictionaries, in [2] one computes the dictionary which best fits the observations. In the following we will discuss the approach used in [46] in more detail.

Best Basis CS

So far we have considered only the canonical basis of $\mathbb{C}^n$ which is defined as the set $\{\mathbf{e}_k\}$ of n vectors, whereby $\mathbf{e}_k \in \mathbb{C}^n$ denotes the vector which has zero coefficients except at the kth position, i.e.,

$$e_k = \begin{pmatrix} 0 \\ \vdots \\ 1 \\ \vdots \\ 0 \end{pmatrix}. \tag{4.64}$$

The assumption of a sparse signal $\mathbf{x}$ in the basic data model (4.1) always refers to the expansion coefficients of $\mathbf{x}$ using the canonical basis $\{\mathbf{e}_k\}$. However, in some cases the signal vector $\mathbf{x}$ is not sparse in the canonical basis but rather in some other orthonormal basis. Let $\mathbf{\Psi}$ denote the matrix whose colums form an orthonormal basis (ONB) $\mathcal{B}$ for $\mathbb{C}^n$ (e.g. the DFT matrix $\mathbb{F}_n$ whose columns are complex sinusoids with equispaced frequencies). The fact that a signal vector $\mathbf{x}$ is sparse with respect to the ONB represented by the matrix $\mathbf{\Psi}$ is expressed by

$$\|\mathbf{\Psi}^H \mathbf{x}\|_0 \ll n. \tag{4.65}$$

An intuitive approach to incorporate the fact that the signal $\mathbf{x}$ is sparse with respect to a certain ONB represented by $\mathbf{\Psi}$ is to search the sparsest approximation of the observed measurement vector $\mathbf{z}$ by trying every ONB $\mathcal{B}_\lambda$ with the associated matrix $\mathbf{\Psi}_\lambda$ out of a proper dictionary $\mathcal{D}_\Lambda = \{\mathcal{B}_\lambda\}_{\lambda \in \Lambda}$. This is the key idea behind the following recovery scheme [46]

$$\hat{\mathbf{x}} = \arg \min_{g \in \mathbb{C}^n} \min_{\lambda \in \Lambda} \left(\frac{1}{2} \|\mathbf{M}g - \mathbf{z}\|_2^2 + t \|\mathbf{\Psi}_\lambda^H g\|_1 + C_0 t^2 \mathrm{pen}(\lambda) \right), \tag{4.66}$$

where the Lagrange multiplier t accounts for stabilization against the noise term $\mathbf{w}$ and that the sparsity of $\mathbf{x}$ is only given approximately. The term $C_0 t^2 \mathrm{pen}(\lambda)$ incorporates a measure for the "complexity" of the basis $\mathcal{B}_\lambda$. The quantity $\mathrm{pen}(\lambda)$ can be interpreted as an equivalent number of bits needed to specify a basis $\mathcal{B}_\lambda$ out of the dictionary (a detailed discussion of this quantity can be found in [46]).

The recovery scheme (4.66) is not feasible for large dictionaries $\mathcal{D}_\Lambda$ without any further assumptions. However, for the practical useful dictionary of local cosine bases, where each basis $\mathcal{B}_\lambda$ can be represented by a tree, there is a fast implementation for the search over the elements of $\mathcal{D}_\Lambda$ available. This implementation exploits the property of the objective function of (4.66), which we will denote by $\mathcal{L}(g, \lambda, t) = \frac{1}{2} \|\mathbf{M}g - \mathbf{z}\|_2^2 + t \|\mathbf{\Psi}_\lambda^H g\|_1 + C_0 t^2 \mathrm{pen}(\lambda)$, that it splits into a sum if the ONB $\mathcal{B}_\lambda$ can be written as a union of two bases:

$$\mathcal{B}_\lambda = \mathcal{B}_{\lambda_1} \cup \mathcal{B}_{\lambda_2} \Rightarrow \mathcal{L}(g, \lambda, t) = \mathcal{L}(g, \lambda_1, t) + \mathcal{L}(g, \lambda_2, t). \tag{4.67}$$

This splitting property of the objective $\mathcal{L}$ together with the tree representation for the elements $\mathcal{B}_\lambda$ of the dictionary of local cosine bases allows an algorithm for the search over the dictionary with a complexity $\mathcal{O}(n)$ where n denotes the dimension of the signal vector $\mathbf{x}$.

Note that this special tree representation for the dictionary consisting of local cosine bases is also exploited to obtain fast algorithms in a different context in [9] and [36].

4.6 Connection to Conventional Bayesian Estimation Theory

4.6.1 Bayesian Setup of CS Recovery

The basic data model of CS (4.1) together with the core problem of recovering the signal vector $\mathbf{x}$ from the incomplete (due to $m < n$) and inaccurate (due to the noise $\mathbf{w}$) measurements $\mathbf{z}$ can also be casted in a traditional estimation framework. We want to give an overview over the possibilities in Bayesian estimation theory (in contrast to classical estimation). As a starting point we cast the central data model of CS (4.1) for the noiseless case in the Bayesian estimation framework:

$$\mathbf{z} = \mathbf{M}\mathbf{x} \tag{4.68}$$

The quantities involved are:

- $\mathbf{x} \in \mathbb{C}^n$ is the *random* data vector, which we would like to estimate.
- $\mathbf{z} \in \mathbb{C}^m$ is the *random* measurement vector that we observe.
- $\mathbf{M} \in \mathbb{C}^{m \times n}$ is the known *deterministic* measurement matrix with typically $m \ll n$.

Within this section we assume that the measurement matrix $\mathbf{M}$ has full row rank, i.e, its rows are linearly independent. This makes sense because we want to perform compression on $\mathbf{x}$. If we would use a measurement matrix $\mathbf{M}$ with linearly dependent rows, we would use a measurement vector $\mathbf{z}$ of size m to encode a linear subspace whose dimension is exactly the row - rank of $\mathbf{M}$ and therefore has a smaller dimension than the "codeword" $\mathbf{z} \in \mathbb{C}^m$ would be able to encode. This would be clearly a waste of resources and therefore make no sense.

Now, as necessary for the Bayesian framework we assign a prior probability density function (pdf) to the signal vector $\mathbf{x}$, which in our specific case moreover has to model the sparsity of the signal vector. An intuitive approach is to use a prior pdf $f_{\mathbf{x}}(\mathbf{x})$ for $\mathbf{x}$ which is of the following form

$$f_{\mathbf{x}}(\mathbf{x}) = C_p e^{-\|\mathbf{x}\|_p^p}, \tag{4.69}$$

where p is a positive real number[10] and C_p is a normalization constant which ensures that the pdf integrates to 1. This specific form for the prior pdf implies that the single coefficients x_k of the signal vector $\mathbf{x}$ are i.i.d.. An important special case poses the choice $p = 1$. For this specific choice, the pdf is called a Laplacian distribution. The Laplacian prior is discussed in [30] where the authors also use Bayesian estimation theory for CS.

Given the prior and the measurement matrix $\mathbf{M}$, the recovery problem of CS can be reformulated as the problem of estimating the signal vector $\mathbf{x}$ from the observed measurement vector $\mathbf{z}$.

[10] The expression $\|\mathbf{x}\|_p^p$ is short for $\sum_k |\mathbf{x}_k|^p$, where $\mathbf{x}_k$ denotes the k-th coefficient of the vector $\mathbf{x}$. For $p < 1$ this expression does *not* define a norm.

In order to be able to calculate the corresponding Bayesian estimators, we have to determine the pdf $f_{\mathbf{z}}(\mathbf{z})$ of $\mathbf{z}$ as well as the conditional pdf $f(\mathbf{z}|\mathbf{x})$ of $\mathbf{z}$ conditioned on $\mathbf{x}$.

To that end, we first perform a singular value decomposition of the measurement matrix $\mathbf{M}$:

$$\mathbf{M} = \mathbf{U}\mathbf{\Sigma}\mathbf{V}^H \tag{4.70}$$

where $\mathbf{U} \in \mathbb{C}^{m\times m}$ and $\mathbf{V} \in \mathbb{C}^{n\times n}$ are orthonormal matrices, i.e, they satisfy

$$\mathbf{U}^H\mathbf{U} = \mathbf{I}_{m\times m} \tag{4.71}$$

and

$$\mathbf{V}^H\mathbf{V} = \mathbf{I}_{n\times n}. \tag{4.72}$$

$\mathbf{\Sigma} \in \mathbb{R}^{m\times n}$ is a rectangular diagonal matrix whose diagonal elements are the singular values of $\mathbf{M}$ arranged in decreasing order.

After some elementary calculations[11] one finds the following expression for the pdf $f_{\mathbf{z}}(\mathbf{z})$

$$f_{\mathbf{z}}(\mathbf{z}) = C_1 \int_{y_{m+1}\dots y_n} f_{\mathbf{x}}(\mathbf{V}\cdot[(\mathbf{\Lambda}^{-1}\mathbf{U}^H\mathbf{z})^H \quad y_{m+1} \quad \dots \quad y_n]^H) dy_{m+1}\dots dy_n. \tag{4.73}$$

where $\mathbf{\Lambda} \in \mathbb{R}^{m\times m}$ is a quadratic diagonal matrix whose diagonal is obtained from the main diagonal of $\mathbf{\Sigma}$. Here m denotes the number of rows of the measurement matrix $\mathbf{M}$ and C_1 is again a normalization constant that ensures that $f_{\mathbf{z}}(\mathbf{z})$ integrates to one and depends only on the measurement matrix $\mathbf{M}$.

For the conditional pdf $f_{\mathbf{z}|\mathbf{x}}(\mathbf{z}|\mathbf{x})$ one obtains:

$$f(\mathbf{z}|\mathbf{x}) = C_2\delta(\mathbf{z} - \mathbf{M}\mathbf{x}) \tag{4.74}$$

where $\delta(\cdot)$ denotes the multidimensional Dirac distribution and C_2 is again a normalization constant.

4.6.2 Recovery Based On Bayesian Estimators

As already mentioned above, the problem of recovering $\mathbf{x}$ from $\mathbf{z}$ can also be interpreted as the problem of estimating $\mathbf{x}$ from $\mathbf{z}$. Within the Bayesian framework we interpret the signal vector $\mathbf{x}$ and the measurement vector $\mathbf{z}$ as a realization of the random vectors $\mathbf{x}$ and $\mathbf{z}$.[12] To model the

[11] $f_{\mathbf{V}^H\mathbf{x}}(\mathbf{a}) = f_{\mathbf{x}}(\mathbf{V}\mathbf{a})$. $f_{\mathbf{\Sigma}\mathbf{V}^H\mathbf{x}}(\mathbf{b}) = \frac{1}{\det\mathbf{\Lambda}}\int_{y_{m+1}\dots y_n} f_{\mathbf{x}}(\mathbf{V}[(\mathbf{\Lambda}^{-1}\mathbf{b})^H \quad y_{m+1} \quad \dots \quad y_n]^H) dy_{m+1}\dots dy_n$ where $\mathbf{\Lambda} \in \mathbb{R}^{m\times m}$ is a quadratic diagonal matrix whose diagonal is obtained from the main diagonal of $\mathbf{\Sigma}$. Because we assume that $\mathbf{M}$ has full rank, the diagonal elements of $\mathbf{\Sigma}$ can be chosen to be positive which implies that the inverse $\mathbf{\Lambda}$ exists.

[12] By an abuse of notation we use the same symbol for the random variable and a specific realization of this random variable. The exact meaning should be clear from the context.

sparsity of $\mathbf{x}$, we use a prior pdf for the random signal vector $\mathbf{x}$ that assigns a relatively large probability to sparse realizations $\mathbf{x}$.

Two prominent Bayesian estimation schemes are the *Minimum Mean Square Error* (MMSE) - estimator and the *Maximum A Posteriori* (MAP) - estimator. They only differ in the performance measure used for their design. Whereas the MMSE estimator minimizes the expected squared error norm between the signal vector $\mathbf{x}$ and the estimated (using only the measurement vector $\mathbf{z}$) signal vector $\hat{\mathbf{x}}$, the MAP estimator minimizes the probability of the event $\{\mathbf{x} \neq \hat{\mathbf{x}}\}$.

MAP estimator

The MAP estimator $\hat{\mathbf{x}}_{\text{MAP}}$ of the signal vector $\mathbf{x}$ using only the measurement vector $\mathbf{z}$ is given by:

$$\hat{\mathbf{x}}_{\text{MAP}} = \arg\max_{\mathbf{x}} f(\mathbf{x}|\mathbf{z}). \tag{4.75}$$

The expression for the MAP estimator can be shown to be equivalent to

$$\begin{aligned} \hat{\mathbf{x}}_{\text{MAP}} &= \arg\max_{\mathbf{x}} \left\{ f(\mathbf{z}|\mathbf{x}) \frac{f_{\mathbf{x}}(\mathbf{x})}{f_{\mathbf{z}}(\mathbf{z})} \right\} \\ &= \arg\max_{\mathbf{x}} \{ f(\mathbf{z}|\mathbf{x}) f_{\mathbf{x}}(\mathbf{x}) \} \end{aligned} \tag{4.76}$$

where we used Bayes' rule for manipulating conditional probabilities and the fact that the term $\frac{1}{f_{\mathbf{z}}(\mathbf{z})}$ is irrelevant for the maximization over $\mathbf{x}$.

MMSE estimator

The MMSE estimator $\hat{\mathbf{x}}_{\text{MMSE}}$ of the signal vector $\mathbf{x}$ using only the measurement vector $\mathbf{z}$ is given by:

$$\hat{\mathbf{x}}_{\text{MMSE}} = \mathrm{E}\{\mathbf{x}|\mathbf{z}\}. \tag{4.77}$$

This expression can be developed as follows

$$\begin{aligned} \hat{\mathbf{x}}_{\text{MMSE}} &= \mathrm{E}\{\mathbf{x}|\mathbf{z}\} \\ &= \int_{\mathbf{x}_1 \ldots \mathbf{x}_n} \mathbf{x} f(\mathbf{z}|\mathbf{x}) \frac{f_{\mathbf{x}}(\mathbf{x})}{f_{\mathbf{z}}(\mathbf{z})} d\mathbf{x}_1 \ldots d\mathbf{x}_n \\ &= \frac{1}{f_{\mathbf{z}}(\mathbf{z})} \int_{\mathbf{x}_1 \ldots \mathbf{x}_n} \mathbf{x} f(\mathbf{z}|\mathbf{x}) f_{\mathbf{x}}(\mathbf{x}) d\mathbf{x}_1 \ldots d\mathbf{x}_n, \end{aligned} \tag{4.78}$$

and furthermore, by inserting the expression (4.74) for the conditional pdf $f(\mathbf{z}|\mathbf{x})$,

$$\begin{aligned}
\hat{\mathbf{x}}_{\text{MMSE}} &= \frac{C_2}{f_{\mathbf{z}}(\mathbf{z})} \int_{\mathbf{x}_1 \ldots \mathbf{x}_n} \mathbf{x}\delta(\mathbf{z} - \mathbf{M}\mathbf{x}) f_{\mathbf{x}}(\mathbf{x}) \quad d\mathbf{x}_1 \ldots d\mathbf{x}_n \\
&= \frac{C_2}{f_{\mathbf{z}}(\mathbf{z})} \int_{\mathbf{x}_1 \ldots \mathbf{x}_n} \mathbf{x}\delta(\mathbf{z} - \mathbf{U}\boldsymbol{\Sigma}\mathbf{V}^H\mathbf{x}) f_{\mathbf{x}}(\mathbf{x}) \quad d\mathbf{x}_1 \ldots d\mathbf{x}_n \\
&= \frac{C_2}{f_{\mathbf{z}}(\mathbf{z})} \int_{\mathbf{y}_{m+1} \ldots \mathbf{y}_n} \int_{\mathbf{y}_1 \ldots \mathbf{y}_m} \delta(\mathbf{z} - \mathbf{U}\boldsymbol{\Lambda}\mathbf{y}_{1..m}) \mathbf{V}\mathbf{y} f_{\mathbf{x}}(\mathbf{V}\mathbf{y}) \quad d\mathbf{y}_1 \ldots d\mathbf{y}_n \\
&= \frac{C_2}{f_{\mathbf{z}}(\mathbf{z}) \det \boldsymbol{\Lambda}} \int_{\mathbf{y}_{m+1} \ldots \mathbf{y}_n} \int_{y'} \delta(\mathbf{z} - \mathbf{y}') \mathbf{V}[\left(\boldsymbol{\Lambda}^{-1}\mathbf{U}^H\mathbf{y}'\right)^H \quad \mathbf{y}_{m+1} \quad \ldots \quad \mathbf{y}_n]^H \\
&\qquad \times f_{\mathbf{x}}(\mathbf{V}[\left(\boldsymbol{\Lambda}^{-1}\mathbf{U}^H\mathbf{y}'\right)^H \quad \mathbf{y}_{m+1} \quad \ldots \quad \mathbf{y}_n]^H) \quad d\mathbf{y}' d\mathbf{y}_{m+1} .. d\mathbf{y}_n \\
&= \frac{C_2}{f_{\mathbf{z}}(\mathbf{z}) \det \boldsymbol{\Lambda}} \int_{\mathbf{y}_{m+1} \ldots \mathbf{y}_n} \mathbf{V}[\left(\boldsymbol{\Lambda}^{-1}\mathbf{U}^H\mathbf{z}\right)^H \quad \mathbf{y}_{m+1} \quad \ldots \quad \mathbf{y}_n]^H \\
&\qquad \times f_{\mathbf{x}}(\mathbf{V}[\left(\boldsymbol{\Lambda}^{-1}\mathbf{U}^H\mathbf{z}\right)^H \quad \mathbf{y}_{m+1} \quad \ldots \quad \mathbf{y}_n]^H) \quad d\mathbf{y}_{m+1} .. d\mathbf{y}_n
\end{aligned} \tag{4.79}$$

where $\boldsymbol{\Lambda} \in \mathbb{R}^{m \times m}$ denotes the diagonal matrix that is made up of the elements of the main diagonal of $\boldsymbol{\Sigma}$ and $\mathbf{y}_{1\ldots m}$ denotes a vector of size m that consists of the first m elements of $\mathbf{y}$. Again, C_2 is just a normalization constant.

Although we have found closed form expressions for the MAP and MMSE estimators for the recovery of the signal vector $\mathbf{x}$ from the observed measurement vector $\mathbf{z}$ the implementation of this scheme is rather expensive regarding computational complexity. However the approach to use MAP and MMSE estimators within a Bayesian framework is also pursued in [51]. There, a modeling of the prior probability of $\mathbf{x}$ is used that differs from our proposal in (4.69). Furthermore, the authors of [51] used a more specific type of measurement matrix $\mathbf{M}$, more precisely they used "sparse" matrices, i.e., only few entries of $\mathbf{M}$ are nonzero. With this assumption they are able to construct algorithms that approximate the solutions of the MAP and MMSE estimators, given in (4.77) and (4.75). Their construction is based on a graph representation of the measurement matrix and a method called "message passing" that is also extensively used for decoders of *low density parity check* (LDPC) codes.

Chapter 5

Spectrum-Estimation Using CS

5.1 Introduction

We already encountered the problem of estimating the WVS of an underspread process in Section 3.5. There, we exploited only the properties of underspread processes.

In this chapter we combine the results for underspread processes and for CS in order to design a CS based WVS estimator for an underspread process $X(t)$. Because the WVS is fully equivalent to the autocorrelation function $r_X(t_1, t_2)$ and therefore also to the correlation operator $\mathbf{R}_X$ we could call the estimator also a "CS based correlation estimator" for underspread processes.

We would like to discuss two approaches which are fundamentally different in their structure. Roughly speaking, the two schemes differ in the order in which CS and estimation is applied. The first scheme will be called "Random Sampling of the Filterbank" and is a quite obvious synthesis of CS results with the theory of underspread processes. The second one, coined "Random Sampling of the EAF" is not such a straightforward combination of CS and underspread processes as the first but we believe that it is an interesting alternative with its pros and cons vs. the other scheme.

5.2 Motivating Example – Cognitive Radio

In this section we would like to present a case study for a potential application of the estimator schemes that will be developed. We consider a cognitive radio system, i.e., we a have L transmitters with associated data sequences $X_k[n]$ with $k = 1...L$, which are modeled as (wide sense) stationary white discrete time random processes. This implies:

$$\mathrm{E}\{X_k[n]X_k^*[n']\} = P_k\delta[n - n']. \tag{5.1}$$

We furthermore assume that the data sequences of different users are statistically independent, i.e., the sequences $X_k[n]$ and $X_{k'}[n]$ are independent (and therefore also uncorrelated) if $k \neq k'$. Let us

consider a further host "R", that wishes to start a transmission. A characteristic of cognitive radio systems is that there is no fix allocation of frequency intervals ("bandwidths") to specific users. Therefore the host R has to scan the complete bandwidth that is reserved for the cognitive radio system and whose size is usually magnitudes larger than the bandwidth required by one single host. If he finds an unoccupied frequency region then he will start his transmission there.

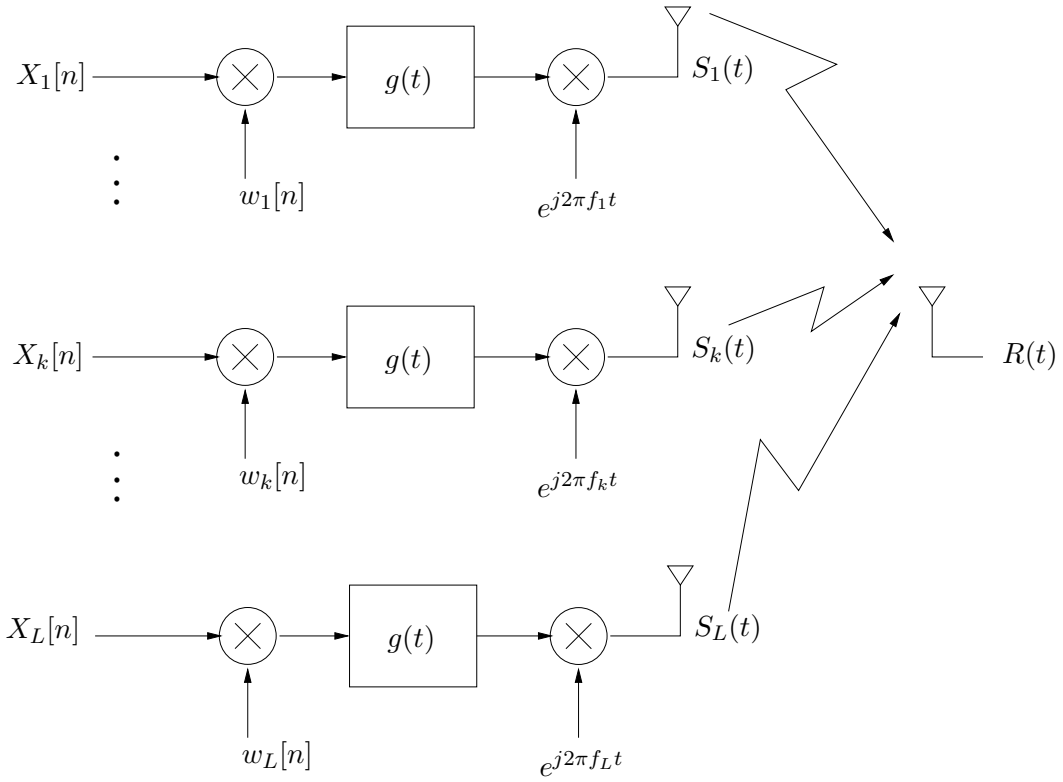

Figure 5.1: Simple model of a cognitive radio system.

A very simple picture of this cognitive radio scenario is shown in Figure 5.1. Each transmitter employs a pulse amplitude modulation (PAM) scheme with a linear time invariant (LTI) pulse filter $g(t)$. The multiplication with the window functions $w_k[n]$ models the fact that data is transmitted in a bursty fashion, which is typical for radio systems that use a CSMA (Carrier Sense Multiple Access) scheme at the data link layer (e.g. IEEE802.11). Each transmitter signal $S_k(t)$ can therefore be written as

$$S_k(t) = \sum_{n=w_{k_1}}^{w_{k_2}} X_k[n] g(t - nT_s) e^{j2\pi f_k t} \tag{5.2}$$

where w_{k_1} and w_{k_2} denotes the (discrete) start and stop time of the window $w[n]$ at node k. For the sake of simplicity, we assume that the physical radio transmission between the antennas only

causes a multiplicative change of the signals and moreover the multiplicative factor is the same for all signals. This multiplicative factor is chosen to be 1. Therefore the scanning signal $R(t)$ at node "R" can be written as a superposition of all transmitted signals, i.e.,

$$R(t) = \sum_{m=1}^{K} S_m(t) \tag{5.3}$$

In the following, we will show that under reasonable conditions $R(t)$ satisfies the two fundamental properties of our thesis, i.e., it is an underspread random process that moreover yields sparse analyzing coefficients using a proper WH-set. Therefore we can use CS in the front end of "R" in order to reduce the effective sampling rates while incurring only small errors. To that end, we calculate the correlation function $r_{S_k}(t_1, t_2)$ of the transmitted signals $S_k(t)$, i.e.,

$$\begin{aligned} r_{S_k}(t_1, t_2) &= \mathrm{E}\{S_k(t_1) S_k^*(t_2)\} \\ &= \mathrm{E}\left\{ \sum_{l=w_{k_1}}^{w_{k_2}} \sum_{l'=w_{k_1}}^{w_{k_2}} X_k[l] X_k^*[l'] g(t_1 - lT_s) g^*(t_2 - l'T_s) \right\} \\ &= P_k \sum_{l=w_{k_1}}^{w_{k_2}} g(t_1 - lT_s) g^*(t_2 - lT_s). \end{aligned} \tag{5.4}$$

Here, P_k denotes the mean signal power of $X_k[n]$. Note that it is assumed here that each transmitter sends only one single burst of data, because we use a box shaped window. However, because each data sequence is white, contributions to the correlation function $r_{S_k}(t_1, t_2)$ of potential additional transmission bursts in each transmitter can be simply added. For multiple bursts the window function of the k-th transmitter has to be replaced by a superposition of non-overlapping box-shaped functions.

From the correlation function we calculate the EAF $\bar{A}_{S_k}(\tau, \nu)$ of the transmitted signals as

$$\begin{aligned} \bar{A}_{S_k}(\tau, \nu) &= \int_t r_{S_k}\left(t + \frac{\tau}{2}, t - \frac{\tau}{2}\right) e^{-j2\pi\nu t} dt \\ &= \int_t P_k \sum_{l=w_{k_1}}^{w_{k_2}} g\left(t + \frac{\tau}{2} - lT_s\right) g^*\left(t - \frac{\tau}{2} - lT_s\right) e^{-j2\pi\nu t} dt \\ &= P_k \sum_{l=w_{k_1}}^{w_{k_2}} \int_t g\left(t + \frac{\tau}{2} - lT_s\right) g^*\left(t - \frac{\tau}{2} - lT_s\right) e^{-j2\pi\nu t} dt \\ &= P_k \sum_{l=w_{k_1}}^{w_{k_2}} A_g(\tau, \nu) e^{-j2\pi\nu l T_s} \qquad (5.5) \\ &= P_k A_g(\tau, \nu) \sum_{l=w_{k_1}}^{w_{k_2}} e^{-j2\pi\nu l T_s}. \qquad (5.6) \end{aligned}$$

For burst lengths not too small (e.g. $w_{k_2} - w_{k_1} \geq 100$) the factor $\sum_{l=w_{k_1}}^{w_{k_2}} e^{-j2\pi\nu l T_s}$ approximates a dirac comb[1] along the ν axis with a period of $\frac{1}{T_s}$ which means that it "masks" the factor $A_g(\tau,\nu)$ in ν direction. This masking effect causes the signal $S_k(t)$ to be underspread, provided that the ambiguity function $A_g(\tau,\nu)$ of the transmit pulse is well concentrated around the origin in τ direction. If we now assume that there are only a few transmitters relative to the whole system bandwidth (which is typical for cognitive radio systems because otherwise it would be wiser to allocate fix frequency bands to the transmitters) then $R(t)$ is the superposition of only a few underspread processes and is therefore underspread and sparse (relative to the whole bandwidth of the cognitive radio system).

To further illustrate the masking effect described above, which has the effect that the effective support of $\bar{A}_{S_k}(\tau,\nu)$ is small, i.e., S_k is underspread, we simulated a PAM transmitter using a raised cosine pulse shape[2], i.e.,

$$g_\alpha(t) = \operatorname{sinc}\left(\frac{t}{T_s}\right) \cdot \frac{\cos\left(\pi\alpha\frac{t}{T_s}\right)}{1 - 4\alpha^2\left(\frac{t}{T_s}\right)^2} \tag{5.7}$$

where the parameter α denotes the roll off factor and takes on values from $[0,1]$ and where we used the "sinc" function:

$$\operatorname{sinc}(x) \triangleq \frac{\sin(x)}{x}. \tag{5.8}$$

For $\alpha = 0$ the raised cosine pulse $g_{\alpha=0}(t)$ degenerates to the conventional "sinc" pulse whose Fourier transform is box shaped. At the other extreme: $\alpha = 1$, the raised cosine pulse $g_{\alpha=1}(t)$ needs twice the bandwidth as the sinc-pulse using the same symbol period T_s. However, $g_{\alpha=1}(t)$ has a much better time concentration, making digital implementations a lot easier.

We simulated two simple PAM transmitters which used the same parameters: A roll-off factor $\alpha = 0.3$ and a burst length of 10 PAM symbols. The symbols are i.i.d. from the alphabet $\{-1,1\}$. In Figure 5.2 we show a gray scale plot of the EAF $\bar{A}_R(\tau,\nu)$ of the received signal

$$R(t) = S_1(t) + S_2(t) \tag{5.9}$$

as well as a contour plot ot the WVS $\overline{W}_R(t,f)$ of $R(t)$. The added reference rectangle in the (τ,ν) plane illustrates the underspreadness of $R(t)$. However, the burst length of 10 symbols is rather low, for more realistic values (say 1000), the masking effect described above should be even stronger leading to a higher degree of underspreadness of $R(t)$.

[1] Carefully note that this approximation is not true in a quantitative sense at all because a dirac comb has an infinite power whereas the power of $\sum_{l=w_{k_1}}^{w_{k_2}} e^{-j2\pi\nu l T_s}$ is always finite. What is meant here is that the effective support of the periodic (w.r.t. ν) signal $\sum_{l=w_{k_1}}^{w_{k_2}} e^{-j2\pi\nu l T_s}$ goes to zero if $w_{k_2} - w_{k_1}$ goes to infinity.

[2] In practice the raised cosine filter is split up into two root raised cosine filters, one located at the transmitter and the other one serving as a matched filter at the receiver.

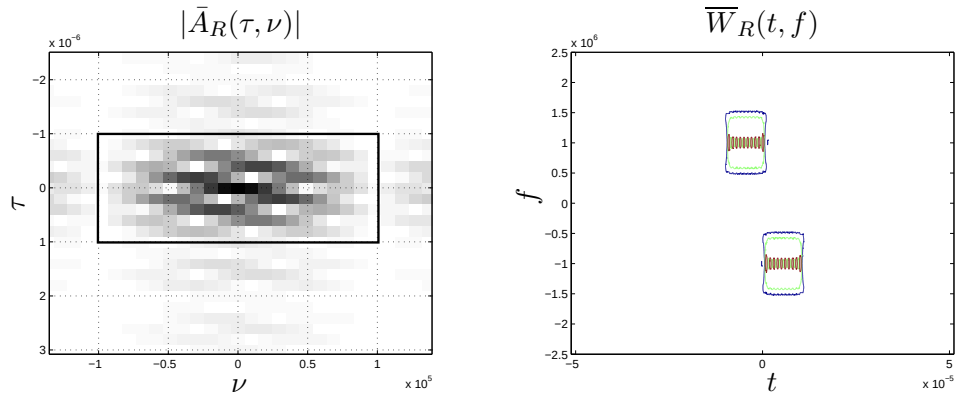

(a) (b)

Figure 5.2: (a) EAF of the received signal (darker shades correspond to larger magnitudes). The rectangle has an area of 0.4, (b) WVS of the received signal (the lowest contour is about 1 percent of the maximum).

5.3 Measuring the Sparsity of an Underspread Random Process $X(t)$

Before we can discuss any CS based estimator scheme we have to clarify the notion of "sparseness" and "sparsity" in the context of underspread random processes. According to Chapter 4, CS operates on the finite dimensional vector space $\mathbb{C}^n$. There, the notion of "sparseness" was identified with the number of (effectively) nonzero entries.

The question arises, how to adopt this definition to a random process $X(t)$. As already mentioned further above, a straightforward way is to consider the coefficients of an analyzing WH-set $\mathcal{G} = (g(t), T, F)$ (not necessarily a Gabor frame):

$$C_{k,l} = \langle X, g_{k,l} \rangle = \int_t X(t) g^*(t - kT) e^{-j2\pi lFt} dt \tag{5.10}$$

and to define the sparsity of $X(t)$ via the sparsity of a (suitable) truncated version[3] of the coefficients $C_{k,l}$. However, the $C_{k,l}$ are random quantities and therefore the sparsity of the $C_{k,l}$ would be a random quantity. As discussed below we will be interested in the mean squared errors of our estimator schemes. Therefore we are primarily interested in a mean sparsity of the $C_{k,l}$.

[3]Throughout this thesis we assume that the WVS $\overline{W}_X(t,f)$ of any random process $X(t)$ always is supported within a sufficiently large rectangle. The lengths of the rectangle can be interpreted as maximum signal duration and effective bandwidth, respectively.

Furthermore as indicated by the central performance results for the BP (Theorem 4.5.1) and ROMP (Theorem 4.5.10) the sparsity of a vector can be defined via the norm of the tail[4] relative to the entire energy (= squared ℓ_2-norm) of the vector. Although in (4.19) and (4.61) the ℓ_1-norm is used we will use the quadratic norm for two reasons: firstly, the ℓ_1-norm can always be upper bounded by the quadratic norm and secondly, the quadratic norm will lead to approximate expressions that are directly related to (sample values of) the WVS $\overline{W}_X(t,f)$ of the process $X(t)$[5].

A drawback of such a definition of a mean sparsity is, that it depends on the lattice (kT, lF) in the TF-plane that is used by the WH-set $\mathcal{G}$ and on the center of gravity of the WD of the prototype function used by the WH-set $\mathcal{G}$. Because we will exclusively use prototype functions that are well localized and centered around the origin in the TF-plane (e.g. a Gaussian) and the fact that the WVS $\overline{W}_X(t,f)$ of an underspread process $X(t)$ does not vary too much within an rectangle of size TF if T and F are chosen not too large relative to the inverse of the effective support of $\bar{A}_X(\tau,\nu)$[6], the exact choice of T and F will have not a dramatic impact on the sparsity measure.

However, it will turn out that it is wiser to define a sparsity without using a Gabor analysis but use directly the exact shape of the WVS of the process, i.e., to stack the sample values of the WVS along the lattice (kT, lF) into a vector $\mathbf{c}$ and use this vector to measure the (TF-) sparsity of the random process. Summarizing this discussion, given an underspread random process $X(t)$ and lattice constants T, F that are such that the effective support of $\bar{A}_X(\tau,\nu)$ is supported within $[-\frac{1}{2F}, \frac{1}{2F}] \times [-\frac{1}{2T}, \frac{1}{2T}]$, we measure the sparsity of an underspread $X(t)$ process as follows:

- Firstly, after suitable truncation of the WVS, we stack the values $\{\overline{W}_X(kT, lF)\}_{k,l}$ into a vector $\mathbf{c}$:

$$\mathbf{c} \triangleq \mathrm{vec}\{\{\overline{W}_X(kT, lF)\}_{k,l}\} \tag{5.11}$$

  where $\mathrm{vec}\{\cdot\}$ denotes the operation that stacks the columns of a matrix into a vector (see the appendix for details).

- Secondly, we measure the sparsity to degree S of the underspread process $X(t)$ via the ratio of the energy that is contained within the tail of $\mathbf{c}$ relative to the energy (squared norm) of $\mathbf{c}$:

$$\sigma_S \triangleq \frac{\|\mathbf{c} - \mathbf{c}_S\|_2^2}{\|\mathbf{c}\|_2^2} \tag{5.12}$$

[4]The tail of a vector refers to the coefficients that are below a certain threshold or to coefficients that are not contained in the set of the S largest coefficients, where $S \in \mathbb{N}$ denotes the sparsity order.

[5]More specifically, the variances $\mathrm{E}\{|C_{k,l}|^2\}$ of the Gabor coefficients $C_{k,l}$ are equal to the values of the physical spectrum (cf. Section 2.6) of $X(t)$ evaluated at the grid of the analyzing WH-set: $\mathrm{E}\{|C_{k,l}|^2\} = \mathrm{PS}_X^{(g)}(t,f)$. However, for an underspread process $X(t)$ the physical spectrum $\mathrm{PS}_X^{(g)}(t,f)$ becomes approximately equal the WVS $\overline{W}_X(t,f)$ [38, 40]

[6]More precisely, the EAF $\bar{A}_X(\tau,\nu)$ should have most of its energy with the rectangle $[-\frac{1}{2F}, \frac{1}{2F}] \times [-\frac{1}{2T}, \frac{1}{2T}]$ in the (τ,ν)-plane.

were $\mathbf{c}_S$ denotes the vector that is obtained from $\mathbf{c}$ by zeroing all coefficients except the specific S ones whose magnitudes are the largest. We will denote the set of (k,l) for which the sample values $\overline{W}_X(kT,lF)$ are not among the S largest of all sample values $\overline{W}_X(kT,lF)$ within the effective support of $\overline{W}_X(t,f)$ by Ω.

For an underspread process the quantity σ_S can be well approximated by:

$$\sigma_S \approx TF\frac{\sum_{(k,l)\in\Omega}\overline{W}_X^2(kT,lF)}{\|R_X\|_2^2} \tag{5.13}$$

where we used the fact that the squared norm of $\overline{W}_X(t,f)$ is approximately equal to $TF\sum_{k,l}\overline{W}_X^2(kT,lF)$ if T,F are suitable chosen, i.e., aliasing effects due to sampling can be neglected (cf. Theorem 3.6).

In the next two sections we will develop approximate performance bounds, more specifically approximate upper bounds on the mean squared error (MSE) of spectrum estimators using CS. These approximate bounds will use the quantity σ_S for a given sparsity degree S in order to measure the (TF-)sparsity of a given process. However, this method leads to pessimistic bounds because the performance of the CS recovery strategies fundamentally depend on the sparsity of the signal vector $\mathbf{x}$ which is in our case a single realization of the process $X(t)$. It may happen that for a single realization of $\mathbf{x}$ the spectrum, more specifically the Wigner Distribution $W_x(t,f)$, has its maximum values at locations in the TF-plane that are different from the locations where the WVS $\overline{W}_X(t,f)$ attains its maximum values. Therefore if we use σ_S, we fix *a priori* the locations which are regarded as the positions of the smaller spectral values in the TF plane even if one single realization has its energy concentrated on a different region in the TF plane. The simulations in the next chapter will support this reasoning.

5.4 Random Sampling of the Filterbank

The WVS estimator scheme "Random Sampling of the Filterbank" has a structure similar to the scheme proposed in Section 3.5. A big difference is that the CS based estimator uses a CS measurement stage after the sampled filterbank. The estimator scheme is illustrated in Figure 5.3. The first two blocks, the sampled filterbank (with the parameters $g(t)$,T and F specifying the

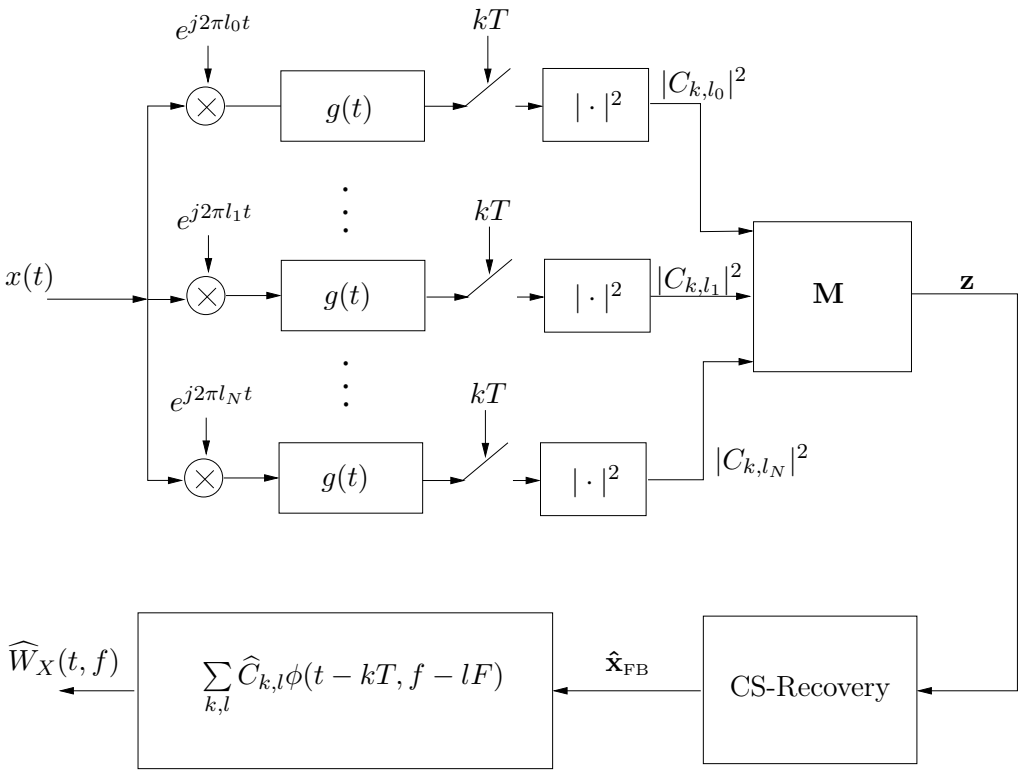

Figure 5.3: Block diagram of the estimator scheme "Random Sampling of the Filterbank" using the analyzing WH-set $\mathcal{G} = (g(t), T, F)$. The summation index l of the last (reconstruction) block ranges over the set $\{l_0, ..., l_N\}$.

corresponding WH-set) which computes the inner products[7] :

$$C_{k,l} = \left\langle X(t), g(t-kT)e^{j2\pi lFt} \right\rangle \tag{5.14}$$

and the measurement stage (represented by the measurement matrix $\mathbf{M}$) might be grouped together in a so called "CS sensor". This naming would indicate that this group represents a device that takes few measurements on the process $X(t)$ in order to finally estimate the WVS $\overline{W}_X(t,f)$. The output of this sensor are the measurements, represented by the vector $\mathbf{z} \in \mathbb{C}^m$, which is given as:

$$\mathbf{z} = \mathbf{M}\mathbf{x}_{\mathrm{FB}} \tag{5.15}$$

where the random vector $\mathbf{x}_{\mathrm{FB}}$ is constructed from the (suitable truncated) set of Gabor coefficients $C_{k,l}$ via the vec operation

$$\mathbf{x}_{\mathrm{FB}} = \mathrm{vec}\{|C_{k,l}|^2\}. \tag{5.16}$$

The measurements $\mathbf{z}$ are then fed into the spectrum estimator, which performs the following tasks:

1. It employs BP or ROMP in order to recover the original coefficients $\mathbf{x}_{\mathrm{FB}}$ from the measurements $\mathbf{z}$ resulting in a vector of estimated coefficients $\hat{\mathbf{x}}_{\mathrm{FB}}$:

$$\hat{\mathbf{x}}_{\mathrm{FB}} = \mathrm{vec}\left\{\widehat{C}_{k,l}\right\}. \tag{5.17}$$

   The elements $\widehat{C}_{k,l}$ of this vector are approximately equal to the magnitude squared Gabor coefficients, i.e., to $|C_{k,l}|^2$.

2. The result of the recovery $\hat{\mathbf{x}}_{\mathrm{FB}}$ is then used for the estimation of WVS $\overline{W}_X(t,f)$ of $X(t)$ by an estimator of the form

$$\widehat{W}_X(t,f) = \sum_{k,l} \widehat{C}_{k,l}\phi(t-kT, f-lF) \tag{5.18}$$

   where the summation range corresponds to the truncated set of Gabor coefficients. Note that for a given underspread process $X(t)$ the output of the estimator $\widehat{W}_X(t,f)$ is in general different to the following estimator:

$$\widetilde{W}_X(t,f) = \sum_{k,l} |C_{k,l}|^2\phi(t-kT, f-lF) \tag{5.19}$$

[7] We assume that the energy, or more precisely the WVS $\overline{W}_X(t,f)$, of the process $X(t)$ is effectively supported within a certain region in the TF plane. Therefore for the computation of the Gabor coefficients $C_{k,l}$ we consider only those indices (k,l) for which the point (kT, lF), where T and F are the lattice constants of the analyzing WH-set, is within the effective support of $\overline{W}_X(t,f)$. For formal convenience we additionally assume that this set of indices forms a "rectangle", i.e., the set is of the form $\{(k,l)|k_0 \le k \le k_1 \,\mathrm{and}\, l_0 \le l \le l_1\}$. In this case the values $C_{k,l}$ can be directly represented as a matrix which then will be denoted by $\{C_{k,l}\}$.

where the summation range corresponds to the truncated set of Gabor coefficients. We note that (5.19) defines the same estimator as in Section 3.5. Indeed, the estimator introduced in Section 3.5 can be regarded as the limiting case of the estimator $\widehat{W}_X(t,f)$ when no compression is used. The reason for the difference between $\widehat{W}_X(t,f)$ and $\widetilde{W}_X(t,f)$ is due to the fact that the estimator here uses the recovered coefficients $\hat{\mathbf{x}}_{\mathrm{FB}}$ which will in general deviate from the coefficients $\mathbf{x}_{\mathrm{FB}}$ which are essentially the output of the filter bank.

It remains to choose the measurement matrix $\mathbf{M}$ (i.e., in particular the number of measurements m which is related to the mean sparsity of $\mathbf{x}_{\mathrm{FB}}$) as well as the analyzing WH-set, i.e., the prototype function $g(t)$ and the lattice constants T and F. The lattice constants T and F are also used for the design of the estimator which furthermore requires a choice for the reconstruction kernel $\phi(t,f)$.

The choice for $g(t)$,T,F and $\phi(t,f)$ is motivated by the discussion of Section 3.5. As mentioned there, we choose the lattice constants T,F such that the effective support of the EAF $\bar{A}_X(\tau,\nu)$ of $X(t)$ is approximately supported within the rectangle $[-\frac{1}{2F},\frac{1}{2F}]\times[-\frac{1}{2T},\frac{1}{2T}]$ in the (τ,ν)-plane. Then we choose a reconstruction kernel $\phi(t,f)$, whose Fourier transform $\Phi(\tau,\nu)$ is given as in (5.26) below (see also the justification for this choice discussed there). It remains to determine $\mathbf{M}$. To that end we use the specific sparsity order $S\in\mathbb{N}$ for which the parameter σ_S, introduced above, is below a certain threshold η, where η is a small positive real number.

If we have fixed the value of S we can choose a specific measurement matrix $\mathbf{M}$. We will use two alternative choices: the Gaussian ensemble and the sampled Fourier matrix (see Section 4.4.5). As a rule of thumb [50, 53] we use the following formulas for m:

- For the Gaussian ensemble $m = 11.7\cdot S\left[1.5+\ln\frac{n}{S}\right]$
- and for the sampled Fourier matrix $m = C_3\,(\ln n)^4\cdot S$ with a constant C_3 whose exact value seems to be unknown yet. However as pointed out in [53] for this choice of m and a dimension n that is not too small, the Fourier matrix will yield a successful CS-recovery for reasonable values of C_3 with extremely high probability.

In the following we present upper bounds on the expected squared estimation error:

$$e_{\mathrm{FB}} \triangleq \mathrm{E}\{\|\widehat{W}_X(t,f)-\overline{W}_X(t,f)\|_2^2\} \tag{5.20}$$

under the assumption that $\mathbf{M}$ satisfies the RIC of BP and ROMP. To that end we rewrite the difference $\widehat{W}_X(t,f)-\overline{W}_X(t,f)$ and use the triangle inequality for norms:

$$\sqrt{e_{\mathrm{FB}}} \le \sqrt{\mathrm{E}\{\|\widehat{W}_X(t,f)-\widetilde{W}_X(t,f)\|_2^2\}} + \sqrt{\mathrm{E}\{\|\widetilde{W}_X(t,f)-\overline{W}_X(t,f)\|_2^2\}}. \tag{5.21}$$

The second term $\sqrt{\mathrm{E}\{\|\widetilde{W}_X(t,f)-\overline{W}_X(t,f)\|_2^2\}}$ is equal to $\sqrt{\varepsilon_{\mathrm{simple}}}$ where $\varepsilon_{\mathrm{simple}}$ denotes the mean squared error of the estimator itself (without considering the CS stage which means to set formally

$\mathbf{x}_{\mathrm{FB}} = \hat{\mathbf{x}}_{\mathrm{FB}}$). For the quantity $\varepsilon_{\mathrm{simple}}$ we found already the approximate expression (3.47) in Section 3.5.

The term $\mathrm{E}\{\|\widehat{W}_X(t,f) - \widetilde{W}_X(t,f)\|_2^2\}$, which will be abbreviated by e_1 in the following, can be bounded as follows:

$$\begin{aligned} e_1 &\leq \mathrm{E}\{\|\mathbf{x}_{\mathrm{FB}} - \hat{\mathbf{x}}_{\mathrm{FB}}\|_2^2\} \max_{\tau,\nu} |\Phi(\tau,\nu)|^2 TF \\ &\leq C_{\mathrm{recovery}} \frac{|\Omega|}{S} \sum_{k,l\in\Omega} \mathrm{E}\{|C_{k,l}|^4\} \max_{\tau,\nu} |\Phi(\tau,\nu)|^2 TF \\ &\approx C_{\mathrm{recovery}} \frac{|\Omega|}{S} \sum_{k,l\in\Omega} 2\overline{W}_X^2(kT,lF) \max_{\tau,\nu} |\Phi(\tau,\nu)|^2 TF \\ &\approx C_{\mathrm{recovery}} \frac{|\Omega|}{S} 2\sigma_S \frac{\|R_X\|_2^2}{TF} \max_{\tau,\nu} |\Phi(\tau,\nu)|^2 TF \\ &= C_{\mathrm{recovery}} \frac{|\Omega|}{S} 2\sigma_S \|R_X\|_2^2 \max_{\tau,\nu} |\Phi(\tau,\nu)|^2 \end{aligned} \tag{5.22}$$

were we used $\|\mathbf{u}\|_1 \leq \|\mathbf{u}\|_2 \cdot \sqrt{\mathrm{supp}(\mathbf{u})}$ (valid for any $\mathbf{u} \in \mathbb{C}^n$) and (5.26) and the fact that if T, F are chosen such that aliasing effects are small then $TF \sum_{k,l} \overline{W}_X^2(kT,lF) \approx \|\overline{W}_X(t,f)\|_2^2 = \|R_X\|_2^2$. Furthermore we used Isserli's fourth order equation for Gaussian RV's and the fact that for a sufficient underspread process the variances $\mathrm{E}\{|C_{k,l}|^2\}$ (remember that the $C_{k,l}$ are zero mean because $X(t)$ is assumed zero mean) are approximately equal to the values $\overline{W}_X(kT,lF)$ of the WVS of $X(t)$.

By combining (5.21),(3.47) and (5.22) we get the following approximate bound:

$$e_{\mathrm{FB}} \leq \left(\sqrt{C_{\mathrm{recovery}} \frac{|\Omega|}{S} 2\sigma_S \|\mathbf{R}_X\|_2^2 \max_{\tau,\nu} |\Phi(\tau,\nu)|^2} + \sqrt{\varepsilon_{\mathrm{simple}}} \right)^2 \tag{5.23}$$

which is the more accurate, the more underspread the process $X(t)$ is. The constant C_{recovery} depends only on the type of the recovery algorithm (BP or ROMP) and the sparsity degree S (the sparsity degree should be chosen such that σ_S is small, e.g. ≤ 0.1).

5.5 Random Sampling of the EAF

The estimator scheme "Random Sampling of the EAF" is based on the heuristic estimator design proposed in [41]. Under the assumption that only one realization $x(t)$ of the random process $X(t)$ can be observed, they propose to estimate the WVS of an underspread random process $X(t)$ by smoothing the WD of a single realization $x(t)$ of $X(t)$, i.e.,

$$\widetilde{W}_X(t,f) = W_x(t,f) ** \phi(t,f) \tag{5.24}$$

where the smoothing kernel $\phi(t,f)$ is chosen such that its 2D Fourier transform

$$\Phi(\tau,\nu) \triangleq \int_f \int_t \phi(t,f) e^{-j2\pi(\nu t - \tau f)} dt df \tag{5.25}$$

is given as

$$\Phi(\tau,\nu) = \begin{cases} 1, & \text{for } (\tau,\nu) \in \text{effective support of } \bar{A}_X(\tau,\nu) \\ 0, & \text{elsewhere} \end{cases} \tag{5.26}$$

whereby the effective support of the EAF $\bar{A}_X(\tau,\nu)$ can be defined in different ways. A possible method could be to define the effective support $\mathcal{A}$ of $\bar{A}_X(\tau,\nu)$ to be those specific rectangle of minimum area for which the quantity $\sigma_{\mathcal{A}} \triangleq \frac{\|\bar{A}_X(\tau,\nu)\cdot\mathcal{I}_{\mathcal{A}}\|_2}{\|\bar{A}_X(\tau,\nu)\|_2}$ satisfies[8]

$$\sigma_{\mathcal{A}} \geq 1 - \eta. \tag{5.27}$$

with a small positive real number η ($\eta \ll 1$).

The original WVS estimator proposed in [41] uses an estimator $\widetilde{W}_X(t,f)$ that incorporates only a single realization $x(t)$ of the form

$$\widetilde{W}_X(t,f) = \langle \hat{\mathbf{C}}_{t,f} x, x \rangle \tag{5.28}$$

with TF-shifted versions[9]

$$\hat{\mathbf{C}}_{t,f} \triangleq \mathbf{S}_{t,f} \hat{\mathbf{C}} \mathbf{S}_{t,f}^* \tag{5.29}$$

of the prototype operator $\hat{\mathbf{C}}$ that parameterizes the estimator $\widetilde{W}_X(t,f)$. The defining expressions (5.28) and (5.24) of the estimator $\widetilde{W}_X(t,f)$ are equivalent if the smoothing function $\phi(t,f)$ is equal to the Weyl symbol of the prototype operator $\hat{\mathbf{C}}$ mirrored at the origin in the TF-plane, i.e.,

$$\phi(t,f) = L_{\hat{\mathbf{C}}}(-t,-f). \tag{5.30}$$

The design of the estimator, i.e., the choice for $\phi(t,f)$ (or equivalently the choice for the prototype operator $\hat{\mathbf{C}}$), is based on the estimator's mean squared error

$$\varepsilon_2 \triangleq \mathrm{E}\left\{ \left\| \widetilde{W}_X(t,f) - \overline{W}_X(t,f) \right\|_2^2 \right\}. \tag{5.31}$$

Because the WVS $\overline{W}_X(t,f)$, which we want to estimate, is a deterministic object we can split ε_2 into a bias and variance term

$$\varepsilon_2 = V_{EAF}^2 + B_{EAF}^2 \tag{5.32}$$

[8] $\mathcal{I}_\Omega(\cdot)$ denotes the indicator function of some domain Ω, i.e., for each point $x \in \Omega$ we have $\mathcal{I}_\Omega(x) = 1$ for all other x we have $\mathcal{I}_\Omega(x) = 0$.

[9] The action of the TF-shift operator $\mathbf{S}_{t,f}$ on a signal $x(t)$ is defined via $(\mathbf{S}_{t,f}x)(t') = x(t'-t)e^{j2\pi f t'}$. Furthermore, for every linear operator $\mathbf{C}$ the Weyl symbol of $\mathbf{S}_{t_0,f_0}\mathbf{C}\mathbf{S}_{t_0,f_0}^*$ is given by $L_{\mathbf{C}}(t-t_0, f-f_0)$ where $L_{\mathbf{C}}$ denotes the Weyl symbol of $\mathbf{C}$.

with the global bias $B^2_{EAF} \triangleq \|\mathrm{E}\{\widetilde{W}_X(t,f) - \overline{W}_X(t,f)\}\|_2^2$ and the global variance $V^2_{EAF} \triangleq \mathrm{E}\{\|\widetilde{W}_X(t,f) - \mathrm{E}\{\widetilde{W}_X(t,f)\}\|_2^2\}$. In some sense the bias term accounts for a systematic (i.e., deterministic) estimation error, whereas the variance term accounts for a random error component due to the random fluctuations of the different realizations. It can be easily shown [41] that the bias term is given as

$$B^2_{EAF} = \int_{\tau,\nu} |1 - \Phi(-\tau,-\nu)|^2 |\bar{A}_X(\tau,\nu)|^2 d\tau d\nu \tag{5.33}$$

and the variance term can be approximated [41] by

$$V^2_{EAF} \approx \|\mathbf{R}_X\|_2^2 \int_{\tau,\nu} |\Phi(\tau,\nu)|^2 d\tau d\nu. \tag{5.34}$$

In order to introduce our CS based estimator scheme "Random Sampling of the EAF" let us consider sampled versions of both[10], the smoothed WD of the realization $x(t)$ (which is equal to the estimator $\widetilde{W}_X(t,f)$ defined in (5.24)), i.e.,

$$\mathbf{x}_{\mathrm{EAF}} = \mathrm{vec}\left\{\left\{\widetilde{W}_X(kT,lF)\right\}_{(k,l)\in\mathcal{W}}\right\} \tag{5.35}$$

and the AF $A_x(\tau,\nu)$ of $x(t)$, constrained to the effective support of $\bar{A}_X(\tau,\nu)$

$$\mathbf{y}_{\mathrm{EAF}} = \mathrm{vec}\left\{\left\{A_x\left(\frac{k}{T_{max}},\frac{l}{B}\right)\right\}_{(k,l)\in\mathcal{L}}\right\} \tag{5.36}$$

where we assume that the smoothed WD of the realization $x(t)$, which is the WVS estimator $\widetilde{W}_X(t,f)$, is effectively supported within $[-\frac{T_{max}}{2},\frac{T_{max}}{2}]\times[-\frac{B}{2},\frac{B}{2}]$ in the TF-plane, $\mathcal{L}\subseteq\mathbb{Z}^2$ denotes the set of pairs $(k,l)\in\mathbb{Z}^2$ for which $(\frac{k}{T_{max}},\frac{l}{B})$ is located within the rectangle $[-\frac{1}{2F},\frac{1}{2F}]\times[-\frac{1}{2T},\frac{1}{2T}]$ and $\mathcal{W}$ denotes the set of pais $(k,l)\in\mathbb{Z}^2$ for which the points (kT,lF) are located within the effective support of $\widetilde{W}_X(t,f)$. The lattice constants of T and F are chosen such that the effective support of $\bar{A}_X(\tau,\nu)$ is contained within the rectangle $[-\frac{1}{2F},\frac{1}{2F}]\times[-\frac{1}{2T},\frac{1}{2T}]$ in the (τ,ν)-plane.

It can then be shown that $\mathbf{x}_{\mathrm{EAF}}$ and $\mathbf{y}_{\mathrm{EAF}}$, by neglecting unavoidable aliasing effects[11], are related via

$$\mathbf{y}_{\mathrm{EAF}} = \frac{1}{TF}\left(\mathbb{F}_{k_1}\otimes\mathbb{F}^*_{k_2}\right)\mathbf{x}_{\mathrm{EAF}} \tag{5.37}$$

where "$\otimes$" denotes the Kronecker product of matrices (see the Appendix for details) and $\mathbb{F}_k$ denotes the DFT matrix ($\in\mathbb{C}^{k\times k}$) as defined in Section 4.5.2.

[10] Independently of this work, the authors of [4] proposed a method that is algorithmically very similar to the approach we use here. However, in that paper there is a completely deterministic framework used. Furthermore the authors use CS methods mainly for regularization and not for data compression as we do.

[11] A function cannot be simultaneously supported within an interval (rectangle) in the original and the Fourier domain. However, approximately, certain functions do have this property provided that the geometries of the two intervals/rectangles are suitable chosen.

Because we assume that the WVS $\overline{W}_X(t,f)$ of $X(t)$ is sparse in the sense defined above, the vector $\mathbf{x}_{\mathrm{EAF}}$ is sparse with high probability. Therefore, we can randomly select a few elements of $\mathbf{y}_{\mathrm{EAF}}$ without, according to the CS recovery results for sampled Fourier matrices, loosing significant information. The overall estimator structure is shown in Figure 5.4. In the first stage, the values

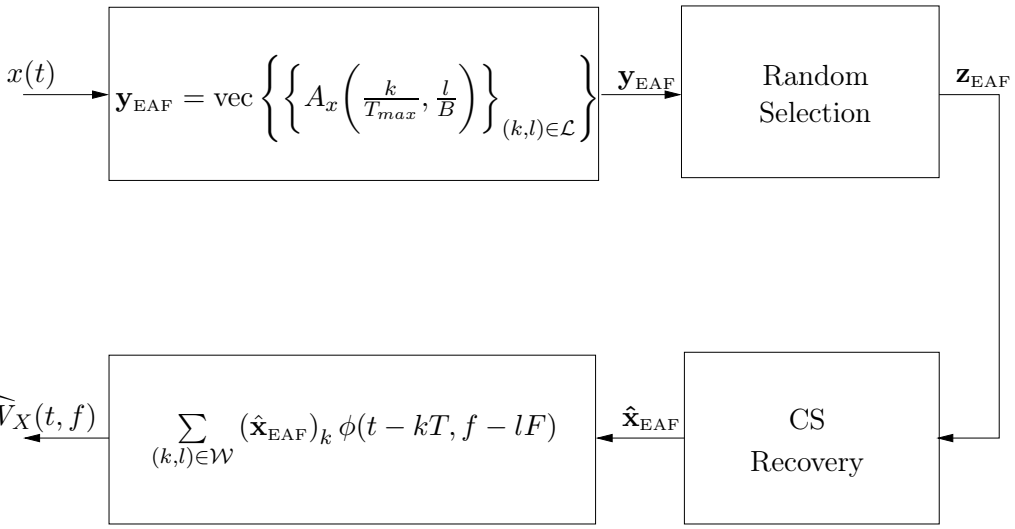

Figure 5.4: Block diagram of the estimator scheme "Random Sampling of The EAF".

of the AF $A_x(\tau,\nu)$ are calculated at the points (τ,ν) which corresponds to the rectangular grid of points $(\frac{k}{T_{max}}, \frac{l}{B})$ as introduced above. The resulting values are then stacked into the finite dimensional vector $\mathbf{y}_{\mathrm{EAF}} \in \mathbb{C}^n$ and are then randomly selected by the CS measurement stage. The randomly selected coefficients of $\mathbf{y}_{\mathrm{EAF}} \in \mathbb{C}^n$ are stacked into the measurement vector $\mathbf{z}_{\mathrm{EAF}} \in \mathbb{C}^m$. Using (5.37) we have the following relationship:

$$\mathbf{z}_{\mathrm{EAF}} = \mathbf{M}\mathbf{x}_{\mathrm{EAF}} \tag{5.38}$$

where the measurement matrix $\mathbf{M}$ is made up of those rows of $\frac{1}{TF}\left(\mathbb{F}_{k_1} \otimes \mathbb{F}^*_{k_2}\right)$ that correspond to the randomly selected (sampled) coefficients of $\mathbf{y}$.

The final stage of our estimator now tries to reconstruct $\mathbf{x}_{\mathrm{EAF}}$ from $\mathbf{z}_{\mathrm{EAF}}$ by using one of the CS recovery schemes (BP or ROMP). The result/output of the recovery $\hat{\mathbf{x}}_{\mathrm{EAF}}$ is an approximation to $\mathbf{x}_{\mathrm{EAF}}$ which will be in general different from $\mathbf{x}_{\mathrm{EAF}}$. However, as shown in the previous chapter for a suitable measurement matrix $\mathbf{M}_{\mathrm{EAF}}$ and sparsity of $\mathbf{x}_{\mathrm{EAF}}$ the error $\|\hat{\mathbf{x}}_{\mathrm{EAF}} - \mathbf{x}_{\mathrm{EAF}}\|_2$ will be small.

The recovered vector $\hat{\mathbf{x}}_{\mathrm{EAF}}$ consists of approximate sample values of $\widetilde{W}_X(t,f)$. Using the elements of the vector $\hat{\mathbf{x}}_{\mathrm{EAF}}$ as sampled estimator outputs of the estimated WVS we calculate the

estimated WVS $\widehat{W}_X(t,f)$ by a 2D reconstruction using $\phi(t,f)$ as the reconstruction kernel

$$\widehat{W}_X(t,f) = \sum_{(k,l)\in\mathcal{W}} (\hat{\mathbf{x}}_{\mathrm{EAF}})_k \, \phi(t-kT, f-lF). \tag{5.39}$$

Here, the function $\phi(t,f)$ is the same as in (5.24) and is in essence a reconstruction kernel for band limited (2D-) functions. The output $\widehat{W}_X(t,f)$ of our estimator is in general different from $\widetilde{W}_X(t,f)$ (the estimator without using CS) defined in (5.24), because the CS stages (random sampling of $\mathbf{y}_{\mathrm{EAF}}$ and recovery) will in general introduce errors.

Now we bound the mean squared error $e_{\mathrm{EAF}} \triangleq \mathrm{E}\left\{\left\|\overline{W}_X(t,f) - \widehat{W}_X(t,f)\right\|_2^2\right\}$, under the assumption that the measurement matrix $\mathbf{M}$ satisfies the RIC of Basis Pursuit and ROMP, in an approximate manner. Again, using the triangle inequality for norms we get:

$$\begin{aligned}
\sqrt{e_{\mathrm{EAF}}} &= \sqrt{\mathrm{E}\left\{\left\|\overline{W}_X(t,f) - \widehat{W}_X(t,f)\right\|_2^2\right\}} = \sqrt{\mathrm{E}\left\{\left\| \left(\widetilde{W}_X(t,f) - \widehat{W}(t,f)\right) + \left(\overline{W}_X(t,f) - \widetilde{W}_X(t,f)\right) \right\|_2^2\right\}} \\
&\leq \sqrt{\mathrm{E}\left\{\left\|\widehat{W}_X(t,f) - \widetilde{W}_X(t,f)\right\|_2^2\right\}} + \sqrt{\mathrm{E}\left\{\left\|\overline{W}_X(t,f) - \widetilde{W}_X(t,f)\right\|_2^2\right\}} \\
&= \sqrt{\mathrm{E}\left\{\left\|\widehat{W}_X(t,f) - \widetilde{W}_X(t,f)\right\|_2^2\right\}} + \sqrt{B_{\mathrm{EAF}}^2 + V_{\mathrm{EAF}}^2} \\
&= \sqrt{\mathrm{E}\{TF\sum_{k,l} |\widehat{W}_X(kT,lF) - \widetilde{W}_X(kT,lF)|^2\}} + \sqrt{B_{\mathrm{EAF}}^2 + V_{\mathrm{EAF}}^2} \\
&\leq \sqrt{\frac{C_{\mathrm{recovery}}|\Omega|}{S} \sum_{(k,l)\in\Omega} \mathrm{E}\{|\widetilde{W}_X(kT,lF)|^2\}} + \sqrt{B_{\mathrm{EAF}}^2 + V_{\mathrm{EAF}}^2}
\end{aligned} \tag{5.40}$$

where the constant C_{recovery} only depends on the actual recovery algorithm, i.e., BP or ROMP and on the sparsity degree S. We used for this derivation the triangle inequality for norms, (5.32), the identity of the 2-norm of bandlimited functions with the 2-norm of a suitable sequence of sample values and Theorem 4.5.10 as well as Theorem 4.5.1 of the previous chapter. As we will show presently the mean power of $\widetilde{W}_X(kT,lF)$ is approximately proportional to $\overline{W}_X^2(kT,lF)$. We note that the sparsity measure σ_S for a fixed sparsity degree S enters in exactly the same manner into the error bound of this scheme as for the scheme "random sampling the Filterbank".

It remains to determine the quantities $\mathrm{E}\{|\widetilde{W}_X(kT,lF)|^2\}$. To that end we use concepts and results from [41]:

- First, we note that $\widetilde{W}_X(t,f)$ can be written as a quadratic form (5.28) using the prototype operator $\hat{\mathbf{C}}$ of the estimator. Because we assume that $\Phi(\tau,\nu)$ is box-shaped, real valued and symmetric w.r.t. the τ and ν axis we have that the Weyl symbol $L_{\hat{\mathbf{C}}_{t_0,f_0}}$ (cf. Section 2.4) of

the TF-shifted prototype operator $\hat{\mathbf{C}}$ is given as

$$L_{\hat{\mathbf{C}}_{t_0,f_0}}(t,f) = \phi(t-t_0, f-f_0) = \frac{1}{TF}\text{sinc}\left(\frac{t-t_0}{T}\right)\cdot\text{sinc}\left(\frac{f-f_0}{F}\right) \tag{5.41}$$

where we assume that the sampling constants T, F are chosen such that the effective support of $\bar{A}_X(\tau,\nu)$ is contained within $[-\frac{1}{2F},\frac{1}{2F}]\times[-\frac{1}{2T},\frac{1}{2T}]$.

- Second, it can be shown [41] that the variance $V_{t,f}^2$ of $\widetilde{W}_x(t,f)$ is given by

$$V_{t,f}^2 = \text{tr}\{\hat{\mathbf{C}}_{t,f}\mathbf{R}_X\hat{\mathbf{C}}_{t,f}^*\mathbf{R}_X\} \tag{5.42}$$

and the mean of $\widetilde{W}_X(t,f)$ is equal to $\overline{W}_X(t,f)$ (because we assume that the EAF is supported within the support of $\Phi(\tau,\nu)$, which is also necessary for an unbiased estimator of the WVS). If the operators C and R_X are jointly underspread (for the definition of joint underspreadness of operators we refer to [40]) then the following approximation holds:

$$\begin{aligned}\text{tr}\{\hat{\mathbf{C}}_{t,f}\mathbf{R}_X\hat{\mathbf{C}}_{t,f}^*\mathbf{R}_X\} &= \int_{t,f} L_{\hat{\mathbf{C}}_{t,f}\mathbf{R}_X}(t,f)L^*_{\mathbf{R}_X\hat{\mathbf{C}}_{t,f}}(t,f)dtdf \\ &\approx \int_{t,f} L^2_{\mathbf{R}_X}(t,f)L^2_{\hat{\mathbf{C}}_{t,f}}(t,f)dtdf \\ &= \int_{t,f} \overline{W}^2_X(t,f)L^2_{\hat{\mathbf{C}}_{t,f}}(t,f)dtdf.\end{aligned} \tag{5.43}$$

Here, we used the identity $L_{\mathbf{R}_X}(t,f) = \overline{W}_X(t,f)$. A result concerning the quality of this approximation is given by Theorem 2.14 in [40]. Therefore we can approximate the variance term as

$$\begin{aligned}V^2_{t_0,f_0} &\approx \|L_{\hat{\mathbf{C}}_{t,f}}\cdot L_{\mathbf{R}_X}\|_2^2 \\ &= \|\frac{1}{TF}\text{sinc}\left(\frac{t-t_0}{T}\right)\cdot\text{sinc}\left(\frac{f-f_0}{F}\right)\cdot \\ &\sum_{k,l}\overline{W}_X\left(t_0+kT, f_0+lF\right)\text{sinc}\left(\frac{t-t_0-kT}{T}\right)\cdot\text{sinc}\left(\frac{f-f_0-lF}{F}\right)\|_2^2 \\ &= \overline{W}^2_X(t_0,f_0).\end{aligned} \tag{5.44}$$

Here, we assumed that the WVS $\overline{W}_X(t,f)$ of $X(t)$ is an exactly bandlimited 2D function. By noting the relationship:

$$\text{E}\{\|\mathbf{x}_{\text{EAF}}\|_2^2\} = \text{E}\{\|\mathbf{x}_{\text{EAF}} - \text{E}\{\mathbf{x}_{\text{EAF}}\}\|_2^2\} + \|\text{E}\{\mathbf{x}_{\text{EAF}}\}\|_2^2 \tag{5.45}$$

valid for any complex valued random vector $\mathbf{x}$ we get the final approximation:

$$\text{E}\{|\widetilde{W}_X(t,f)|^2\} \approx 2\overline{W}^2_X(t,f). \tag{5.46}$$

The final approximate bound for the error $\mathbf{e}$ is given as:

$$\begin{aligned} e_{\text{EAF}} &\leq \left(\sqrt{\frac{C_{\text{recovery}}|\Omega|}{S} \sum_{(k,l)\in\Omega} \mathrm{E}\{|\widetilde{W}_X(kT, lF)|^2\}} + \sqrt{B_{\text{EAF}}^2 + V_{\text{EAF}}^2} \right)^2 \\ &\approx \left(\sqrt{\frac{C_{\text{recovery}}|\Omega|}{S} \sum_{(k,l)\in\Omega} 2\overline{W}_X^2(t, f)} + \sqrt{B_{\text{EAF}}^2 + V_{\text{EAF}}^2} \right)^2 \\ &\approx \left(\sqrt{\frac{C_{\text{recovery}}|\Omega|}{S} 2\sigma_S \frac{\|\mathbf{R}_X\|_2^2}{TF}} + V_{\text{EAF}} \right)^2 \\ &\approx \left(\sqrt{\frac{C_{\text{recovery}}|\Omega|}{S} 2\|\mathbf{R}_X\|_2^2 \frac{\sigma_S}{TF}} + \|\mathbf{R}_X\|_2 \|\Phi(\tau, \nu)\|_2 \right)^2 \\ &= \left(\sqrt{\frac{C_{\text{recovery}}|\Omega|}{S} 2\frac{\sigma_S}{TF}} + \|\Phi(\tau, \nu)\|_2 \right)^2 \|\mathbf{R}_X\|_2^2 \end{aligned} \tag{5.47}$$

Where we used (5.46), the fact that we will use approximately unbiased ($B_{\text{EAF}}^2 \approx 0$) estimators and the approximate expression for the variance (5.34).

Chapter 6

Simulations

In this chapter we discuss various experiments in MATLAB to demonstrate how the CS based estimator schemes perform compared to traditional (non CS based) estimator schemes. But first we discuss the problem of going from the analog domain into the discrete and finite length setting of a computer simulation. Furthermore, we discuss a scheme that allows to synthesize random processes with a freely designable geometry of the WVS or equivalently the EAF. In particular we can use this tool for generating (TF-) sparse and underspread processes.

6.1 From Analog to Digital

Within our simulations we represent any signal $s(t)$ (e.g. the realization of a random process) by a finite length vector $\mathbf{s}' \in \mathbb{C}^N$ that is obtained by truncating the signal $s(t)$ to a finite interval of length T_{sig} and subsequently sampling this truncated signal with a sampling period T_s. Using this vector we can compute digitalized (= sampled and truncated) versions of the Wigner distribution $W_s(t,f)$ and the ambiguity function $A_s(\tau,\nu)$ of the signal $s(t)$. However this will work only with little errors, if

- the energy of the Fourier transform $\hat{s}(f)$ of $s(t)$ is well concentrated within the interval $[-\frac{1}{4T_s}, \frac{1}{4T_s}]$ at the frequency axis [8, 42]
- and the energy of the signal $s(t)$ is well concentrated within the truncation interval of size T_{sig}. Without loss of generality we assume that the energy of $s(t)$ is concentrated within the interval $[0, T_{\text{sig}}]$.

It these two conditions are satisfied then it can be shown that

$$W_{\mathbf{s}}\left(nT_s, \frac{m}{2NT_s}\right) \approx 2T_s \sum_{k=-\infty}^{\infty} {\mathbf{s}'}_{n+k} {\mathbf{s}'}^*_{n-k} e^{-j2\pi\frac{m}{N}k} \tag{6.1}$$

where the vector $\mathbf{s}' \in \mathbb{C}^N$ is given by the sample valued of the truncated function $s(t)$, i.e.,

$$\mathbf{s}'_k = s(kT_s) \quad k = 0...N-1. \tag{6.2}$$

Similarly, it can be shown that

$$A_{\mathbf{s}}\left(2kT_s, \frac{m}{NT_s}\right) \approx T_s \sum_{n=-\infty}^{\infty} \mathbf{s}'_{n+k}\mathbf{s}'^*_{n-k} e^{-j2\pi\frac{m}{N}n}, \tag{6.3}$$

where in both expressions $\mathbf{s}'_l$ is 0 if the index l is not within $\{0, ..., N-1\}$.

6.2 Minimum Error Synthesis

For the generation of an underspread random process $X(t)$ that has also a sparse WVS $\overline{W}_X(t,f)$ we use the synthesis scheme for random processes presented in [27]. This scheme starts with an arbitrary 2D-function in the TF-plane, the so called model function $W'(t,f)$. We would like to calculate a process, more specifically the correlation operator $\mathbf{R}_X$ of a process $X(t)$ whose WVS $\overline{W}_X(t,f)$ has the minimum distance (measured in the standard norm) to the model function $W'(t,f)$. This amounts to solving the following optimization problem:

$$X(t) = \arg\min_{X'(t)} \|W' - \overline{W}_{X'}\|_2^2. \tag{6.4}$$

Because the WVS is the Fourier transform of the EAF $\bar{A}_X(t,f)$ the process $X(t)$ which solves (6.4) will also minimize the distance between $\bar{A}_X(\tau,\nu)$ and the model EAF $A'(\tau,\nu)$, where the model EAF $A'(\tau,\nu)$ is defined via

$$A'(\tau,\nu) \triangleq \int_t \int_f W'(t,f) e^{-j2\pi(\nu t - \tau f)} dt df. \tag{6.5}$$

This observation is important because we want to generate a process with an EAF that is well concentrated around the origin in the (τ,ν) plane and this observation shows that the process $X(t)$ which solves the optimization (6.4) has an EAF that is near to the model EAF and is therefore likely to be concentrated if the model $A'(\tau,\nu)$ is concentrated around the origin in the (τ,ν) plane. The synthesizing scheme allows to specify a subspace $\mathcal{S} \subseteq L^2(\mathbb{R})$ in which the realizations $x(t)$ of $X(t)$ should be located.

The complete synthesis works as follows:

- We assume that $\mathcal{S}$ is a finite dimensional space with dimension N. Is has to be chosen such that it contains all signals that are located within the effective support of the model function in the TF plane. E.g. if the model function $W'(t,f)$ is contained within a rectangle in the TF-plane with a certain bandwidth and time duration. Then a suitable subspace $\mathcal{S}$ would

be given by the span of all sinc pulses with the same bandwidth that are centered on a regular grid on the time axis (the grid constant is equal to the inverse of the bandwidth) and located within the effective duration of $W'(t,f)$. A simple calculation [26] yields the following relationship between the maximum duration T_{dur}, maximum bandwidth $B_{\max}$ and dimension N:

$$N \approx T_{\mathrm{dur}} \cdot B_{\max}. \tag{6.6}$$

- Start with a given WVS model $W'(t,f)$, or equivalently a given EAF model $A'(\tau,\nu)$ and an ONB $\{u_k\}_k$ for the subspace $\mathcal{S}$. It can then be shown that the set of linear operators $\{\mathbf{U}_{k,l}\}_{k,l}$ that are given by the kernels $h_{\mathbf{U}_{k,l}}(t_1,t_2) = u_k(t_1)u_l^*(t_2)$ constitute an orthonormal basis for the set of correlation operators corresponding to random processes with realizations in $\mathcal{S}$.

- We transform the model $W'(t,f)$ into a model correlation operator $\mathbf{R}'$ whose kernel is given as:

$$h_{\mathbf{R}'}(t_1,t_2) = \int_f W'\left(\frac{t_1+t_2}{2}, f\right) e^{j2\pi(t_1-t_2)} df. \tag{6.7}$$

  Now we compute the expansion coefficients $\gamma_{k,l}$ of $\mathbf{R}'$ with respect to the ONB $\{\mathbf{U}_k\}$:

$$\gamma_{k,l} = \langle \mathbf{R}', \mathbf{U}_{k,l} \rangle = \int_{t_1}\int_{t_2} h_{\mathbf{R}'}(t_1,t_2) u_k^*(t_1) u_l(t_2) dt_1 dt_2. \tag{6.8}$$

- We collect the coefficients $\gamma_{k,l}$ into the matrix $\mathbf{\Gamma} \in \mathbb{C}^{N\times N}$, $\mathbf{\Gamma}_{k,l} = \gamma_{k,l}$. Now we determine the N_+ positive eigenvalues λ_k and the corresponding normalized eigenvectors $\mathbf{v}_k$ $(k = 1, ..., N_+)$ of the positive semi-definite matrix $\mathbf{\Gamma}$.

- The resulting process $X(t)$ can be represented with the ONB $\{u_k(t)\}_k$ via a linear expansion:

$$X(t) = \sum_{k=1}^{N} a_k u_k(t) \tag{6.9}$$

  where N denotes the dimension of $\mathcal{S}$ and the scalar coefficients a_k are random variables. Because we exclusively work with zero mean Gaussian processes, we require these random variables to be jointly Gaussian with zero mean. Therefore this random variables are fully determined by its correlation matrix $\mathbf{R}_{\mathbf{a}} = \mathrm{E}\{\mathbf{a}\mathbf{a}^H\}$ where $\mathbf{a}$ is constructed by stacking the a_k into a column vector:

$$\mathbf{a} \triangleq \begin{pmatrix} a_1 \\ a_2 \\ \vdots \\ a_N \end{pmatrix}. \tag{6.10}$$

The process $X(t)$ which minimizes the quantity $\|W'(t,f) - \overline{W}_X(t,f)\|_2^2$ and which is represented as in (6.9) is determined by the zero mean Gaussian coefficients $\mathbf{a}$ whose correlation matrix is given by

$$\mathbf{R_a} = \sum_{k=1}^{N_+} \lambda_k \mathbf{v}_k \mathbf{v}_k^H. \tag{6.11}$$

where the λ_k are the positive eigenvalues of $\mathbf{\Gamma}$ and the $\mathbf{v}_k$ are the corresponding eigenvectors of $\mathbf{\Gamma}$. A zero mean Gaussian random vector $\mathbf{a}$ (of length N) with given correlation matrix $\mathbf{R_a}$ can be conveniently generated by first generating a vector (of length N) of uncorrelated Gaussian variables whose variances are equal to the eigenvalues of the correlation matrix and then multiplying this vector with the specific matrix $\mathbf{V}$ that has the eigenvectors of the correlation matrix $\mathbf{R_a}$ as its columns. This method is also known under the name "innovation system representation".

Of course for the simulations on a real computer all signals and operators have to be digitalized (sampled and truncated). The detailed reformulation of the synthesis procedure above for the discrete-time case can be obtained from [27].

Finally, we present an example for the minimum error synthesis. Because we use discrete time signals for this example, we implicitly constrain the subspace $\mathcal{S}$ to be contained within the set of all bandlimited functions where the maximum bandwidth is given by[1] $\frac{1}{2T_s}$ where T_s is the sampling period. The model function is a box shaped spectrum with a rectangular support. The sizes of the model function are 40 and 0.1 respectively (we use a sampling period of $T_{sym} = 1$. In Figure 6.1 the TF model function $W'(t,f)$ as well as the the WVS $\overline{W}_X(t,f)$ and the EAF $\bar{A}_X(t,f)$ of the synthesized process $X(t)$ are shown.

6.3 Cognitive-Radio Model

For this simulation we used the received signal $R(t)$ of the cognitive radio system model of Section 5.2 for the process $X(t)$:

$$X(t) = S_1(t) + S_2(t) \tag{6.12}$$

where $S_1(t)$ and $S_2(t)$ are two PAM signals with the same PAM parameters (raised cosine pulse, transmit length of 3 symbols and symbol period $T_s = 6$s) but using different carrier frequencies and transmission times (i.e., the WVS of $S_1(t)$ and $S_2(t)$ are centered around different points in the TF plane).

[1] The maximum bandwidth is $\frac{1}{2T_s}$ an not $\frac{1}{T_s}$ because we want to use a direct sampling (both in time and frequency direction) of the Wigner Ville spectrum which is only possible for this maximum bandwidth.

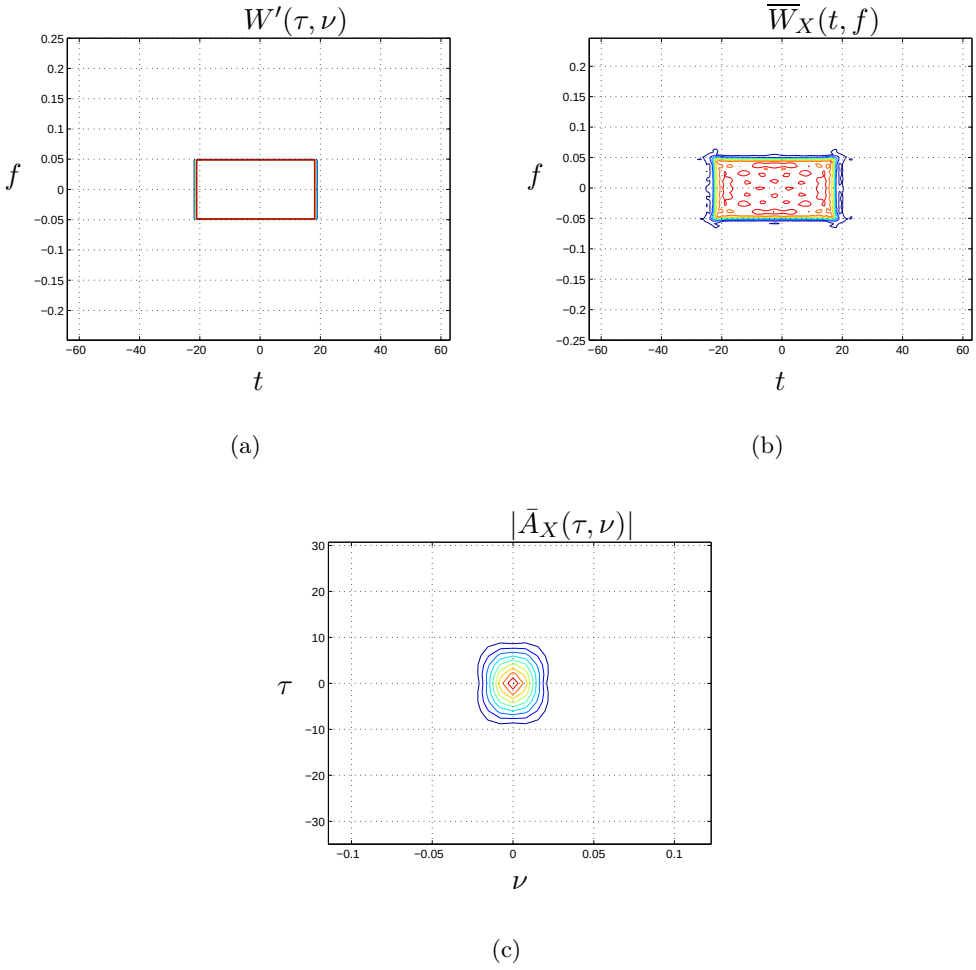

Figure 6.1: (a) Model function $W'(t,f)$ used to synthesize the process $X(t)$. (b) WVS $\overline{W}_X(t,f)$ of the synthesized process $X(t)$. (c) Magnitude of the EAF $\bar{A}_X(\tau,\nu)$ of the synthesized process $X(t)$.

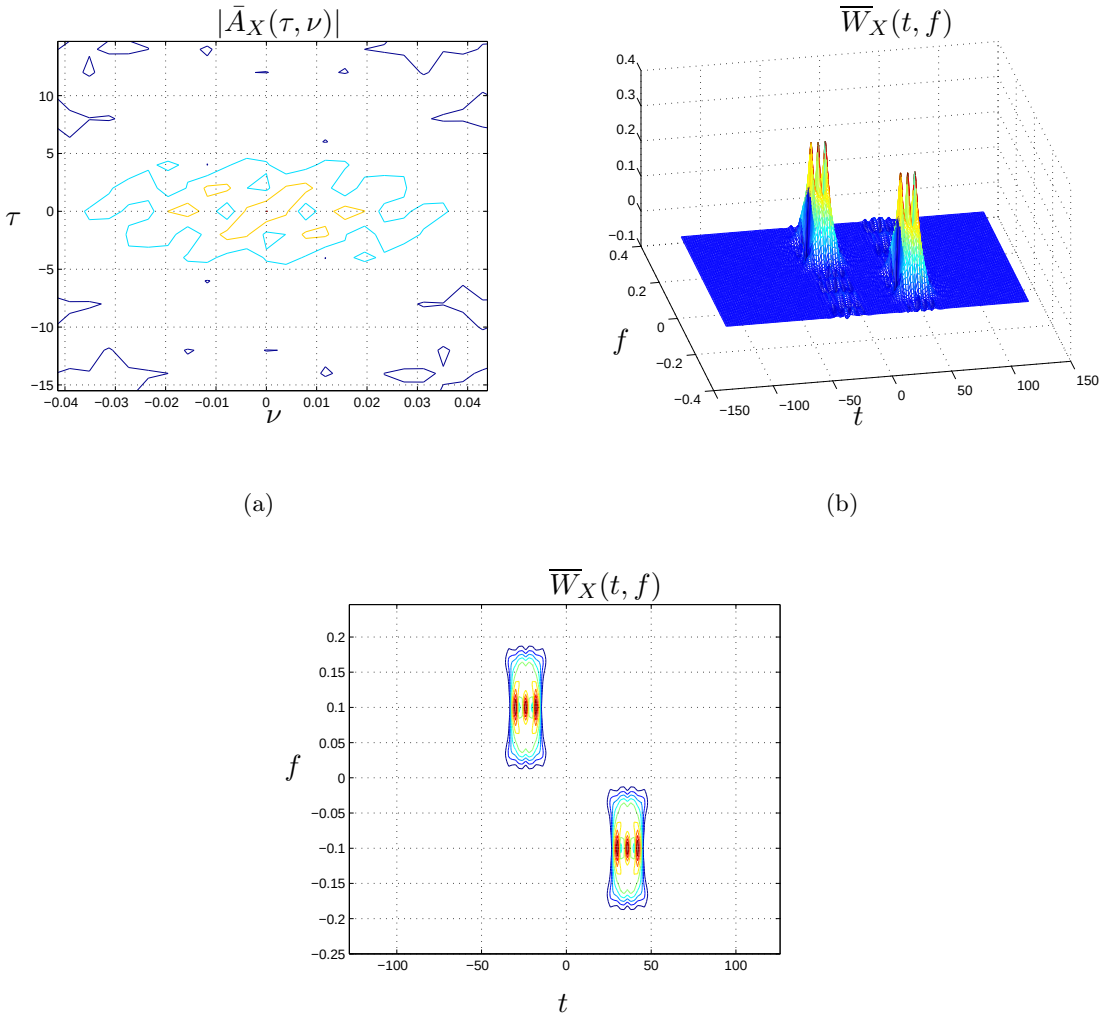

(a) (b)

(c)

Figure 6.2: Cognitive Radio signal detection. (a) Magnitude of the EAF $\bar{A}_X(\tau,\nu)$ of the received signal. The lowest contour level is about 0.01 and the maximum at the origin is equal to 1. (b) (c) WVS $\overline{W}_X(t,f)$ of the received signal.

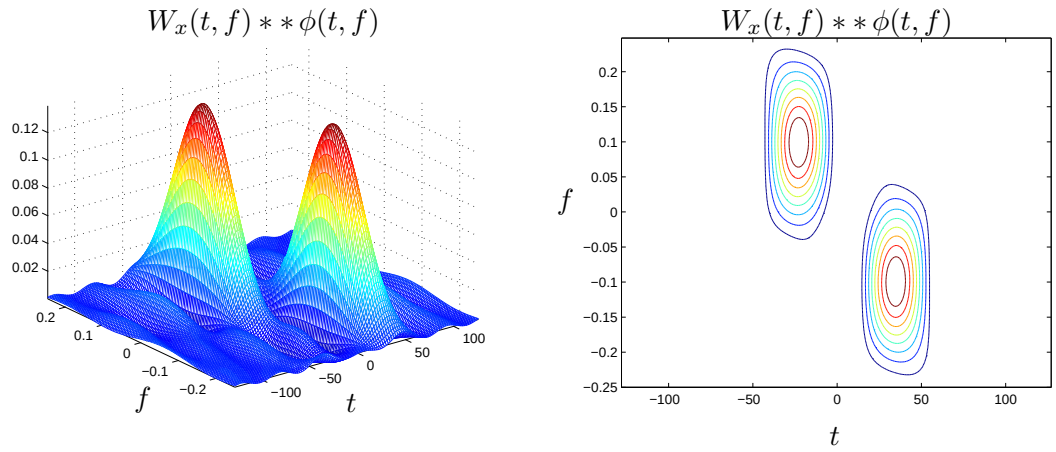

Figure 6.3: Cognitive Radio signal detection. Here we used the smoothed WD of the realization $x(t)$ as an estimate for $\overline{W}_X(t,f)$.

In Figure 6.2 we plotted the WVS $\overline{W}_X(t,f)$ as well as the magnitude of the EAF $\bar{A}_X$. The WVS $\overline{W}_X(t,f)$ consists of two TF - components, one for each of the two transmitters ($S_1(t)$ and $S_2(t)$). We used a carrier frequency of 0.1 for the first and -0.1 for the second transmitter. The symbol period T_{sym} has been fixed to 6. The dimension of the digitalized input was $n = 256$.

As a reference for the CS based estimator we show in Figure 6.3 the result of the conventional non CS based estimator which performs a smoothing of the WD of the realization $x(t)$. The smoothing kernel $\phi(t,f)$ we use here (cf. (5.24)) has the same shape as the corresponding kernels (which are all denoted by $\phi(t,f)$) for the CS based estimator schemes (cf. Figure 5.3 and Figure 5.4) which will be simulated next.

We compared both CS based estimator schemes proposed in the previous Chapter. In the scheme "Random Sampling of the Filterbank" the measurement vector $\mathbf{z}$ had a length of $m = 26$ and a Gaussian ensemble was used for the measurement matrix $\mathbf{M}$. The reconstruction kernel $\phi(t,f)$ was chosen such that its Fourier transform $\Phi(\tau,\nu)$ is box shaped and has as its support the rectangle $[-4,4] \times [-0.025, 0.025]$ in the (τ,ν) plane. For the scheme "Random Sampling of the EAF" we used also a length of $m = 26$ for the measurement vector $\mathbf{z}$ and the same shape for reconstruction kernel $\phi(t,f)$ as for the previous estimator scheme (the height of $\Phi(\tau,\nu)$ is however different from that used in the previous scheme), but here we used implicitly a randomly sampled Fourier matrix for the measurement matrix $\mathbf{M}$. Because the "nominal" signal dimension was 256, this is equivalent to compression factors of nearly 10 that is reached in the CS sensor stages.

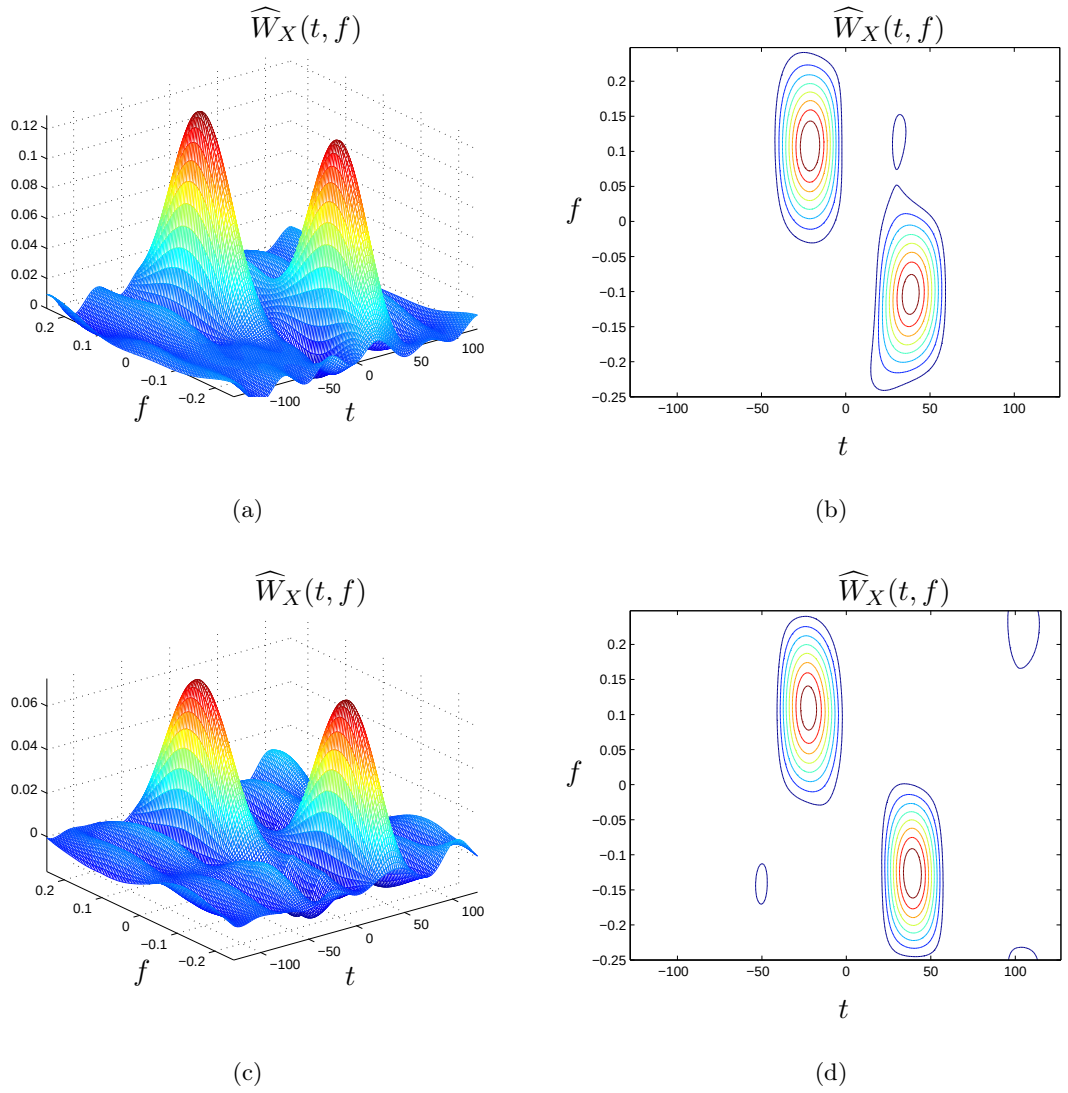

Figure 6.4: Cognitive Radio signal detection using $m = 26$ measurements for the CS based estimators. (a) (b) Estimated WVS $\widehat{W}_X(t,f)$ using the CS based estimator scheme "Random Sampling of the EAF". (c) (d) Estimated WVS $\widehat{W}_X(t,f)$ using the CS based estimator scheme "Random Sampling of the Filterbank".

For the recovery we used the BP (more specifically a real valued reformulation of the BP, see the Appendix for details). As can be seen from Figure 6.4, the estimated WVS $\widehat{W}(t,f)$ that were computed using a single realization of $X(t)$ clearly shows the two spectral components corresponding to the transmitters for both estimator schemes.

We conclude that both estimator schemes allow an accurate detection of the occupied regions in the TF plane for the specific example of transmit signals we used here while using a significant reduction of the input data rate. The difference between both schemes is their structure which may led to different requirements for their implementation.

Finally we present the estimator results for different compression factors m/n, where m and n denotes the number of rows and columns of the measurement matrix $\mathbf{M}$ respectively, in Figure 6.5 to Figure 6.9. The reconstruction kernel $\phi(t,f)$ of both schemes where chosen box shaped ant with the support $[-4,4] \times [-0.025, 0.025]$. The sparsity measure σ_4 was equal to 0.0014 for the scheme "Random Sampling of the EAF" and equal to 0.45 for the scheme "Random Sampling of the Filterbank". The higher value for the latter scheme is due to the fact that the lattice constants T and F have to be chosen smaller than the theoretical anti-aliasing condition suggests (cf. Section 5.4, 3.5) because of two effects. First the process is not exactly underspread (the EAF is not exactly contained within a rectangle) and second because we simulated only finite length discrete signals the anti-aliasing conditions from the continuous time setting does not hold in general exactly. The smaller lattice constants result in a bigger measurement vector because the support of the WVS of the process in the TF plane is fixed. This implies that for the same compression factor m/n we have to use more measurements in the scheme "Random Sampling of the Filterbank" compared to the scheme "Random Sampling of the EAF". However, for the scheme "Random Sampling of the EAF" we used straightforward discretizations of the WD of the AF of a signal and this requires that the discrete time signals only occupy half of the entire bandwidth (which is equal to 1 for discrete time signals). Therefore, for a fair comparison of compression abilities this has to be taken into account. As can be obtained from Figure 6.5 both estimator schemes allow an accurate localization of the PAM transmissions in the TF plane even for compression factors as low as $m/n = 0.2$.

6.4 Random Sampling of the Filterbank

Here, we investigate the performance of our CS based estimator scheme "Random Sampling the Filterbank" with the help of a synthetic process $X(t)$ that was generated using minimum error synthesis as presented above using a Gaussian shaped TF - model function that is centered at the origin in the TF-plane. The WVS $\overline{W}_X(t,f)$ and the EAF $\bar{A}_X(\tau,\nu)$ are shown in Figure 6.10. For the Gabor analysis we used a Gaussian prototype whose variance has been empirically adjusted in

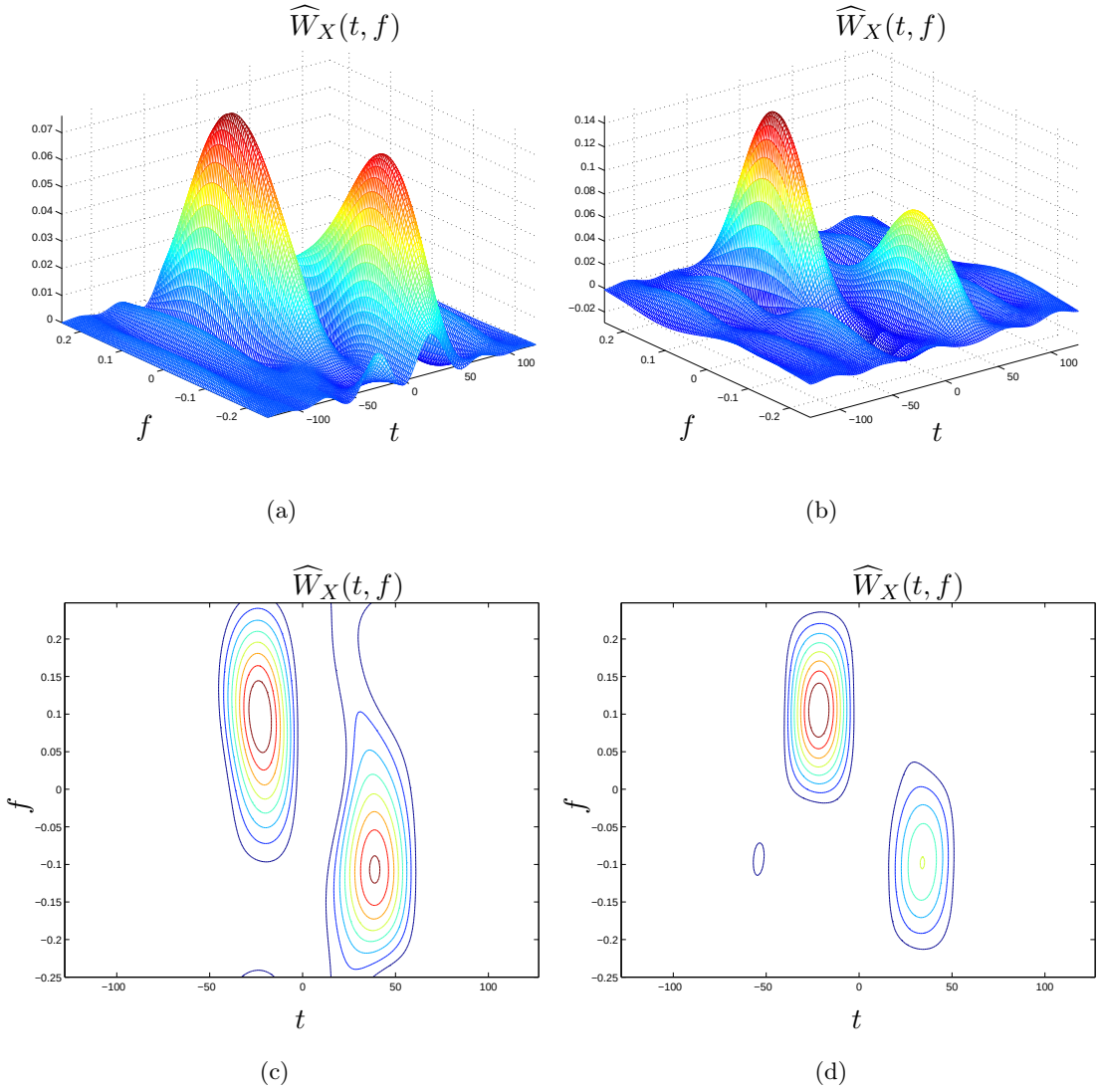

Figure 6.5: Cognitive Radio signal detection using a compression factor $m/n = 0.2$ where m and n denotes the number of rows and columns of the measurement matrix $\mathbf{M}$ respectively. The contour level plot shows the positive part of the estimated spectra. (a) (c) "Random Sampling of the EAF" (b) (d) "Random Sampling of the Filterbank".

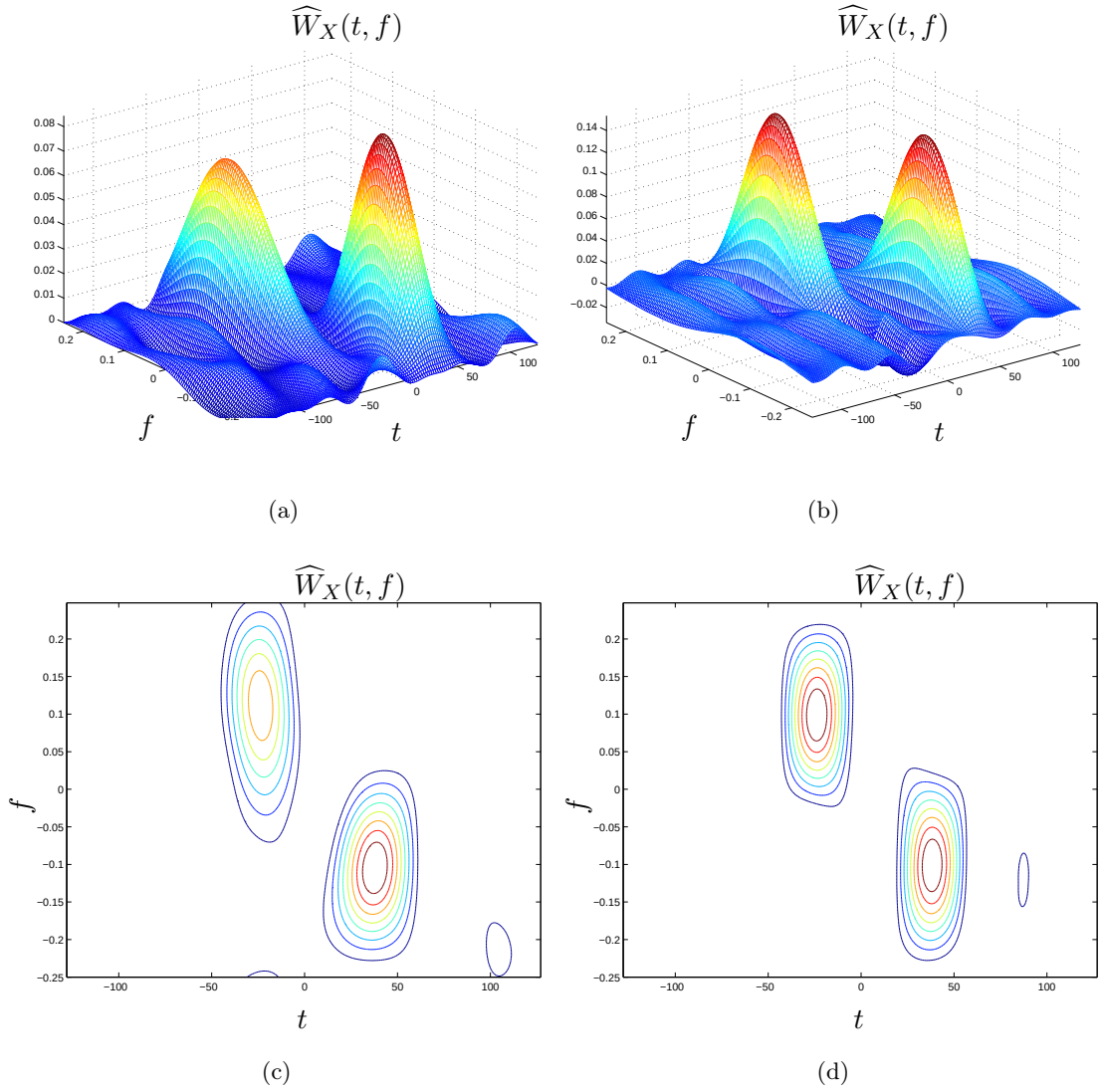

Figure 6.6: Cognitive Radio signal detection using a compression factor $m/n = 0.25$ where m and n denotes the number of rows and columns of the measurement matrix $\mathbf{M}$ respectively. The contour level plot shows the positive part of the estimated spectra. (a) (c) "Random Sampling of the EAF" (b) (d) "Random Sampling of the Filterbank".

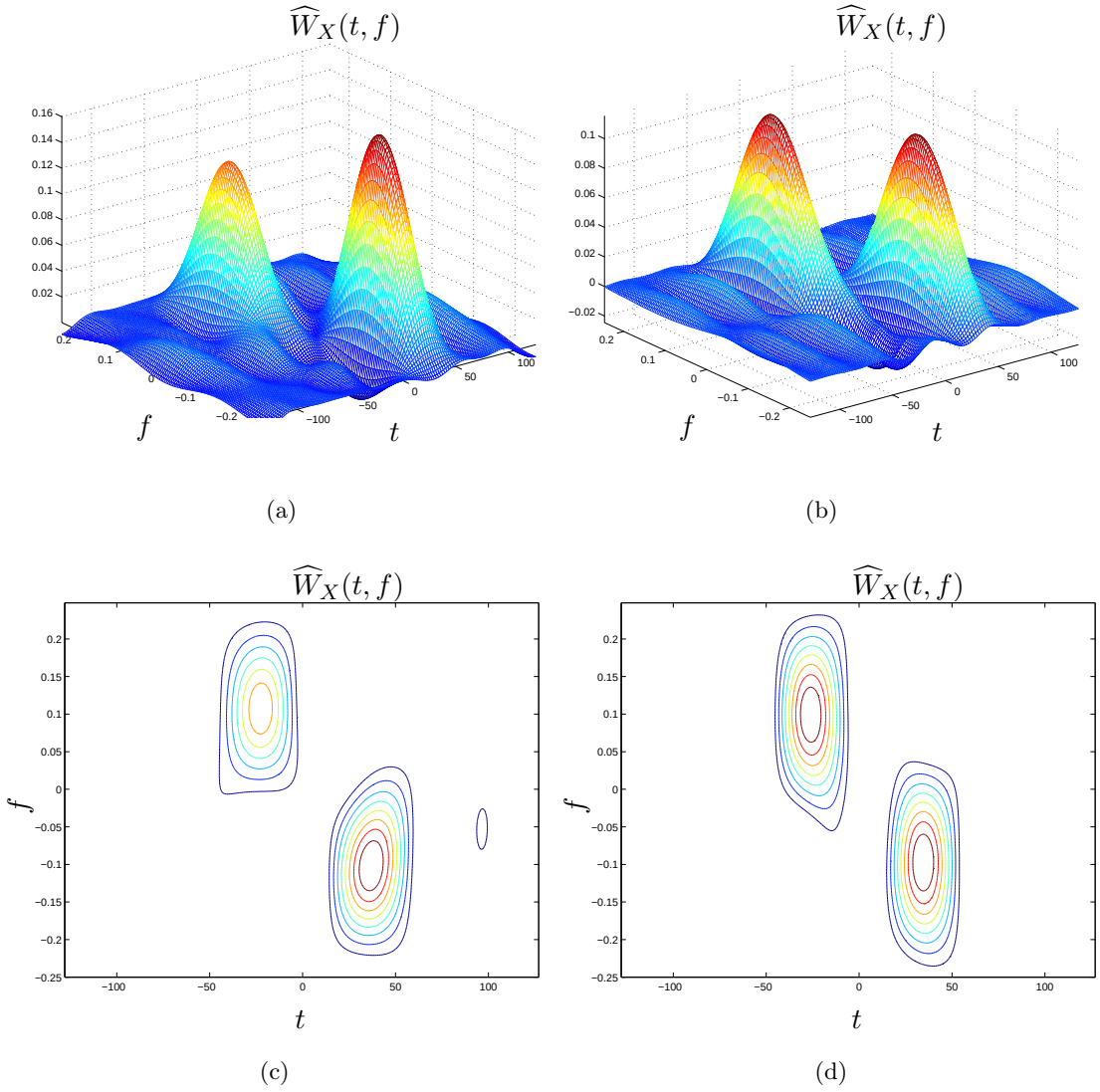

Figure 6.7: Cognitive Radio signal detection using a compression factor $m/n = 0.5$ where m and n denotes the number of rows and columns of the measurement matrix $\mathbf{M}$ respectively. The contour level plot shows the positive part of the estimated spectra. (a) (c) "Random Sampling of the EAF" (b) (d) "Random Sampling of the Filterbank".

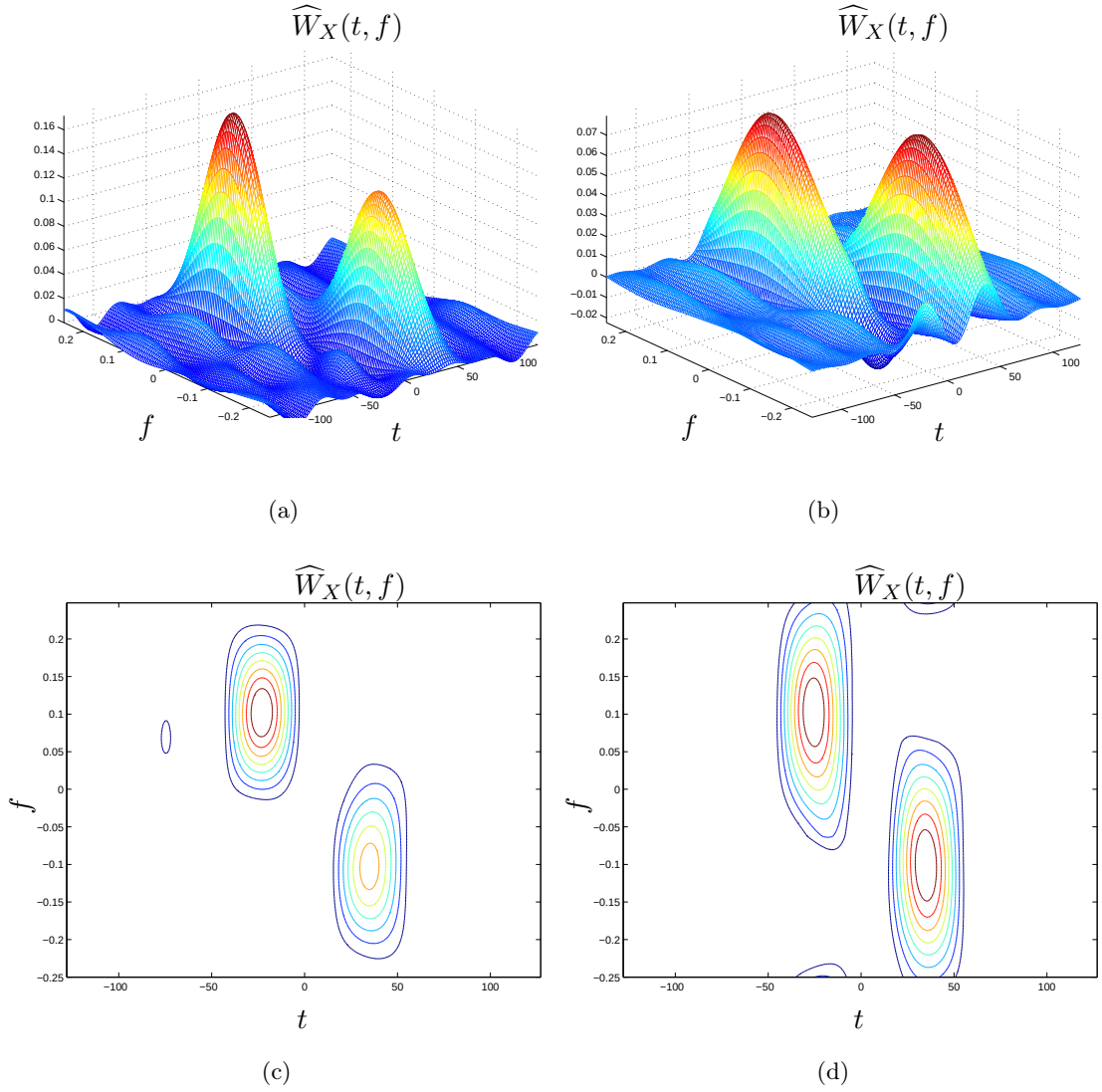

Figure 6.8: Cognitive Radio signal detection using a compression factor $m/n = 0.75$ where m and n denotes the number of rows and columns of the measurement matrix $\mathbf{M}$ respectively. The contour level plot shows the positive part of the estimated spectra. (a) (c) "Random Sampling of the EAF" (b) (d) "Random Sampling of the Filterbank".

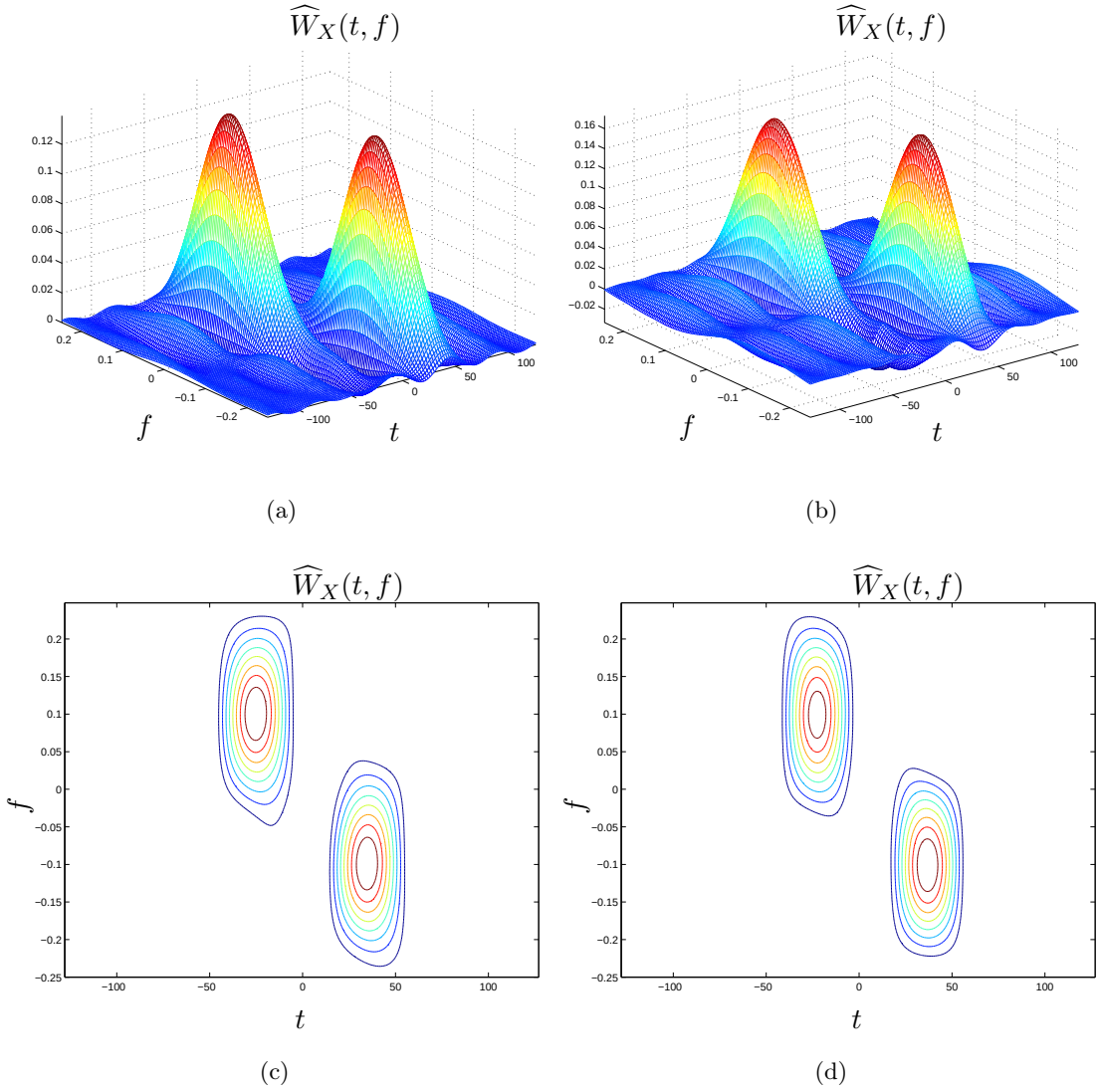

Figure 6.9: Cognitive Radio signal detection using a compression factor $m/n = 1$ (i.e., no compression) where m and n denotes the number of rows and columns of the measurement matrix $\mathbf{M}$ respectively. The contour level plot shows the positive part of the estimated spectra. (a) (c) "Random Sampling of the EAF" (b) (d) "Random Sampling of the Filterbank".

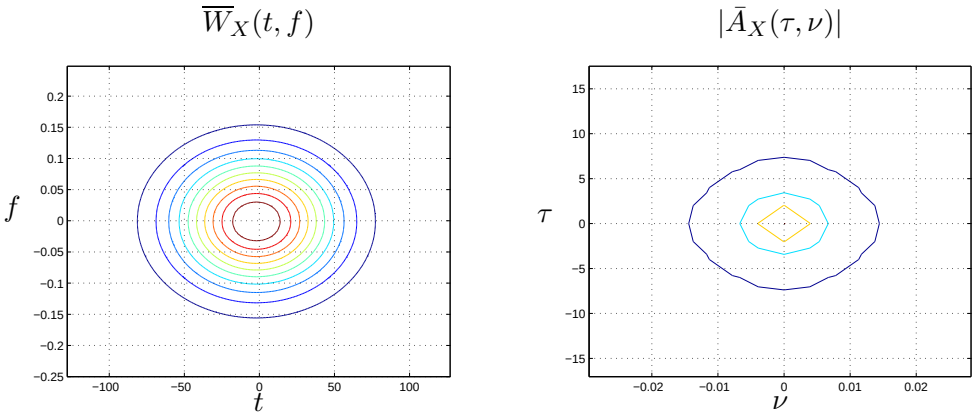

Figure 6.10: (a) WVS $\overline{W}_X(t,f)$ of the process $X(t)$, (b) Magnitude of the EAF $\bar{A}_X(\tau,\nu)$ of the process $X(t)$ (the lowest contour level is below 0.01 and the maximum is 1 because the process is energy normalized).

order to match the EAF. A profound theoretical discussion of the matching problem can be found in [32].

First we investigate the estimator without the CS stage which can be considered as performing CS with compression factor 1, i.e., no compression is performed at all[2]. The results that are obtained here should validate the approximate expressions for the variance, the bias and the mean squared error for the estimator scheme presented in Section 3.5. In Figure 6.13 the variance term $V^2 = \int_t \int_f \mathrm{E}\left\{\left\|\widehat{W}_X(t,f) - \mathrm{E}\{\widehat{W}_X(t,f)\}\right\|_2^2\right\} dtdf$, the bias term $B^2 = \int_t \int_f \left|\mathrm{E}\{\widehat{W}_X(t,f) - \overline{W}_X(t,f)\}\right|^2 dtdf$ and the normalized MSE are shown for different choices for the lattice constants T and F. All quantities are normalized to the squared mean energy $\overline{E}_X^2$ of the process. The reconstruction kernel $\phi(t,f)$ has been chosen such that its Fourier transform $\Phi(\tau,\nu)$ is box shaped and centered at the origin in the (τ,ν) plane with height TF in order to get an approximately unbiased estimator. The lengths of the box was $2 \cdot 7$ and $2 \cdot 0.015$ in the τ- and ν - direction respectively. However, as indicated in Figure 6.13 the estimator was not exactly unbiased because the EAF $\bar{A}_X(\tau,\nu)$ was not ideally concentrated within the support of $\Phi(\tau,\nu)$ (cf. 6.10). The values for T and F have been chosen such that the product TF is in the order of 1.

[2]Indeed, a compression factor of 1 implies a quadratic measurement matrix $\mathbf{M}$ which in turn implies that the measurement matrix is regular because we assume throughout this thesis that a measurement matrix for CS is always full rank. Therefore the BP for the noiseless case yields the original signal vector $\mathbf{x}$ of the CS signal model if we choose the constant ε in the inequality constraint of BP very small (ideally 0).

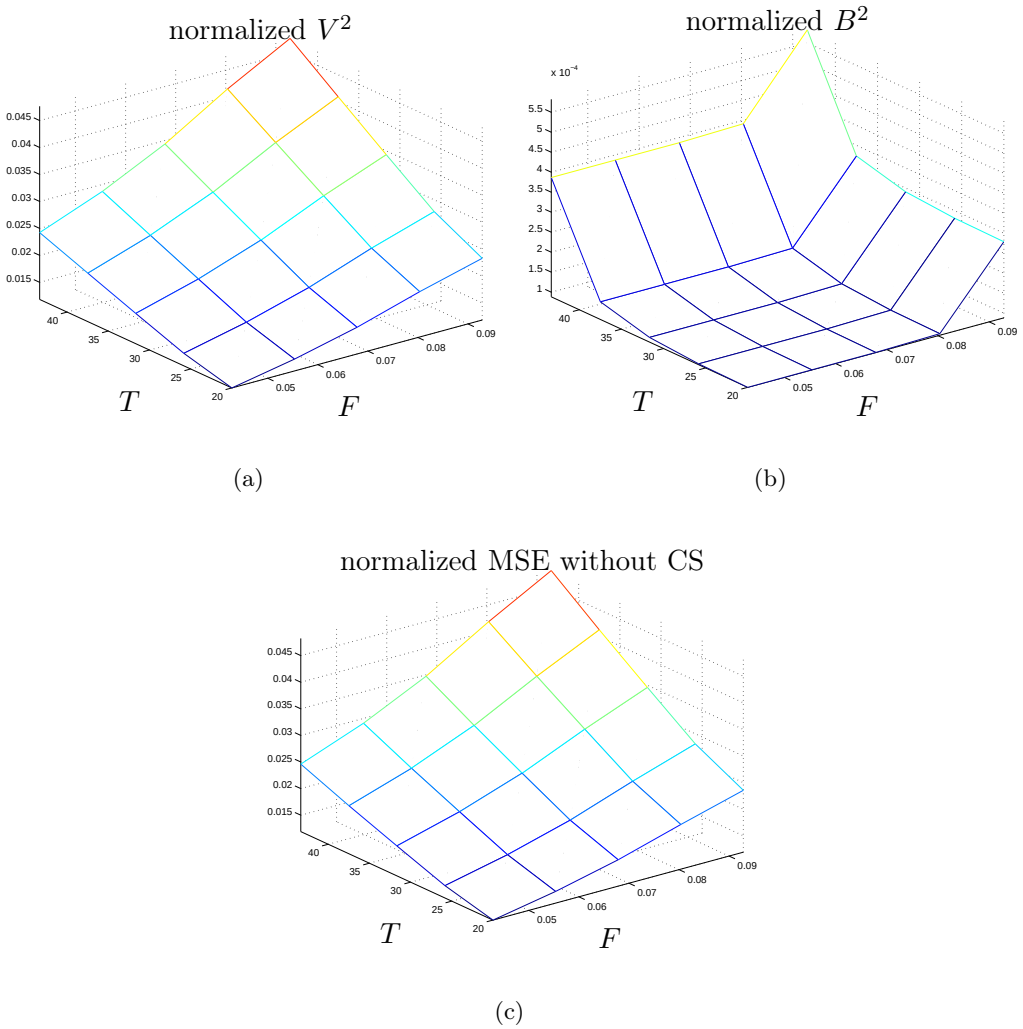

Figure 6.11: (a) Global normalized variance term V^2 (cf. (3.32)). (b) Global normalized bias term B^2 (cf. (3.31)) of the estimator.(c) Normalized MSE ($= B^2 + V^2$) without compression.

We compared the obtained values for the variance term to the approximate expression (3.47) for the variance term. Figure 6.12 shows the ratio of the true variance V^2 to the approximate simulated variance V^2 normalized to the approximation (3.47)

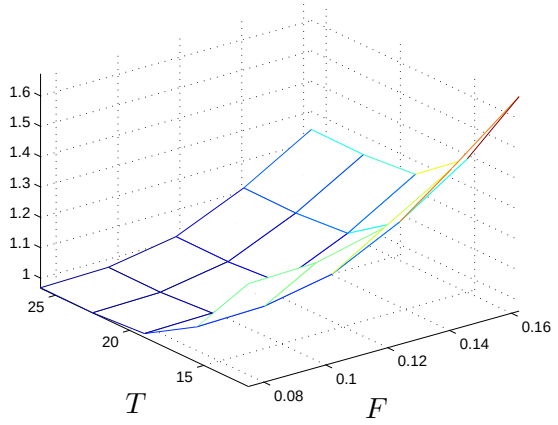

Figure 6.12: Ratio of the simulated variance term V^2 to the approximation (3.47).

expression given in (3.47). We see that except for small values of sampling interval T in time direction and large values of the product TF the approximation is relatively accurate. The deviation of the approximation from the true variance for small values of T is due to non negligible correlations between the Gabor coefficients $C_{k,l}$ which was one of the necessary assumptions for the derivation of the approximation (3.47). On the other hand, for large values of TF aliasing effects are introduced because the lattice constants are too large compared to the support of $\Phi(\tau, \nu)$ which has an area of $4 \cdot 7 \cdot 0.015 = 0.42$ which gives a maximum value of $\frac{1}{0.42} = 2.38$ for the product TF in order to avoid undesired aliasing effects.

Next, we included the CS stage with a compression factor of 2, i.e., the length of the measurement vector $\mathbf{z}$ is half of that of the vector $\mathbf{x}_{\mathrm{FB}}$ consisting of the squared magnitudes of the Gabor coefficients (cf. (5.16)). The measurement matrix $\mathbf{M}$ was the Gaussian ensemble, i.e., the elements of $\mathbf{M}$ are i.i.d. normally distributed. For the recovery we used BP. In contrast to the numerical results above, which have been computed semi-analytically (the variances of the Gabor coefficients have been computed by a quadratic form using discrete versions of the correlation operator $\mathbf{R}_X$ and the Gabor atoms $g_{k,l}$), we here performed a random simulation using 100 realizations of the process $X(t)$ and computed the squared error between $\widehat{W}_X(t,f)$ and $\overline{W}_X(t,f)$ for each realization separately and then took the average. The resulting average MSE is shown in Figure 6.13(c).

Another simulation investigated the dependency of the CS recovery accuracy with the sparsity measure σ_S of the process $X(t)$. For the simulation we fixed the sparsity degree to $S = 4$. We used different TF-model functions $W'(t,f)$, which are all superpositions of 2D Gaussian functions with

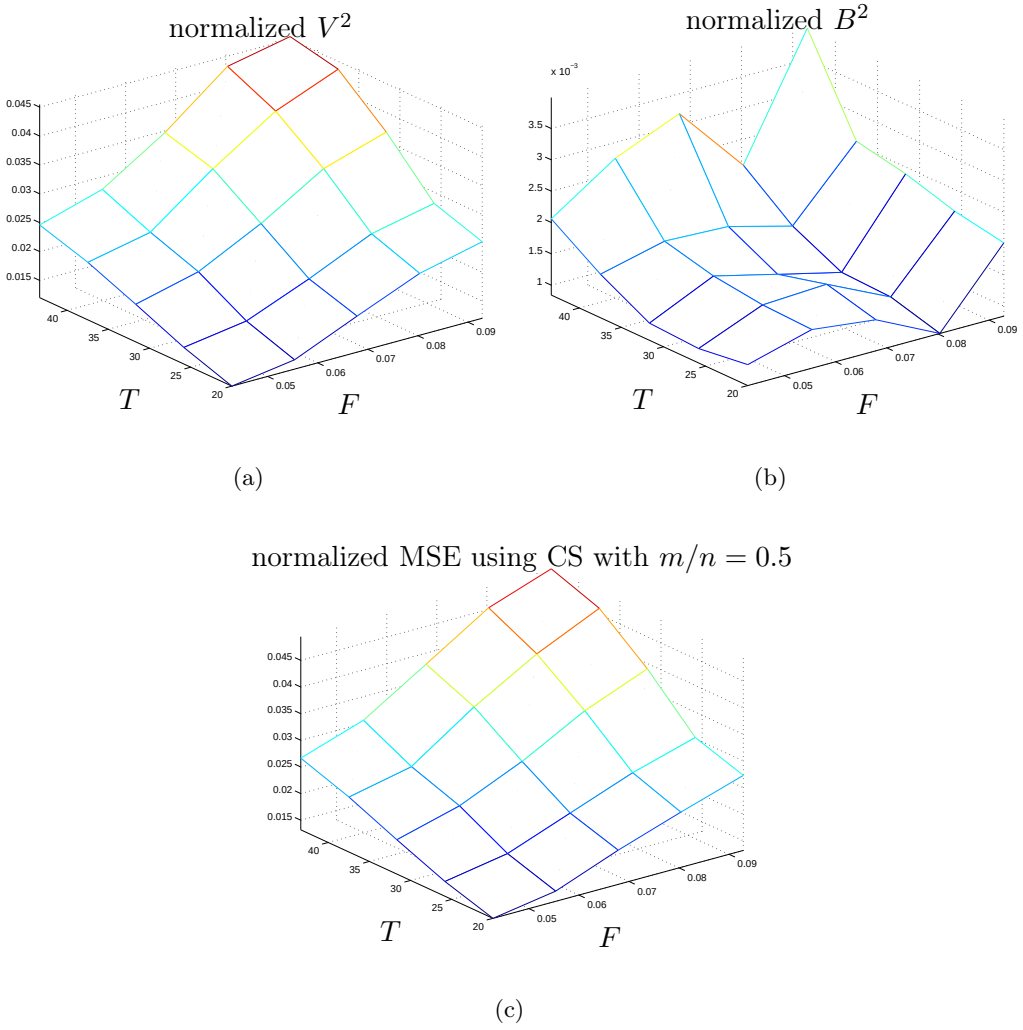

(a) (b)

(c)

Figure 6.13: (a) Global normalized variance term V^2. (b) Global normalized bias term B^2 of the estimator.(c) Normalized MSE ($= B^2+V^2$) using CS with a compression factor of $m/n = 0.5$ where m and n denotes the number of rows and columns of the measurement matrix $\mathbf{M}$ respectively.

process	$\sigma_{S=4}$	$M_{\mathbf{X}}^{(1,1)}$
G_1	0.09	0.055
G_2	0.21	0.047
G_3	0.32	0.041
G_4	0.41	0.038

Table 6.1: Sparsity and underspread parameter for the different processes.

identical spreads in the t and f direction. In order to generate processes with varying sparsity we added different numbers of Gaussian functions, i.e., for a fixed sparsity degree S we generated processes possessing different sparsity measures σ_S. We plotted the different TF models together with the WVS of the resulting processes in Figure 6.14. The Fourier transform $\Phi(\tau, \nu)$ of the reconstruction kernel $\phi(t, f)$ (cf. Section 3.5) of the estimator was chosen to be a box shaped function with support $[-5, 5] \times [-0.05, 0.05]$ in the (τ,ν) plane. The lattice constants T and F of the estimator were chosen such that aliasing is avoided (cf. Section 3.5). The exact value have been optimized empirically.

In the following we will caption the four processes that correspond to the four model functions by G_1,G_2,G_3 and G_4 where the digit indicates the number of summed Gaussian functions that are used for the corresponding model. For the interpretation of the results shown below we list in Table 6.1 the sparsity measure $\sigma_{S=4}$ and the quantity $M_{\mathbf{X}}^{(1,1)}$ (cf. (3.2)) of the different processes (whenever we use the notation $X(t)$ for a process this means that it is clear from the context which of the four processes G_1 to G_2 is meant). The lower the value $M_{\mathbf{X}}^{(1,1)}$ is the more underspread is the process and the lower the value of $\sigma_{S=4}$ for a process is the more sparse is the process.

We simulated the error that is introduced by the CS stage for the different process models, i.e., for different values of $\sigma_{S=4}$ and for different values of the CS compression factor m/n where m and n denotes the number of rows and columns of the measurement matrix $\mathbf{M}$ respectively. In Figure 6.15 we plotted the error energy of the CS stage, measured by $\hat{\varepsilon}_{\mathrm{FB,CS}}$:

$$\hat{\varepsilon}_{\mathrm{FB,CS}} \triangleq \frac{1}{100} \sum_{k=1}^{100} \|\hat{\mathbf{x}}_{\mathrm{FB}}^k - \mathbf{x}_{\mathrm{FB}}^k\|_2^2 \tag{6.13}$$

normalized to the squared HS norm of the correlation operator $\|\mathbf{R}_X\|_2^2$. Here $\hat{\mathbf{x}}_{\mathrm{FB}}^k$ and $\mathbf{x}_{\mathrm{FB}}^k$ denote the output of the CS recovery stage and the sampled input vector respectively when the k-th realization of $X(t)$ is used as the input (cf. Figure 5.3). For this plot the value of m/n is used as the parameter. We note that the measured error curves are all significantly below the theoretical bounds for the CS recovery errors derived in Chapter 4 and Section 5.4. This agrees with the observations in the well known CS literature.

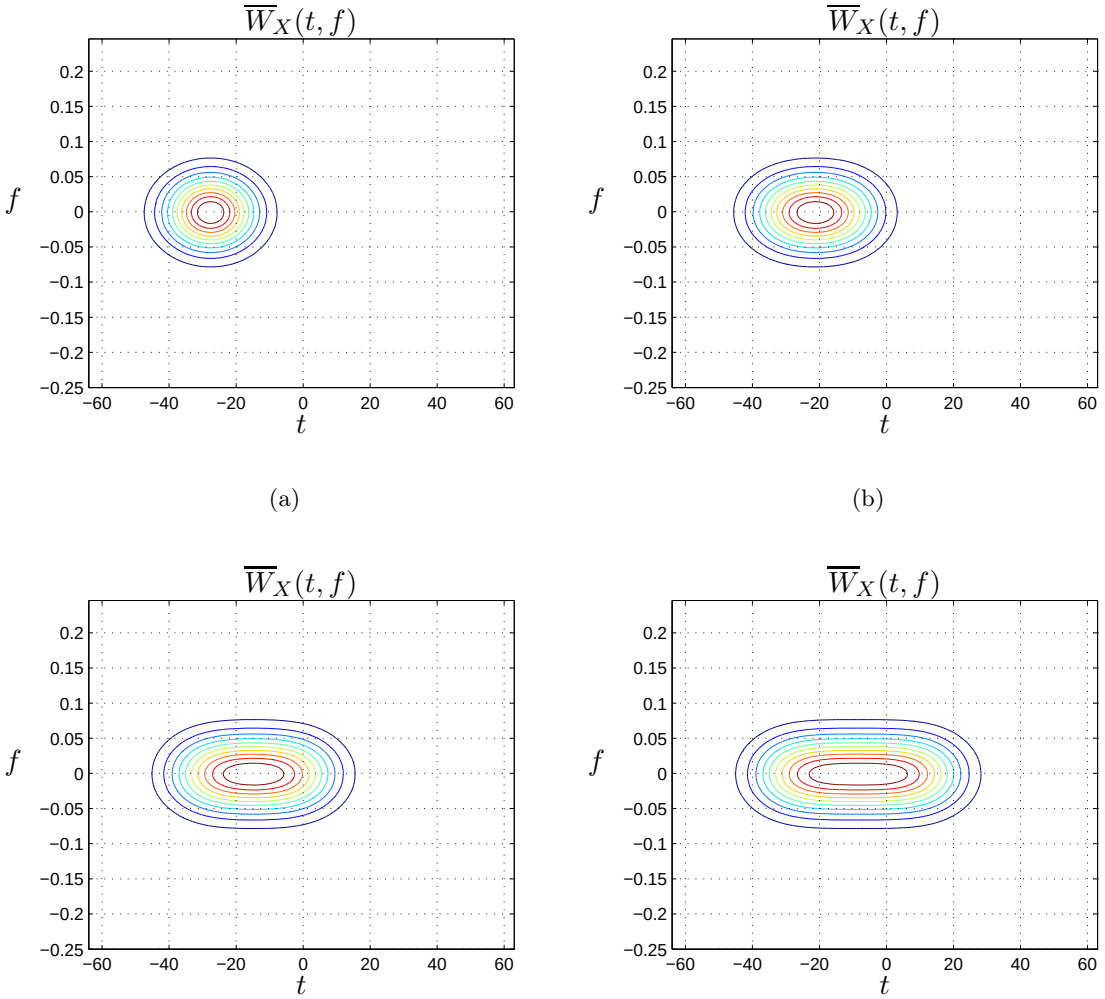

Figure 6.14: WVS of different processes that are generated using as a model function $W'(t,f)$ a superposition of (a) 1 (G_1), (b) 2 (G_2), (c) 3 (G_3), and (d) 4 (G_4) Gaussian functions with identical shape and height. The corresponding four processes are used to simulate the estimator performance for different degrees of sparsity.

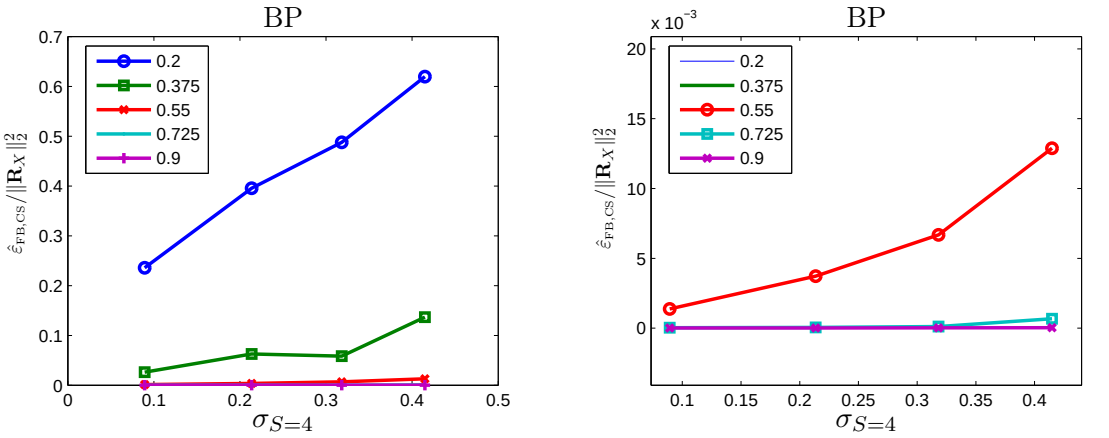

(a) (b)

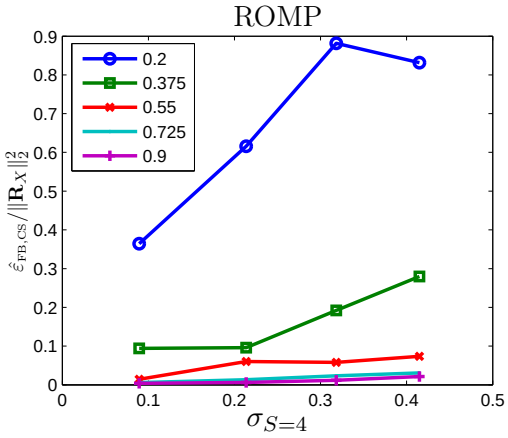

(c)

Figure 6.15: Error of the CS stage against the sparsity measure σ_4 (i.e., the sparsity degree S is set to 4) for different compression factors m/n (a) recovery by BP, (b) zoom in of (a), (c) recovery by ROMP.

In Figure 6.16 we plotted the empirical mean squared error of the estimator $\hat{\varepsilon}_{\mathrm{FB}}$

$$\hat{\varepsilon}_{\mathrm{FB}} \triangleq \frac{1}{100} \sum_{k=1}^{100} \left\| \widehat{W}_X^k(t,f) - \overline{W}_X(t,f) \right\|_2^2 \tag{6.14}$$

and the empirical bias term $\hat{B}_{\mathrm{FB}}^2$

$$\hat{B}_{\mathrm{FB}}^2 \triangleq \left\| \left(\frac{1}{100} \sum_{k=1}^{100} \widehat{W}_X^k(t,f) \right) - \overline{W}_X(t,f) \right\|_2^2 \tag{6.15}$$

as a function of the CS compression factor m/n. Here, $\widehat{W}_X^k(t,f)$ denotes the estimator output $\widehat{W}_X(t,f)$ (cf. Figure 5.3 and (5.16),(5.17)) when the k-th realization of $X(t)$ is used as the input. We normalized both quantities to the squared mean energy $\bar{E}_X^2$ of the process. Each curve in Figure 6.16 corresponds to one of the processes with the model functions shown in Figure 6.14. The dashed curves in Figure 6.16 correspond to the standard estimator of the form (5.24), where the same $\phi(t,f)$ is used as for the estimator simulated here.

As indicated by Figure 6.16 the performance of the estimator "Random Sampling of the Filterbank" mainly depends on the underspreadness (as measured by $M_{\mathbf{X}}^{(1,1)}$) of the process $X(t)$. The dependency of the MSE and the bias term on the compression factor m/n is very low for values above 0.4. For compression factors below 0.4 the error introduced by the CS stages is very high, which seems to indicate that the RIP/RIC condition for the measurement matrix $\mathbf{M}$ is violated with a non-negligible probability.

6.5 Random Sampling of the EAF

For the simulation of the estimator scheme "Random Sampling of the EAF" we also used the minimum error synthesis described above. Furthermore, we again used the ensemble of the TF models shown in Figure 6.14 to generate different processes. The reconstruction kernel $\phi(t,f)$ of the estimator was designed such that its Fourier transform $\Phi(\tau,\nu)$ is box shaped with the support $[-5,5] \times [-0.05, 0.05]$ in the (τ,ν) plane.

The sparsity degree was fixed to $S = 4$. In order to ensure that the measurement matrix $\mathbf{M}$, which in the estimator scheme "Random Sampling of the EAF" is obtained by randomly selecting rows out of a unitary matrix and subsequent renormalization of the columns such that they have unit norm, fulfills the RIP and RIC conditions, for compression factors m/n above 0.5, of the recovery schemes (ROMP and BP) we performed empirical tests in a separate simulation.

As before, we simulated the error that in introduced by the CS stage for the different process models, i.e., for different values of $\sigma_{S=4}$ and for different values of the CS compression factor m/n

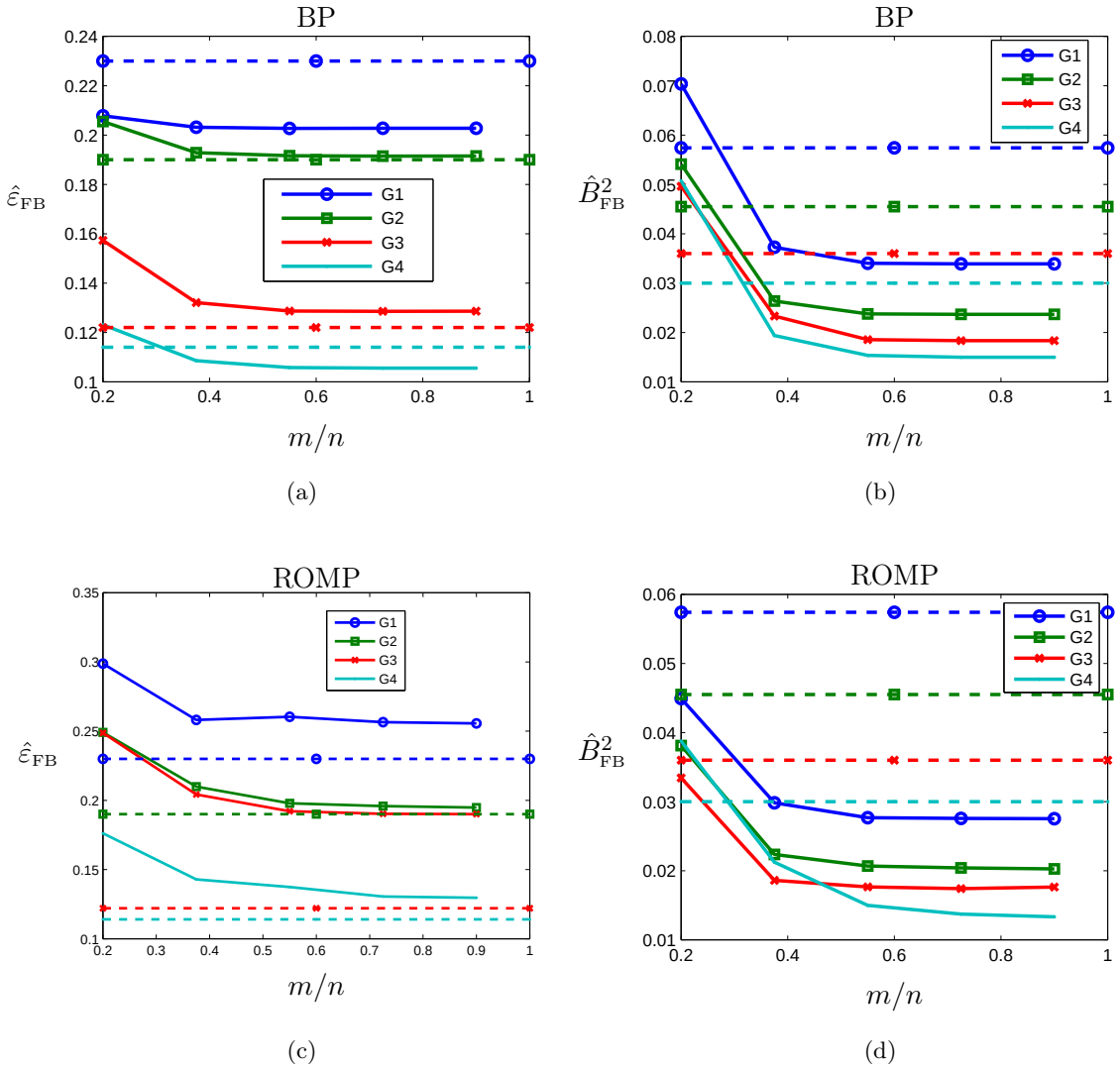

Figure 6.16: MSE and bias against the compression factors m/n for processes G_1 to G_4, generated from different TF models (a) (b) recovery by BP, (c) (d) recovery by ROMP.

where m and n denote the number of rows and columns of the measurement matrix $\mathbf{M}$ respectively. In Figure 6.17 we plotted the error energy of the CS stage, measured by $\hat{\varepsilon}_{\mathrm{EAF,CS}}$:

$$\hat{\varepsilon}_{\mathrm{EAF,CS}} \triangleq \frac{1}{100} \sum_{k=1}^{100} \|\hat{\mathbf{x}}_{\mathrm{EAF}}^k - \mathbf{x}_{\mathrm{EAF}}^k\|_2^2 \tag{6.16}$$

normalized to the squared HS norm of the correlation operator: $\|\mathbf{R}_X\|_2^2$. Here $\hat{\mathbf{x}}_{\mathrm{EAF}}^k$ and $\mathbf{x}_{\mathrm{EAF}}^k$ denote the output of the CS recovery stage and the sampled input vector when the k-th realization of $X(t)$ is used as the input (cf. Figure 5.4). For this plot the value of m/n is used as the parameter. As in the previous section we note that the measured error curves are all significantly below the theoretical bounds for the CS recovery errors derived in Chapter 4 and Section 5.5. This agrees with the observations in the well known CS literature.

In Figure 6.18 we plotted the empirical mean squared error of the estimator $\hat{\varepsilon}_{\mathrm{EAF}}$

$$\hat{\varepsilon}_{\mathrm{EAF}} \triangleq \frac{1}{100} \sum_{k=1}^{100} \left\| \widehat{W}_X^k(t,f) - \overline{W}_X(t,f) \right\|_2^2 \tag{6.17}$$

and the empirical bias term $\hat{B}_{\mathrm{EAF}}^2$

$$\hat{B}_{\mathrm{EAF}}^2 \triangleq \left\| \left(\frac{1}{100} \sum_{k=1}^{100} \widehat{W}_X^k(t,f) \right) - \overline{W}_X(t,f) \right\|_2^2 \tag{6.18}$$

as a function of the CS compression factor m/n. Here, $\widehat{W}_X^k(t,f)$ denotes the estimator output $\widehat{W}_X(t,f)$ (cf. Figure 5.4 and (5.35)) when the k-th realization of $X(t)$ is used as the input. We normalized both quantities to the squared mean energy $\bar{E}_X^2$ of the process $X(t)$. Each curve in Figure 6.18 corresponds to one of the processes with the model functions shown in Figure 6.14. The dashed curves in Figure 6.18 correspond to the standard estimator of the form (5.24), where the same $\phi(t,f)$ is used as for the estimator simulated here. Note that this reference estimator can be viewed as a special case of the CS-based estimator "Random Sampling of the EAF" using a BP and a compression factor of $m/n = 1$.[3]

Similarly to the simulation of the estimator "Random Sampling of the Filterbank", as indicated by Figure 6.18 the performance of the estimator "Random Sampling of the EAF" mainly depends on the underspreadness (as measured by $M_{\mathbf{X}}^{(1,1)}$) of the process $X(t)$. The dependency of the MSE and the bias term on the compression factor m/n is very low for values above 0.4. For compression factors below 0.4 the error introduced by the CS stages is very high, which seems to indicate that the RIP/RIC condition for the measurement matrix $\mathbf{M}$ is violated with a non-negligible probability. Another conclusion suggested by Figure 6.18 is that the performance of the two different CS recovery schemes (BP and ROMP) is very similar, although the computational costs of ROMP are much lower than that of BP.

[3]This is true exactly only when for the BP the constant ϵ in (4.18) is set to zero.

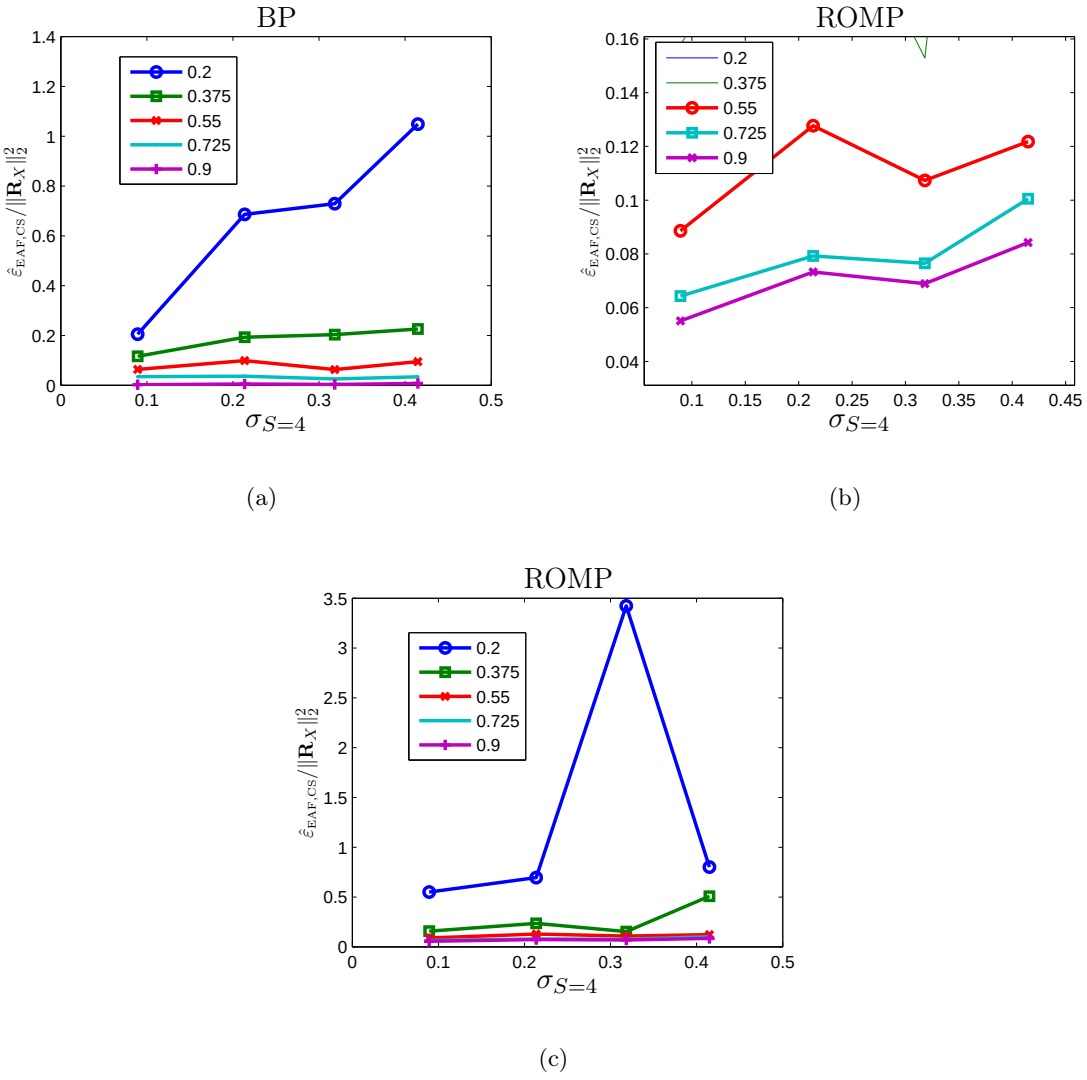

(a) (b)

(c)

Figure 6.17: Error of the CS stage against the sparsity measure σ_4 (i.e., the sparsity degree S is set equal to 4) for different compression factors m/n (a) recovery by BP, (b) zoom in of (c), (c) recovery by ROMP.

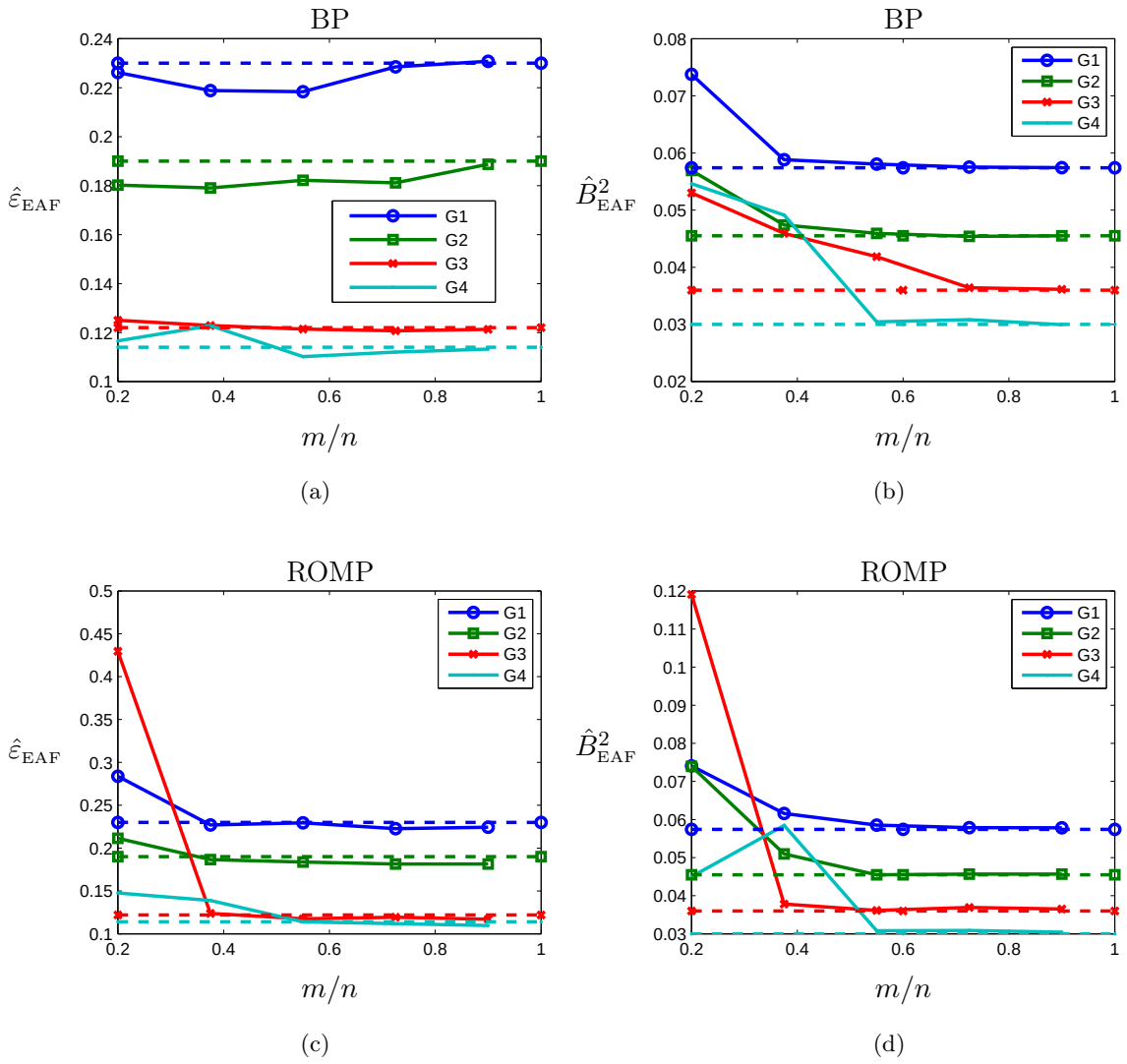

Figure 6.18: MSE and bias against the compression factors m/n for processes G_1 to G_4 generated from different TF models (a) (b) recovery by BP, (c) (d) recovery by ROMP.

Chapter 7

Conclusion and Outlook

7.1 Conclusions

In this thesis we considered the problem of estimating the Wigner Ville spectrum of an underspread random process that is moreover (TF-) sparse. By sparsity we mean that the energy of the process is distributed among a few relatively small (compared to the overall bandwidth and signal duration) regions in the TF plane. We proposed two different estimator schemes that used a CS stage in order to reduce the signal dimension, i.e., to perform compression. We gave detailed performance bounds of these schemes in terms of the mean squared error of the estimators. Furthermore, we conducted numerical experiments which suggested that a spectrum estimation is possible even with a significantly reduced signal dimension, i.e., a relatively high compression factor. However, we want to note that the effective compression is due two to influences. The first source of compression is the usage of Compressed Sensing which allows explicitly for a reduction of the data rate.

But in our CS based estimator schemes there is also a second source of compression, namely the estimation process itself. One on hand this is because the spectrum estimators for underspread processes essentially uses a smoothing of the Wigner distribution of each process realization (cf. estimator scheme "Random Sampling of the EAF"). This smoothing is equivalent to a restriction of the realization AF to a small domain in the (τ, ν) domain and this restriction leads also to a data reduction. On the other hand the inherent smoothness of the spectrum of an underspread process is exploited in order sample the values of the realization WD (cf. estimator scheme "Random Sampling of the Filterbank") on a very coarse lattice in the TF plane specified by the lattice constants T and F whose values are relatively large. Therefore relatively few samples of the WD, which are within the effective support of the WVS of the process, are used.

It should be noted that for practical reasons, we could only simulate scenarios with relatively small dimensions of the signals. For more realistic scenarios even higher compression factors can

be expected to yield satisfactory performance.

7.2 Outlook

Finally we give a list of open questions and directions that turned out to be interesting during this thesis:

- **Efficient Implementations of the CS Measurement Stage:** From our view the most critical component for the practical usefulness of our results is the CS measurement stage which consists in a sampled filterbank followed by a squaring of the magnitude and a multiplication with a measurement matrix for the scheme "Random Sampling of the Filterbank". For the scheme "Random Sampling of the EAF" the CS measurement stage consists of computing the values of the EAF at randomly selected points in the (τ, ν) plane. The problem is that these operations have to be performed on the nominal signal rate which is in general very high compared to the rate after the CS stage.

- **Theoretical Performance Analysis of Adaptive Recovery Schemes:** It would be interesting to theoretically analyze the performance bound of adaptive schemes. However we expect this to be difficult because of the adaptivity.

- **Links to Distributed Sensing Setting:** Compressed Sensing can be generalized to the theory of Distributed sensing which models the fact that the measurements of a signal $\mathbf{x}$ are taken at different sensor locations [17].

- **Sparsity Measures for an Underspread Process:** The definition of sparsity of an underspread process was formulated in terms of sample values of the WVS at a rectangular lattice with lattice constants T, F that are also used for the analyzing WH-set of the process. This definition is rather general and does not allow for sophisticated sampling methods. E.g. a simple random sampling in the time domain is not possible for a process that is sparse in our sense, because it is not known if the sparse energy is distributed "spike"-like or if it is distributed over a small number of frequency components that have a narrow bandwidth. A more specialized notion of sparsity would allow to investigate such random sampling schemes (in the time- or frequency domain).

- **RIP/RIC Analysis of Measurement Matrices:** At the time of finishing this thesis there seemed to be no efficient method for verifying the RIP/RIC properties of a given deterministic measurement matrix. Moreover, even for the well known random constructions of measurement matrices the results regarding the RIP performance still lack of accuracy. The corresponding performance bounds (e.g. bounds on the probability that a random matrix

satisfies certain RIP/RIC conditions) are relatively pessimistic compared with empirical studies. It would be very interesting to have more and better theoretical tools for the RIP/RIC analysis of measurement matrices.

Appendix A

Kronecker Product and Vec Operation

The vec$\{\cdot\}$ operation assigns a column vector $\mathbf{x} \in \mathbb{C}^K$ to each matrix $\mathbf{A} \in \mathbb{C}^{m \times n}$ where $K = m \cdot n$. This assignment is given by stacking all the columns of $\mathbf{A}$ into a signal column vector $\mathbf{x}$:

$$\mathbf{x} = \text{vec}\{\mathbf{A}\} \triangleq \begin{bmatrix} \mathbf{A}_{1,1} \\ \mathbf{A}_{2,1} \\ \vdots \\ \mathbf{A}_{m,1} \\ \vdots \\ \mathbf{A}_{m,n} \end{bmatrix} \tag{A.1}$$

where the first m elements of $\mathbf{x}$ are given by the first column of $\mathbf{A}$, the second m elements are given by the second column and so on.

Another operation that we use within this thesis is the Kronecker product $\mathbf{A} \otimes \mathbf{B}$ of two matrices $\mathbf{A} \in \mathbb{C}^{m \times n}$ and $\mathbf{B} \in \mathbb{C}^{k \times l}$. The resulting matrix $\mathbf{C} = \mathbf{A} \otimes \mathbf{B}$ lies in $\mathbb{C}^{mk \times nl}$ and is given by multiplying each entry of $\mathbf{A}$ by the complete matrix $\mathbf{B}$.

The most important property of the Kronecker product for our purposes is that if the two matrices $\mathbf{A}$ and $\mathbf{B}$ are unitary, i.e., $\mathbf{A}\mathbf{A}^H = \mathbf{I}$ and $\mathbf{B}\mathbf{B}^H = \mathbf{I}$ (which implies of course that $\mathbf{A}$ and $\mathbf{B}$ are square matrices) then also the product is unitary:

$$(\mathbf{A} \otimes \mathbf{B})\,(\mathbf{A} \otimes \mathbf{B})^H = \mathbf{I} \tag{A.2}$$

where the dimension of the identity matrix $\mathbf{I}$ is clear from the context.

Appendix B

Complex Valued Basis Pursuit

Most of the CS literature about BP uses exclusively the real valued setting. As often mentioned there, it is an easy step to generalize results from the real valued to the complex valued setting.

Remember that in CS we observe a measurement vector $\mathbf{z}$ that is given by $\mathbf{z} = \mathbf{M}\mathbf{x}$ where $\mathbf{M}$ denotes a (full rank) measurement matrix that has fewer rows than columns. All vectors and matrices so far are modeled as complex valued. We also showed that the solution to the minimization problem (whose implementation is called BP):

$$\hat{\mathbf{x}} = \arg\min \|\mathbf{x}\|_1 \quad \text{subject to} \quad \|\mathbf{z} - \mathbf{M}\mathbf{x}\|_2 \leq \varepsilon \tag{B.1}$$

can be used to recover the signal $\mathbf{x}$ from $\mathbf{z}$ accurately.

As mentioned above, most implementations of this minimization presuppose that all objects are real valued. Therefore we want to show how one can reformulate the complex valued minimization problem to a real valued one without loosing significant recovery accuracy.

We present two different methods to to this. The first method assumes a special structure of the measurement matrix $\mathbf{M}$ and is not an exact reformulation of the original problem but we will show that the errors introduced by this inexactness are small. The second method, which is exact, reformulates the optimization problem as a convex optimization problem for which efficient implementations also already exist.

The first method we want to present assumes that the measurement matrix $\mathbf{M}$ is a randomly sampled unitary matrix, more specifically the DFT matrix. We now consider the matrix $\mathbf{M}'$ which is defined as

$$\mathbf{M}' = \begin{pmatrix} \Re\{\mathbf{M}\} & -\Im\{\mathbf{M}\} \\ \Im\{\mathbf{M}\} & \Re\{\mathbf{M}\} \end{pmatrix} \tag{B.2}$$

and the vector $\mathbf{x}'$ that is defined as

$$\mathbf{x}' = \begin{pmatrix} \Re\{\mathbf{x}\} \\ \Im\{\mathbf{x}\} \end{pmatrix} \tag{B.3}$$

i.e., by stacking the real part and the imaginary part of the signal vector $\mathbf{x}$ into a "super"-vector of twice the size of $\mathbf{x}$. Now we note that we can express the observed measurements $\mathbf{z}$ fully equivalently via

$$\mathbf{z}' = \mathbf{M}'\mathbf{x}' + \mathbf{w}' \tag{B.4}$$

where

$$\mathbf{z}' = \begin{pmatrix} \Re\{\mathbf{z}\} \\ \Im\{\mathbf{z}\} \end{pmatrix} \qquad \mathbf{w}' = \begin{pmatrix} \Re\{\mathbf{w}\} \\ \Im\{\mathbf{w}\} \end{pmatrix} \tag{B.5}$$

and furthermore it can be shown that $\mathbf{M}'$ satisfies the same RIP/RIC properties as $\mathbf{M}$ because of the relationship (B.2).[1] Finally, because if the vector $\mathbf{x}$ is sparse then also the vector $\mathbf{x}'$ we have that the all results regarding recovery performance of the Basis Pursuit that are valid for the measurement matrix $\mathbf{M}$ and the signal vector $\mathbf{x}$ are also valid for the real-valued measurement matrix $\mathbf{M}'$ and the real valued signal vector $\mathbf{x}'$. Moreover, the noise energy $\|\mathbf{w}'\|_2^2$ of the real valued noise $\mathbf{w}'$ where is identical to the energy $\|\mathbf{w}\|_2^2$ of the complex valued noise $\mathbf{w}$. Putting it all together we have obtained a new CS signal model (B.4) where all quantities are real valued and in particular, as can be shown the signal $\mathbf{x}'$ and measurement matrix $\mathbf{M}'$ have the same sparsity and RIP/RIC properties as the original complex valued signal $\mathbf{x}$ and measurement matrix $\mathbf{M}$. Therefore we can use the real valued optimization problem:

$$\hat{\mathbf{x}}' = \arg\min_{\mathbf{x}'} \|\mathbf{x}'\|_1 \quad \text{such that} \quad \|\mathbf{M}'\mathbf{x}' - \mathbf{z}'\|_2 \leq \varepsilon \tag{B.7}$$

and the relation:

$$\hat{\mathbf{x}}' = \begin{pmatrix} \Re\{\hat{\mathbf{x}}\} \\ \Im\{\hat{\mathbf{x}}\} \end{pmatrix} \tag{B.8}$$

to get the (approximate) solution of the original complex-valued minimization through a real-valued minimization. Note that this translation of complex valued quantities ($\mathbf{z}$,$\mathbf{w}$,$\mathbf{M}$) to real valued quantities can also be used for the usage of ROMP, which is stated in this thesis only for the real valued setting.

The second approach reformulates in an exact way the optimization problem (B.1) as the following new optimization problem:

$$\hat{\mathbf{x}}' = \arg\min_{\mathbf{x}',\mathbf{t}} \sum_k \mathbf{t}_k \quad \text{such that} \quad |\mathbf{x}'_k| \leq \mathbf{t}_k \quad \text{and} \quad \|\mathbf{M}'\mathbf{x}' - \mathbf{z}\|_2 \leq \varepsilon \tag{B.9}$$

with $\mathbf{M}'$ defined as before in (B.2). Note that this optimization can be performed only using real valued quantities by optimizing over all real valued vectors $\mathbf{x}'$ of twice the length of $\mathbf{x}$. The

[1] The proof of this statement essentially relies on these equalities:

$$\|\mathbf{M}\mathbf{x}\|_2^2 = \|\mathbf{z}\|_2^2 = \|\mathbf{z}'\|_2^2 = \|\mathbf{M}'\mathbf{x}'\|_2^2. \tag{B.6}$$

solution $\hat{\mathbf{x}}$ of the original problem (B.1) is then given through the solution $\hat{\mathbf{x}}'$ of the real valued optimization (B.9) and the relation (B.8), i.e., the first half of $\hat{\mathbf{x}}'$ is equal to the real part of $\hat{\mathbf{x}}$ and the second half to the imaginary part. The real valued optimization problem (B.9) can easily shown [7] to be an convex optimization problem, more specifically a second order cone programm (SOCP) for which efficient implementations [5] exist.

List of Abbreviations

ONB	Orthonormal Basis
WVS	Wigner Ville Spectrum
WD	Wigner Distribution
EAF	Expected Ambiguity Function
AF	Ambiguity Function
TF-plane	Time-Frequency plane, i.e., the set of all pairs (t, f) of (absolute) time and frequency values
DMD	Digital Micro-Mirror Device
KLT	$Karhunen - Loéve$ Transformation
LTI	Linear Time Invariant
CSMA	Carrier Sense Multiple Access
PAM	Pulse Amplitude Modulation
TOMP	Tree Based Orthogonal Matching Pursuit
ROMP	Regularized Orthogonal Matching Pursuit
StOMP	Stage Wise Orthogonal Matching Pursuit
MSE	Mean Squared Error
MAP	Maximum A - Posteriori
MMSE	Minimum Mean Squared Error
FFT	Fast Fourier Transform
IFFT	Inverse Fast Fourier Transform
RV	Random Variable
AIC	Analog to Information Converter
BP	Basis Pursit
HS	Hilbert Schmidt
CS	Compressed Sensing
iff	if and only if
DSP	Digital Signal Processing
MP	Matching Pursuit
PSD	Power Spectral Density
HS	Hilbert Schmidt
WH	Weyl Heisenberg
SF	Spreading Function
w.r.t.	with respect to
pdf	probability density function

Bibliography

[1] Dimitris Achlioptas. Database-friendly random projections. In *PODS '01: Proceedings of the twentieth ACM SIGMOD-SIGACT-SIGART symposium on Principles of database systems*, pages 274–281, New York, NY, USA, 2001. ACM.

[2] Michal Aharon, Michael Elad, and Alfred Bruckstein. K-svd: Design of dictionaries for sparse representation. 2005.

[3] Richard Baraniuk, Mark Davenport, Ronald De Vore, and Michael Wakin. A simple proof of the restricted isometry property for random matrices. 2007.

[4] Pierre Borgnat and Patrick Flandrin. Time-frequency localization from sparsity constraints. 2008.

[5] Steven Boyd and Lieven Vandenberghe. *Convex Optimization*. Cambridge Press, 2004.

[6] Emmanuel Candes and Justin Romberg. Quantitative robust uncertainty principles and optimally sparse decompositions. *Found. of Comput. Math.*, 6:227–254, 2004.

[7] Emmanuel Candes and Justin Romberg. l1-magic: Recovery of sparse signals via convex programming. 2005.

[8] David S. K. Chan. A non-aliased discrete-time wigner distribution for time-frequency signal analysis. 1982.

[9] R. R. Coifman and M. Wickerhauser. Entropy-based algorithms for best basis selection. *IEEE Trans. Inf. Theory*, 38(2):713–718, March 1992.

[10] Ingrid Daubechies. The wavelet transform, time-frequency localization and signal analysis. *IEEE Trans. Inf. Theory*, 36:961–1005, Sept. 1990.

[11] Ronald A. DeVore. Deterministic constructions of compressed sensing matrices. 2007.

[12] Thong T. Do, Trac D. Tran, and Lu Gan. Fast compressive sampling with structurally random matrices. 2007.

[13] David L. Donoho. Compressed sensing. *IEEE Transactions on Information Theory*, 52:1289–1306, 2006.

[14] David L. Donoho and Michael Elad. Optimally sparse representation in general (nonorthogonal) dictionaries via ℓ^1 minimization. 2002.

[15] David L. Donoho, Michael Elad, and Vladimir N. Temlyakov. Stable recovery of sparse overcomplete representations in the presence of noise. *IEEE Transactions on Information Theory*, 52:6 – 18, 2006.

[16] David L. Donoho, Yaakov Tsaig, Iddo Drori, and Jean-Luc Starck. Sparse solution of underdetermined linear equations by stagewise orthogonal matching pursuit. 2006.

[17] Marco F. Duarte, Shriram Sarvotham, Dror Baron, Michael B. Wakin, and Richard G. Baraniuk. Distributed compressed sensing of jointly sparse signals. In *Proc. 39th Asilomar Conf. Signals, Systems, Computers*, pages 1537 – 1541, 2005.

[18] Justin Romberg Emmanuel Candes and Terence Tao. Stable signal recovery from incomplete and inaccurate measurements. *Comm. Pure Appl. Math.*, 59:1207–1223, 2005.

[19] Anna Gilbert et. al. Implementation models for analog-to-information conversion via random sampling. 2007.

[20] Jarvis D. Haupt et. al. Toeplitz-structured compressed sensing matrices. In *14th IEEE Workshop on Statistical Signal Processing*, pages 294 – 298, 2007.

[21] Jason N. Laska et. al. Theory and implementation of an analog-to-information converter using random demodulation. In *IEEE International Symposium on Circuits and Systems*, pages 1959 – 1962, 2007.

[22] M.B. Wakin et.al. An architecture for compressive imaging. In *IEEE Conference on Image Processing*, pages 1273 – 1276, 2006.

[23] Karlheinz Gröchenig. *Foundations of Time-Frequency Analysis*. Birkhäuser, Boston, 2001.

[24] Matthew A. Herman and Thomas Strohmer. High-resolution radar via compressed sensing. *IEEE Transactions on Signal Processing*, submitted, 2007.

[25] F. Hlawatsch. *Information Theory and Coding*. Lecture notes; Institut für Nachrichtentechnik und Hochfrequenztechnik, Technische Universität Wien, March 2007.

[26] F. Hlawatsch. *Modulation and Detection Methods*. Lecture notes; Institut für Nachrichtentechnik und Hochfrequenztechnik, Technische Universität Wien, March 2007.

[27] F. Hlawatsch and W. Kozek. Second-order time-frequency synthesis of nonstationary random processes. *IEEE Trans. Inf. Theory*, 41(1):255–267, Jan. 1995.

[28] A. J. E. M. Janssen. Positivity and spread of bilinear time-frequency distributions. In W. Mecklenbräuker and F. Hlawatsch, editors, *The Wigner Distribution — Theory and Applications in Signal Processing*, pages 1–58. Elsevier, Amsterdam (The Netherlands), 1997.

[29] A.J.E.M. Janssen. A classroom proof of the density theorem for gabor systems.

[30] Shihao Ji, Ya Xue, and Lawrence Carin. Bayesian compressive sensing. *IEEE Transactions on Signal Processing*, 56:2346 – 2356, 2008.

[31] W. Kozek. Matched generalized Gabor expansion of nonstationary processes. In *Proc. 27th Asilomar Conf. Signals, Systems, Computers*, pages 499–503, Pacific Grove, CA, Nov. 1993.

[32] W. Kozek. *Matched Weyl-Heisenberg Expansions of Nonstationary Environments*. PhD thesis, Vienna University of Technology, March 1997.

[33] W. Kozek and K. Riedel. Quadratic time-varying spectral estimation for underspread processes. In *Proc. IEEE-SP Int. Sympos. Time-Frequency Time-Scale Analysis*, pages 460–463, Philadelphia, PA, Oct. 1994.

[34] Chinh La and Minh N. Do. Tree-based orthogonal matching pursuit algorithm for signal reconstruction. In *IEEE Conference on Image Processing*, pages 1277 – 1280, 2006.

[35] S. G. Mallat. *A Wavelet Tour of Signal Processing*. Academic Press, San Diego, 1998.

[36] S. G. Mallat, G. Papanicolaou, and Z. Zhang. Adaptive covariance estimation of locally stationary processes. *Ann. Stat.*, 26(1):1–47, Feb. 1998.

[37] S. G. Mallat and Z. Zhang. Matching pursuits and time-frequency dictionaries. *IEEE Trans. Signal Processing*, 41(12):3397–3415, Dec. 1993.

[38] G. Matz and F. Hlawatsch. Nonstationary spectral analysis based on time-frequency operator symbols and underspread approximations. *IEEE Trans. Inf. Theory*, 52(3):1067–1086, March 2006.

[39] G. Matz, D. Schafhuber, K. Groechenig, M. Hartmann, and F. Hlawatsch. Analysis, optimization, and implementation of low-interference wireless multicarrier systems. *IEEE Trans. Wireless Comm.*, 6:1921 – 1931, 2007.

[40] Gerald Matz. *A time-frequency calculus for time-varying systems and nonstationary processes with applications*. PhD thesis, Vienna University of Technology, Nov. 2000.

[41] Gerald Matz and Franz Hlawatsch. *Time-Frequency Analysis: Concepts and Methods*, chapter Time-frequency methods for statistical signal processing. 2007.

[42] W. Mecklenbräuker and F. Hlawatsch, editors. *The Wigner Distribution – Theory and Applications in Signal Processing*. 1997.

[43] A. W. Naylor and G. R. Sell. *Linear Operator Theory in Engineering and Science*. Springer, New York, 2nd edition, 1982.

[44] Deanna Needell and Roman Vershynin. Signal recovery from incomplete and inaccurate measurements via regularized orthogonal matching pursuit. 2007.

[45] Deanna Needell and Roman Vershynin. Uniform uncertainty principle and signal recovery via regularized orthogonal matching pursuit. 2007.

[46] Gabriel Peyre. Best basis compressed sensing. 2006.

[47] Holger Rauhut. Stability results for random sampling of sparse trigonometric polynomials. 2006.

[48] Holger Rauhut. On the impossibility of uniform sparse reconstruction using greedy methods. 2007.

[49] Holger Rauhut, Karin Schnass, and Pierre Vandergheynst. Compressed sensing and redundant dictionaries. *IEEE Transactions on Information Theory*, 54:2210–2219, 2008.

[50] Mark Rudelson and Roman Vershynin. Sparse reconstruction by convex relaxation: Fourier and gaussian measurements. In *Proc. of the 40th Annual Conference on Information Sciences and Systems*, pages 207–212, March 2006.

[51] Shriram Sarvotham, Dror Baron, and Richard G. Baraniuk. Compressed sensing reconstruction via belief propagation. 2006.

[52] A. M. Sayeed and D. L. Jones. Optimal kernels for nonstationary spectral estimation. *IEEE Trans. Signal Processing*, 43(2):478–491, Feb. 1995.

[53] Georg Tauböck and Franz Hlawatsch. A compressed sensing technique for OFDM channel estimation in mobile environments: Exploiting channel sparsity for reducing pilots. In *Proc. IEEE ICASSP 2008*, 2008.

[54] Zhi Tian and Georgios B. Giannakis. Compressed sensing for wideband cognitive radios. In *Proc. IEEE ICASSP 2007*, volume 4, pages 1357 – 1360, 2007.

[55] Joel A. Tropp. Greed is good: Algorithmic results for sparse approximation. *IEEE Transactions on Information Theory*, 50(10):2231–2242, 2004.

[56] Joel A. Tropp. Random filters for compressive sampling. In *Proc. of the 40th Annual Conference on Information Sciences and Systems*, pages 216–217, March 2006.